

# Nuclear Interaction from Effective Field Theory

Damon Binder

A thesis submitted for the degree of  
Bachelor of Science (Advanced) with Honours in Physics, at  
The Australian National University

October, 2016



---

# Declaration

---

This thesis is an account of research undertaken between February 2016 and October 2016 at The Department of Nuclear Physics, Research School of Physics and Engineering, The Australian National University, Canberra, Australia.

Except where acknowledged in the customary manner, the material presented in this thesis is, to the best of my knowledge, original and has not been submitted in whole or part for a degree in any university.

---

Damon J. Binder  
October, 2016



---

# Acknowledgments

---

First, I thank my supervisor Cédric Simenel, for his patience, guidance, and ability to catch numerous errors in my thesis. I must also thank him for introducing me to the wonderful topic of quantum field theory, and for putting up with the many tangents I found along the way.

Thanks go to both my fellow Bruce residents and fellow honours students, for their companionship, ability to provide distraction, and for many meal-time conversations. In particular thanks go to Matthew Alger, who proofread my thesis and provided valuable advice throughout the year. I would also like to thank Abigail, for her constant support throughout the year.

Finally, I thank my family, for raising me and for always valuing my education.



---

# Abstract

---

In order to predict the properties of atomic nuclei, a quantitative understanding of the in-medium inter-nucleon forces is required. The Skyrme energy density functional provides a popular phenomenological description of these interactions, with parameters fitted to experimental data. Unfortunately, these parameters are under-constrained by data. This prevents reliable predictions for exotic systems, such as weakly-bound nuclei, super-heavy elements, and reactions.

Through the use of effective field theory, we will examine the origin of nuclear interactions from higher energy physics. By systematically considering the non-relativistic limit, we are able to efficiently relate meson models to non-relativistic energy density functionals. We show that constraints can be placed on Skyrme parametrisations provided generic properties of this high energy physics. On the other hand, details of high energy physics are shown to be largely irrelevant for a description of low energy nuclear phenomenology. We finish with a comparison of our results to a series of commonly used Skyrme parametrisations.



---

# Contents

---

<b>Declaration</b>	<b>iii</b>
<b>Acknowledgments</b>	<b>v</b>
<b>Abstract</b>	<b>vii</b>
<b>1 Introduction</b>	<b>3</b>
<b>2 A Toy Model</b>	<b>9</b>
<b>3 Effective Field Theory</b>	<b>13</b>
3.1 Overview . . . . .	13
3.2 Formalism . . . . .	15
3.3 Gaussian Path Integrals . . . . .	16
3.4 The Semiclassical Expansion . . . . .	18
3.5 Density Dependence in the Quark-Meson Coupling Model . . . . .	20
3.6 Feynman Diagrams for Effective Field Theories . . . . .	23
<b>4 The Non-Relativistic Limit</b>	<b>27</b>
4.1 Overview . . . . .	27
4.2 Schrödinger from Dirac . . . . .	28
4.3 Non-Relativistic Dirac Bilinears . . . . .	29
4.4 Non-Relativistic Densities and Skyrme Functionals . . . . .	33
<b>5 Meson Models for Nuclear Forces</b>	<b>37</b>
5.1 Strong Quantum Chromodynamics . . . . .	37
5.2 Light Hadrons . . . . .	38
5.3 Meson-Nucleon Interactions . . . . .	40
5.3.1 The Sigma . . . . .	40
5.3.2 The Pion . . . . .	41
5.3.3 The Omega and the Rho . . . . .	42
5.3.4 Summary of Results . . . . .	43
5.4 Meson-Meson Interactions . . . . .	45
5.4.1 Relationship to Relativistic Mean-Field Theory . . . . .	48
5.4.2 Expanding around Nuclear Saturation Density . . . . .	49
5.5 Rescaling Parameters . . . . .	49
5.6 Vector and Tensor Couplings . . . . .	50
5.7 Discussion . . . . .	52
<b>6 The Energy Density Functional for Time-Even Systems</b>	<b>55</b>
6.1 The Time-Even EDF . . . . .	55
6.2 Skyrme Parametrisations . . . . .	56

---

6.2.1	Parametrisations Used . . . . .	56
6.2.2	Fitting Parameters and Uncertainties . . . . .	58
6.3	Relating the Central and Spin-Orbit Terms . . . . .	59
6.3.1	Inequalities . . . . .	59
6.3.2	The Isovector Dependence of the Spin-Orbit Term . . . . .	60
6.3.3	Calculating $\mu^2$ . . . . .	62
6.4	Gradient and Effective Mass Terms . . . . .	64
6.4.1	The Pion Contribution . . . . .	64
6.4.2	Calculating the Isovector Effective Mass Term . . . . .	65
6.4.3	The Tensor Terms . . . . .	66
<b>7</b>	<b>Conclusion</b>	<b>67</b>
<b>A</b>	<b>Quark-Meson Coupling to One-Loop</b>	<b>71</b>
<b>B</b>	<b>The Källén-Lehmann Spectral Representation</b>	<b>73</b>
<b>C</b>	<b>Expectation Values of Time-Even Densities</b>	<b>75</b>
C.1	Time-Even Densities . . . . .	75
C.2	Evaluating Bilinears . . . . .	76
	<b>Bibliography</b>	<b>79</b>

---

# List of Figures

---

1.1	Landscape of Even-Even Nuclei . . . . .	4
3.1	Infinite Nuclear Matter in the Quark-Meson Coupling Model . . . . .	23
6.1	Isospin Dependence of the Spin-Orbit Force . . . . .	62
6.2	Values of $\mu^2$ from Skyrme and Relativistic Mean-field Theory . . . . .	63
6.3	Values of $\alpha^2$ from Skyrme Parametrisations . . . . .	65
6.4	Calculated and Fitted Values of the Isovector Effective Mass Term . . . . .	66



---

# List of Tables

---

1.1	Double-Dutied Notation . . . . .	7
4.1	Non-Relativistic Limit of Dirac Bilinears . . . . .	29
5.1	Symmetries of Quantum Chromodynamics . . . . .	38
5.2	Light Mesons . . . . .	39
5.3	Light Baryons . . . . .	39
5.4	Origin of Lagrangian Terms . . . . .	45
6.1	Skyrme Parametrisations Used . . . . .	57
6.2	Uncertainties in UNEDF1 . . . . .	59
6.3	Central and Spin-Orbit Inequalities . . . . .	61
6.4	Relativistic Mean-Field Parametrisations Used . . . . .	63



---

# Introduction

---

Understanding the structure and composition of the atomic nucleus has challenged physicists for almost a century. Nuclei are complex objects: they are bound states of strongly interacting protons and neutrons, and in turn these protons and neutrons are bound states of strongly interacting quarks and gluons. The fundamental theory underlying these interactions, quantum chromodynamics (QCD), was discovered in the 1970s. Yet QCD is highly non-perturbative at low energies, and so it is currently impossible to systematically calculate nuclear properties using QCD.

There are two primary difficulties in the study of nuclear forces. The first is that the nuclear interactions currently cannot be derived from QCD, nor can they be measured experimentally inside the nucleus. As a result, our descriptions of nuclear forces are poorly constrained by both theory and experiment.

The second difficulty is that even once given a microscopic nuclear interaction, utilising this to predict the macroscopic properties of nuclei is highly non-trivial. Nuclei are many-body systems and may contain over 300 nucleons. This is far too many to solve directly, even on a supercomputer, yet too few for statistical techniques to be useful. Numerous approximation techniques have been developed — or just as commonly, adapted from other fields — to make the problem tractable [1]. These approximations are usually grounded in self-consistent mean-field theory, which simplifies the problem by ignoring correlations between nucleons. The errors inherent in this approach further obscure the relationship between microscopic nuclear forces and the observable properties of nuclei.

There are various approaches used in nuclear many-body calculations which can be applied to study nuclei across the periodic table [2]. Relativistic mean-field theory begins with an interacting theory of mesons and nucleons, and then self-consistently solves the equations of motion for the meson field [3]. Non-relativistic methods on the other hand contain only nucleons, interacting with each other by some phenomenological force [4]. Though countless possibilities exist, the two most commonly used in calculations are the Skyrme [5, 6] and Gogny interactions [7]. The form of both interactions were chosen for computational convenience: the Skyrme force is zero-range and the Gogny force is Gaussian.

These models share a common defect: they are phenomenological, requiring many parameters that must be fitted to experimental data. Furthermore, these parameters are under-constrained: various choices of parameters are able to fit experimental data with comparable quality. For instance, there are over 240 parametrisations of the Skyrme interaction found in the literature [8]. Extrapolating these interactions to new regimes is fraught with difficulty, and the predictions of different parametrisations may give divergent results.

This is unfortunate, as exotic systems are of immense interest in contemporary nu-

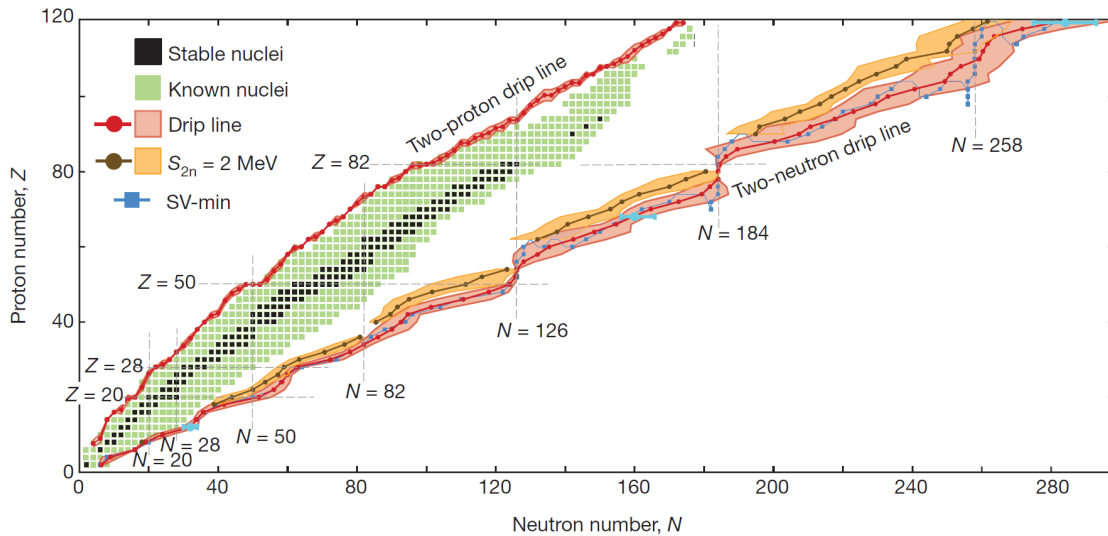


**Figure 1.1:** Landscape of even- $Z$  even- $N$  nuclei as of 2012. Mean drip lines and their uncertainties were calculated by averaging the results of different Skyrme functionals. Adapted from [14].

clear physics. The study of super-heavy elements, and in particular the possibility of an ‘island of stability’ around  $N = 184$  has resulted in much work both theoretically [10] and experimentally [9]. Astrophysical applications have motivated the study of neutron-rich nuclei, which play a critical role in the formation of elements via the  $r$ -process [11, 12]. Predicting the properties of neutron stars require a detailed understanding of the properties of pure neutron matter [13], which again is lacking as we cannot access such matter experimentally.

The location of the two-neutron drip line is a concrete example of a problem originating in our inability to extrapolate Skyrme interactions to new regimes. In *Figure 1.1*, calculations of the two-neutron drip line are shown [14]. The uncertainty in its location was calculated by comparing the results of different Skyrme interactions. Understanding the two-neutron drip line is critical for mapping the limits of the nuclear landscape, and in particular plays a crucial role in the  $r$ -process [15].

Phenomenological forces are also limited in their ability to describe reaction dynamics [16]. They are usually fitted to the ground-state properties of even-even nuclei — these nuclei possess a time-reversal symmetry. Reactions, however, do not possess this symmetry, allowing contributions from time-odd densities that cannot be constrained by standard phenomenological fits [17].

In light of these difficulties, it is logical to ask “Can we constrain nuclear forces using our knowledge of higher-energy physics?” After all, protons and neutrons are just two particles in a veritable “particle zoo” of strongly interacting baryons and mesons. Since the proposal of meson-exchange by Yukawa in 1935 [18] and the discovery of the pion in 1947, a plethora of models have been developed seeking to relate meson exchange to the nuclear forces [19, 20]. By relating phenomenological forces to this higher-energy physics, we may hope to gain a deeper understanding of the nuclear forces. Ideally, this would provide qualitative and quantitative restrictions on the force. We may also hope for insight into the validity of extrapolating our phenomenological fitted forces to new regimes.

In this thesis, we will develop a systematic derivation of nuclear forces using field theoretic techniques and effective field theory. Although this thesis is focused on nuclear

---

theory, the tools we discuss are general and are related to modern techniques in both particle and condensed matter physics. This allows us to concisely relate Skyrme interactions to models of the higher energy physics.

Chapter 2 describes a toy model for nuclear forces. This model illustrates the three steps required to derive non-relativistic forces from higher-energy processes:

1. Choose a relativistic field theory, of nucleons interacting with various mesons and baryons.
2. Use the methods of effective field theory to ‘integrate out’ the mesons, yielding a relativistic theory of interacting nucleons.
3. Take the non-relativistic limit of the interacting nucleon theory, resulting in a non-relativistic theory of nucleons interacting via zero-ranged potentials.

The next two chapters are devoted to developing the theoretical tools necessary to perform the three steps. Chapter 3 describes effective field theory, which is necessary to perform the first two steps. The third step — taking the non-relativistic limit of a theory — is discussed in Chapter 4.

Chapter 5 describes the applications of our tools to the problem of nuclear forces. Beginning with a theory of nucleons linearly interacting with a number of mesons — the sigma, omega, rho and pion — we show that an interaction of Skyrme-like form will result in the low energy limit. Our techniques are able to efficiently reproduce the results of meson-exchange models.

Mesons interact with each other, sometimes quite strongly, and these interactions must be included in any realistic model. A quantitative understanding of strongly interacting field theories does not currently exist, so the predictive power of these theories is questionable. We show however that by judicious rescaling of parameters, the low energy limit will only slightly generalise the linear case. This justifies the success of simple meson models in describing nuclear forces — but this success does not necessarily validate the physics postulated by these models.

To the contrary, we demonstrate that minimal physics is needed in order to reproduce the known properties of the nuclear forces. If the necessary symmetries and interaction channels are included, a Skyrme-like interaction will generically result, with sufficient freedom to describe nuclei across the entire nuclear chart.

In spite of these results, we are still able to provide some constraints on the form of low energy nuclear forces. For instance, the ratio of the vector-to-tensor couplings of the vector mesons to the nucleon may be preserved in the low energy limit, even if both couplings are rescaled by non-perturbative and in-medium effects. Utilising this, we are able to describe low energy nucleon-interactions in terms of only six parameters. This is an improvement on the 18 or so needed in a standard Skyrme functional parametrisation.

Chapter 6 applies the results of Chapter 5 to the case of time-even systems. Time-reversal symmetry greatly simplifies calculations. We are able to relate twelve coefficients in the Skyrme energy density functional to six underlying parameters, allowing us to provide constraints on the parameters of the Skyrme functional. We derive a series of six inequalities relating Skyrme coefficients to each other, and explore the isospin dependence of both the spin-orbit and the effective mass terms. Our predictions are tested against a series of nine commonly used Skyrme parametrisations.

We conclude with a discussion of future directions to take, and in particular of how future theoretical and experimental work could be used to further develop our understanding of nuclear forces.

## Contributions of this Thesis

By systematically applying modern techniques, this thesis aimed to clearly demonstrate the difficulties of relating low energy nuclear phenomenology to higher energy physics.

Chapters 2 and part of Chapter 3 present standard techniques and concepts which can be found in the literature. We present a novel derivation of the effective Lagrangian for a simplified version of the Quark-Meson Coupling (QMC) model (Section 3.5). This is the first time that standard effective field theory techniques have been utilised for this problem.

We have proved that for any scalar field theory, the two-point function in Fourier space can be expanded as

$$G(p) = a + O(p^2) \quad (1.1)$$

where  $a$  is positive (Section 3.6).

A systematic derivation of the non-relativistic limit of all 16 Dirac bilinears is presented in Section 4.3. Though the techniques used are well known, we believe this is the first time that a systematic calculation has been presented.

Chapters 5 and 6 comprise the major contributions of this thesis. In Section 5.3, the low energy limits of various linear meson theories are computed, and these calculations are extended to include meson-meson interactions in Section 5.4. The results are in agreement with previous work, but we believe that our methods are clearer and more concise. In particular, we emphasise that many different models of high energy physics will give the same low energy physics, so that at low energies these models are functionally indistinguishable.

Although various models include tensor couplings of the omega and rho mesons, our discussion in 5.6 is the first we are aware of to suggest a plausible reason that the ratio of the vector to tensor couplings may be relevant in nuclear physics. We also suggest that the experimental values should be used, rather than assuming they are the same as the nucleon magnetic moments.

Chapter 6 relates the Skyrme energy density functional to higher energy physics in a novel way. Using this, we derive a series of new equalities and inequalities relating Skyrme coefficients to each other.

## Notations and Conventions

Unless otherwise stated, in this thesis we shall follow the conventions found in the book of Peskin and Schroeder [21]. In particular, we shall work in natural units with  $\hbar = c = 1$ , and we adopt the mostly-minus convention for the metric tensor:

$$g_{\mu\nu} = \begin{pmatrix} 1 & 0 & 0 & 0 \\ 0 & -1 & 0 & 0 \\ 0 & 0 & -1 & 0 \\ 0 & 0 & 0 & -1 \end{pmatrix}.$$

---

Symbol	Meanings
$\pi$	Mathematical Constant
$\pi, \pi_a$	Pion
$\sigma$	Sigma Meson
$\vec{\sigma}$	Pauli Matrix
$\sigma^{\mu\nu}$	Dirac Bilinears
$\rho$	Nucleon Density
$\rho$	Rho Meson
$\tau$	Kinetic Energy Density
$\tau_a$	Isospin Pauli Matrix
$J$	Source in Lagrangian
$J_{ij}, \vec{J}_v$	Tensor Kinetic Density

**Table 1.1:** Double-dutied notation.

We use Greek letters for space-time indices, Latin letters in the middle of the alphabet for space indices, and Latin letters at the beginning of the alphabet for isospin indices. Hence  $p^\mu$  is a 4-vector,  $\vec{\sigma}$  and  $\sigma^i$  are 3-vectors, and  $\rho_a$  is an isovector scalar. We use Einstein summation notation, so that

$$a^\mu b_\mu = g_{\mu\nu} a^\mu b^\nu = a^0 b^0 - a^1 b^1 - a^2 b^2 - a^3 b^3. \quad (1.2)$$

After taking the non-relativistic limit, space and time are treated asymmetrically, and so we do not need to use covariant notation. We will instead adopt  $a_i = a^{\mu=i}$  to denote the components of the vector  $\vec{a}$ . We will keep all indices lowered, and denote the scalar product as:

$$a_i b_i = \delta_{ij} a_i b_j = a_1 b_1 + a_2 b_2 + a_3 b_3. \quad (1.3)$$

In path integrals, we always assume fields to go to 0 at infinity, allowing integration by parts without worrying about boundary terms. We occasionally abuse the mathematical “=” sign by considering actions to be physically equal if they produce the same action — for example, if two actions are equal up to a boundary term. For Feynman diagrams, we use the convention that time flows upwards, so that the bottom of the page represents the past and the top of the page the future.

There are only so many letters in the Greek and Latin alphabet, and unfortunately what may be standard notation in one field is often at odds with standard notation in another. In *Table 1.1* the most egregious are listed.



---

# A Toy Model

---

In this chapter we shall discuss a toy model which illustrates the techniques which we shall develop in the next few chapters. Imagine there is a single species of spin-1/2 nucleon, described by a Dirac field  $N$ , which interacts with a scalar meson field  $\sigma$ , via the Lagrangian

$$\mathcal{L} = \bar{N}(i\not{\partial} - M)N + \frac{1}{2}(\partial\sigma)^2 - \frac{m^2}{2}\sigma^2 - g\sigma\bar{N}N. \quad (2.1)$$

The term

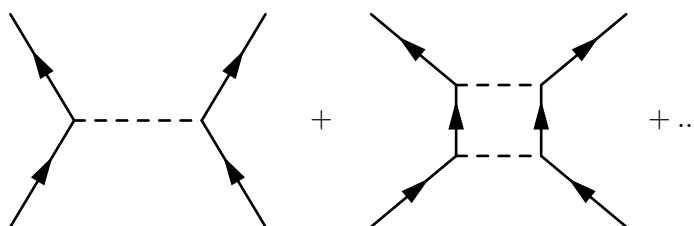
$$\bar{N}(i\not{\partial} - M)N = N^\dagger\gamma^0(i\gamma^\mu\partial_\mu - M)N \quad (2.2)$$

is the Dirac Lagrangian for a free nucleon of mass  $M$ , where  $\gamma^\mu$  are the gamma matrices. Likewise the Klein-Gordon Lagrangian for a free scalar meson of mass  $m$  is  $\frac{1}{2}(\partial\sigma)^2 - \frac{m^2}{2}\sigma^2$ . Finally the  $g\sigma\bar{N}N$  term is an interaction term, with the coupling constant  $g$  governing the strength of the nucleon-sigma interaction.

We will quantise the theory using the Feynman path-integral formulation of quantum mechanics:

$$Z = \int D\sigma D\bar{N}DN e^{i\int dx^4\mathcal{L}[\sigma,N,\bar{N}]}. \quad (2.3)$$

Our theory is non-linear, and cannot be solved exactly for  $g \neq 0$ . Traditionally, calculations would be performed perturbatively, expanding in powers of  $g$ . In this approach the nucleon-nucleon interaction is described diagrammatically as



Here the solid lines represent nucleons, and the dashed lines the mesons. The above diagrams represent nucleons interacting via the exchange of mesons. Using standard Feynman diagram techniques, the first diagram can be evaluated. At low energies it gives a Yukawa potential (see for instance page 122 of [21])

$$V(r) = -\frac{g^2 e^{-mr}}{4\pi r}, \quad (2.4)$$

where  $r$  is the distance between the nucleons. The second diagram gives an  $O(g^4)$  contribution, and if  $g$  is small compared to unity this could be neglected. However, in nuclear physics, we typically have  $g \sim 10$ , and so perturbation theory is not applicable.

We need another small parameter to expand in. In nuclei, the binding energy per nucleon is typically  $\sim 8$  MeV and the nucleon momentum  $\sim 30$  MeV. On the other hand, meson masses (with the exception of the pion) are around 700 MeV or more. In the limit where the meson mass  $m \rightarrow \infty$ , we would expect the mesons to decouple from the nucleons. So we could try expanding in powers of  $m^{-1}$ .

Our theory is Gaussian with respect to  $\sigma$ . Because of this, we can perform the path-integral (2.2) for the  $\sigma$  field. We now define the *effective action*  $\Gamma[N, \bar{N}]$  via the equation

$$e^{i\Gamma[N, \bar{N}]} = \int D\sigma e^{i \int dx^4 \mathcal{L}[\sigma, N, \bar{N}]} \quad (2.5)$$

Using standard path-integral techniques (see for example Section 1.4 of [22]), we can derive the equation

$$\Gamma[N, \bar{N}] = \int dx^4 \bar{N}(i\cancel{\partial} - M)N - \frac{g^2}{2} \int dx^4 dy^4 \bar{N}(x)N(x)D(x-y)\bar{N}(y)N(y) \quad (2.6)$$

where  $D(x-y)$  is the free Feynman propagator for the scalar theory:

$$D(x-y) = \int \frac{dk^4}{(2\pi)^4} \frac{e^{-ik(x-y)}}{k^2 - m^2 + i\varepsilon} \quad (2.7)$$

(Here  $\varepsilon$  is a positive infinitesimal quantity, needed to define the integral as a contour integral.) Now we expand the propagator

$$\begin{aligned} D(x-y) &= \int \frac{dk^4}{(2\pi)^4} \frac{e^{ik(x-y)}}{k^2 - m^2 + i\varepsilon} = -\frac{1}{m^2} \int \frac{dk^4}{(2\pi)^4} \frac{e^{ik(x-y)}}{1 - \frac{k^2}{m^2} + i\varepsilon} \\ &= -\frac{1}{m^2} \int \frac{dk^4}{(2\pi)^4} e^{ik(x-y)} \sum_{n=0}^{\infty} \frac{(k^2)^n}{m^{2n}}. \end{aligned} \quad (2.8)$$

This expansion of the propagator in powers of  $k^2/m^2$  is not rigorous; in particular, we only have convergence if  $k^2/m^2 < 1$ . If, however, the nucleon density  $\bar{N}(x)N(x)$  varies with a characteristic length much larger than  $m$ , then the region where  $k^2 \ll m^2$  will dominate (this can be made rigorous by introducing a cutoff in the integral). With this caveat in mind, we now write

$$D(x-y) = -\frac{1}{m^2} \sum_{n=0}^{\infty} \frac{(-1)^n \partial^{2n} \delta(x-y)}{m^{2n}} = -\frac{\delta(x-y)}{m^2} + \frac{\partial^2 \delta(x-y)}{m^4} + \dots \quad (2.9)$$

and so

$$\begin{aligned} \Gamma[N, \bar{N}] &= \int dx^4 \bar{N}(i\cancel{\partial} - M)N + \frac{g^2}{2m^2} \int dx^4 dy^4 \bar{N}(x)N(x) \sum_{n=0}^{\infty} \frac{(-1)^n \partial^{2n} \delta(x-y)}{m^{2n}} \bar{N}(y)N(y) \\ &= \int dx^4 \left( \bar{N}(i\cancel{\partial} - M)N + \frac{g^2}{2m^2} \sum_{n=0}^{\infty} (-1)^n \frac{\bar{N}N \partial^{2n} \bar{N}N}{m^{2n}} \right) \\ &\approx \int dx^4 \left( \bar{N}(i\cancel{\partial} - M)N + \frac{g^2}{2m^2} (\bar{N}N)^2 - \frac{g^2}{2m^4} \bar{N}N \partial^2 \bar{N}N \right). \end{aligned} \quad (2.10)$$

We will now define the effective Lagrangian,

$$\mathcal{L}_{\text{eff}}[\bar{N}, N] = \bar{N}(i\not{\partial} - M)N + \frac{g^2}{2m^2}(\bar{N}N)^2 - \frac{g^2}{2m^4}\bar{N}N\partial^2\bar{N}N \quad (2.11)$$

to describe the low-energy behaviour of our theory without any reference to the meson fields. The meson field has been “integrated out.”

In traditional approaches to describing atomic nuclei, non-relativistic theories are often used. This can be justified since  $M$  is around 940 MeV, which is much greater than the kinetic energy of nucleons in nuclei. In Chapter 4 we will discuss in detail the procedure to take non-relativistic limits. In this chapter we will simply note the correspondences between relativistic (left) and non-relativistic (right) quantities:

$$\begin{aligned} \bar{N}(i\not{\partial} - M)N &\rightarrow \Psi^\dagger \left( i\frac{\partial}{\partial t} + \frac{\Delta}{2M} \right) \Psi, \\ \bar{N}N &\rightarrow \Psi^\dagger\Psi = \rho, \\ \partial^2 &\rightarrow -\Delta, \end{aligned} \quad (2.12)$$

and defer a proper derivation to Chapter 4. We introduce  $\Psi$  to describe the non-relativistic nucleon field, which has two rather than four components (the other two degrees of freedom in the Dirac spinor correspond to antiparticles, which decouple in the non-relativistic limit). We now take the non-relativistic limit of Lagrangian (2.11):

$$\mathcal{L}_N = \Psi^\dagger \left( i\frac{\partial}{\partial t} + \frac{\Delta}{2M} \right) \Psi + \frac{g^2}{2m^2}\rho^2 + \frac{g^2}{2m^4}\rho\Delta\rho, \quad (2.13)$$

yielding a non-relativistic theory of nucleon interaction. From this, it is easy to derive the energy for the system:

$$E = \int dx^3 \left( -\frac{1}{2M}\Psi^\dagger\Delta\Psi - \frac{g^2}{2m^2}\rho^2 - \frac{g^2}{2m^4}\rho\Delta\rho \right). \quad (2.14)$$

We now see that the  $\sigma$ -meson gives an attractive force. Our toy model is able to explain nuclear binding!

However problems arise when we attempt to calculate the energy of nuclear matter — that is, for the case of constant nucleon density  $\rho$ . For a system of non-interacting fermions, the energy is given by

$$E_0 = \int dx^3 \frac{C}{2M}\rho^{5/3} \quad (2.15)$$

where  $C$  is a constant (see Section 7.3 of [23]). So the energy of nuclear matter in our model is

$$E = E_0 + E_{\text{int}} = \int dx^3 \left( \frac{C}{2M}\rho^{5/3} - \frac{g^2}{2m^2}\rho^2 \right). \quad (2.16)$$

This is not bound, as the energy density becomes infinitely negative as  $\rho \rightarrow \infty$ . If our toy model were correct then all nuclei would collapse. We are clearly missing some important physics.

Through our toy model, we have seen how non-relativistic nuclear forces can arise from a quantum field theory. In doing so we have raised some interesting questions, which will be answered in the following three chapters:

1. *How can we study the low-energy behaviour of theories?*
2. *How can we produce non-relativistic theories from relativistic ones?*
3. *Can we use these tools to provide realistic descriptions of nuclear forces?*

---

# Effective Field Theory

---

## 3.1 Overview

The purpose of effective field theory is to describe physics at low energies in a simple way. If we have two vastly different energy scales,  $E_l \ll E_h$ , then we can use effective field theory to analyse the system in powers of  $E_l/E_h$ . Choosing the correct degrees of freedom, we may be able to produce a simple and universal description of the low-energy physics.

We used effective field theory techniques last chapter to remove the  $\sigma$  meson. Our model possessed two energy scales: the nucleon kinetic energy which is around  $\sim 30$  MeV and the meson mass  $m$  around  $\sim 700$  MeV. This led us to ‘integrate out’ the  $\sigma$  meson from the path integral. The result was a theory of interacting nucleons, and we discovered that the most important dynamic quantities were the  $\rho^2$  and  $\rho\Delta\rho$  terms. All other couplings were suppressed by higher powers of  $m$ .

We also used effective field theory in a second, more subtle way. Nucleons and mesons are composite particles made of quarks and mesons. Yet when we decided to write a toy model for nuclear forces, we only considered nucleon and meson fields. This is because in QCD quarks and gluons only become relevant at energy scales around a few GeV. Since we are only interested in energies considerably below this, we can use our low energy effective field theory of nucleons and mesons — blissfully unaware of the complexity of QCD. Conversely it is difficult to study QCD by studying nuclei: the details of QCD are largely irrelevant in the context of nuclear physics. Whilst in principle we should be able to derive our nucleon and meson model from QCD, QCD has so far proved impossible to solve for large systems such as nuclei.

These two examples illustrate the two primary motivations for effective field theory. We use it when it simplifies calculations, and we use it out of necessity. This might seem quite straightforward, but nevertheless the philosophy of effective field theory revolutionised modern physics.

When quantum field theory was first developed, it was believed to be a fundamental theory. As a consequence, the infinities which plagued early calculations were disturbing to physicists (see Chapter 1 of [24]). The development of renormalisation allowed calculations to be made in a small class of theories, known as ‘renormalisable’ theories. The mathematics behind proving these theories to be renormalisable is quite formidable [25]. Yet in practice the condition required for renormalisability is quite simple: the units of the coupling constant must be non-negative. Explaining what exactly this means requires a quick overview of dimensional analysis.

We work with natural units where  $\hbar = c = 1$ . In this system we find that

$$[M] = [\text{energy}] = [\text{mass}] = [\text{length}]^{-1} = [\text{time}]^{-1},$$

and in nuclear and particle physics the convention is to measure everything in terms of the electron-Volt. Since the action (which has the same unit as  $\hbar$ ) is unitless:

$$S = \int dx^4 \mathcal{L} \implies [\mathcal{L}] = [M]^4, \quad (3.1)$$

so that the Lagrangian has mass dimension 4. We can then determine that a scalar field  $\phi$  has units  $[M]$  — as does the derivative operator  $\partial$  — and a spinor field, such as the nucleon field, has units  $[M]^{3/2}$ . More generally, the coefficient  $c_k$  in the Lagrangian  $c_k \phi^k$  will have dimension  $[M]^{4-k}$ . Because of this, the most general renormalisable Lagrangian we can have for a scalar field is

$$\mathcal{L} = \frac{1}{2}(\partial\phi)^2 - \frac{1}{2}m^2\phi^2 + \frac{\mu}{3!}\phi^3 + \frac{\lambda}{4!}\phi^4. \quad (3.2)$$

A term such as  $\phi^5$  or  $(\partial\phi)^4$  would have a negative dimension coupling constant, and the resulting theory would therefore not be renormalisable.

The Standard Model is renormalisable, as are both quantum electrodynamics and quantum chromodynamics. However, many historically important theories were not renormalisable and this stalled progress for decades. Most famously, the Fermi theory for weak interactions involves 4-fermion interaction terms like  $c\bar{\psi}\psi\bar{\psi}\psi$ , but the dimensions of  $c$  are  $[M]^{-2}$  and so the theory is not renormalisable.

A proper understanding of renormalisation would originate not in particle physics but in condensed matter physics. In this field, we are interested in describing systems such as metals. Microscopically we know these are comprised of ions and electrons interacting according to well-understood laws — the difficulty is in describing macroscopic behaviour such as superconductivity. This was achieved by developing quantum field theories for the macroscopically interesting variables, whilst ignoring the irrelevant microscopic interactions. Like their particle physics brethren, these theories had infinities. But for condensed matter physicists, this was not a problem. They knew that their field theories would break down at high energies: at these energies the detailed physics of ions and electrons becomes important. The divergences were caused by extrapolating field theories to inappropriately high energies.

Furthermore, condensed matter physics shed light on the importance of renormalisable theories in particle physics. In condensed matter, we typically have a characteristic length scale  $l = 10^{-9}$  m due to the separation of atoms in the ionic lattice. Say we have a certain term in our Lagrangian,  $aT_1$ , and we know by dimensional analysis that  $a$  has units m. We would then expect that  $a$  should be of order  $l$ , since the relevant physics is the atomic physics. So if we are interested in macroscopic properties, say around  $L = 1$  m, then in most situations we can set  $a$  to zero since its effect should be negligible. The renormalisation group provides a more rigorous foundation for this idea [26].

These ideas would eventually propagate to particle physics. It was realised that all quantum field theories should come with a high energy cut-off,  $\Lambda$ . Every term allowed by symmetries must be included in the Lagrangian. Terms which have negative energy units are however suppressed by powers of  $\Lambda^{-1}$ , as we would naively expect by unit analysis. If  $\Lambda$  is much greater than the energy of the physics we are probing, our theory will ap-

pear renormalisable. This is the reason why many of our theories in particle physics are renormalisable — the energy scales for which a given theory is valid is often separated from higher energy physics by many orders of magnitude. The Standard Model of particle physics [27] is now seen as merely an effective field theory which will eventually break down, and the same is thought of general relativity [28] (a theory which is infamously non-renormalisable). The discovery of neutrino masses has provided confirmation of this viewpoint, requiring a non-renormalisable extension to the Standard Model at energies around  $10^{14}$  GeV [29].

The philosophy of effective field theory had a significant impact on nuclear models. Meson models were originally required to be renormalisable. These models were often simplified further by ignoring even renormalisable physics such as meson-meson interactions.

The introduction of effective field theory techniques by Weinberg [30] revolutionised the approach physicists used to understand the nuclear forces. It was realised that to properly understand these forces, the Lagrangians used should be as general as possible to capture all physics. In particular, non-renormalisable physics will be needed. The rest of this chapter will develop further the tools of effective field theory.

### 3.2 Formalism

Say we have two fields, a light field  $\phi$  and a heavy field  $\Phi$ , with their interactions governed by an action  $S[\phi, \Phi]$ . We will quantise this theory using path integrals:

$$Z = \int D\phi D\Phi e^{iS[\phi, \Phi]}. \quad (3.3)$$

We now define the effective action for the light field by

$$e^{i\Gamma[\phi]} = \int D\Phi e^{iS[\phi, \Phi]}. \quad (3.4)$$

Our path integral becomes

$$Z = \int D\phi e^{i\Gamma[\phi]}, \quad (3.5)$$

and from this we can see the rationale behind the effective action. It is the action for  $\phi$  after we have removed  $\Phi$ . All of this so far has been a matter of book-keeping: in general  $\Gamma$  will be non-local and will contain the full information of the original theory.

The utility of the EFT method is in the approximations we can make to  $\Gamma$ . Given a  $\Phi$  with mass  $\Lambda$ , we may expand  $\Gamma$  as a power series

$$\Gamma[\phi] = \int dx^4 \mathcal{L}_{\text{eff}}[\phi] = \int dx^4 \left( \mathcal{L}_0[\phi] + \frac{1}{\Lambda} \mathcal{L}_1[\phi] + \frac{1}{\Lambda^2} \mathcal{L}_2[\phi] \dots \right). \quad (3.6)$$

If we can evaluate the various terms in the expression, then for practical calculations at energies far below  $\Lambda$ , we can truncate  $\mathcal{L}_{\text{eff}}$  to the desired accuracy in  $O(\Lambda^{-n})$ . This procedure generalises the one followed in the previous chapter.

We have yet to justify that an expansion like that in (3.6) exists. In quantum field theory, the rigorous formulation of this is known as the Appelquist-Carazzone theorem [31]. Essentially it proves that as  $\Lambda \rightarrow \infty$ , the  $\Phi$  field should decouple completely from the  $\phi$  field. The only influence of the  $\Phi$  field will be through renormalisations which are

not observable at low energies. For completeness, we note that in certain situations the theorem fails (in particular for spontaneous symmetry breaking and for chiral fermions), but these will not be relevant for this thesis (a detailed discussion of these cases can be found in [27]).

Now we turn to the difficulties of calculating the effective action using (3.4). In field theories, we usually demand that the action comes from a local Lagrangian, so we write

$$S[\phi, \Phi] = \int dx^4 \mathcal{L}[\phi, \Phi] = \int dx^4 (\mathcal{L}_l[\phi] + \mathcal{L}_h[\Phi] + \mathcal{L}_I[\phi, \Phi]). \quad (3.7)$$

Here we have separated out the interactions between the light and heavy fields from the rest of the Lagrangian. Plugging the above formula into (3.4), we can now write

$$e^{i\Gamma[\phi]} = \int D\Phi e^{iS[\phi, \Phi]} = e^{i \int dx^4 \mathcal{L}_l[\phi]} \int D\Phi e^{i \int dx^4 (\mathcal{L}_h[\Phi] + \mathcal{L}_I[\phi, \Phi])}. \quad (3.8)$$

Furthermore we can expand the interaction Lagrangian

$$\mathcal{L}_I[\phi, \Phi] = \sum_k f_k[\phi] \mathcal{L}_k[\Phi] = \sum_k J_k(x) \mathcal{L}_k[\Phi], \quad (3.9)$$

where we have defined the operators  $J_k(x) = f_k[\phi(x)]$ . We are then able to write

$$e^{i\Gamma[\phi]} = e^{i \int dx^4 \mathcal{L}_l[\phi]} \int D\Phi e^{i \int dx^4 (\mathcal{L}_h[\Phi] + \sum_k J_k(x) \mathcal{L}_k[\Phi])}. \quad (3.10)$$

This means that if we can perform the path integral for general sources  $J_k(x)$  first, we can then afterwards substitute  $J_k(x) = f_k[\phi]$  to find the effective action in terms of  $\phi$ .

Whilst this book-keeping simplifies our calculations, we still need to evaluate the path integral. In general path integrals do not admit simple solutions, and so we must use approximation techniques. A few methods exist for performing calculations. The first method is to utilise Feynman diagrams:  $\Gamma$  is the sum of closed connected diagrams. Another method is the saddle point technique, where we expand around the classical value of  $\Phi$ . This gives a semiclassical expansion of the effective action. Finally, we could use numerical techniques such as a lattice to evaluate the integral in 3.10.

There is however one situation where we can evaluate the path integral exactly: the case where  $\mathcal{L}[\Phi]$  is quadratic in  $\Phi$ . This is precisely the situation we had in the previous chapter, which was why we were able to so easily calculate the effective action. We will begin with this case, and then afterwards describe both the semiclassical expansion and the Feynman diagram approach.

### 3.3 Gaussian Path Integrals

We will return to the Lagrangian from the previous chapter, Eq. (2.1):

$$\mathcal{L} = \bar{N}(i\partial - M)N + \frac{1}{2}(\partial\sigma)^2 - \frac{m^2}{2}\sigma^2 - g\sigma\bar{N}N. \quad (3.11)$$

Using (3.7), we can split the Lagrangian into three parts

$$\begin{aligned}\mathcal{L}_l &= \bar{N}(i\cancel{\partial} - M)N, \\ \mathcal{L}_h &= \frac{1}{2}(\partial\sigma)^2 - \frac{m^2}{2}\sigma^2, \\ \mathcal{L}_I &= -g\sigma\bar{N}N.\end{aligned}\tag{3.12}$$

The idea is to treat the nucleon field ( $N$ ) as the ‘light’ field, and the  $\sigma$  as the ‘heavy’ field. This can be justified, because, in nuclei nucleons are essentially non-relativistic with kinetic energies much lower than the mass of the  $\sigma$ . Now define the source  $J(x) = -g\bar{N}(x)N(x)$ , and use (3.10) to calculate the effective action:

$$e^{i\Gamma[N,\bar{N}]} = e^{i\int dx^4 \bar{N}(i\cancel{\partial} - M)N} \int D\sigma e^{i\int dx^4 (\frac{1}{2}(\partial\sigma)^2 - \frac{1}{2}m^2\sigma^2 + J\sigma)}.\tag{3.13}$$

To evaluate this expression we simply need to calculate the path integral

$$W[J] = -i \log \left( \int D\sigma e^{i\int dx^4 (\frac{1}{2}(\partial\sigma)^2 - \frac{1}{2}m^2\sigma^2 + J\sigma)} \right).\tag{3.14}$$

This is a slight generalisation of the path integral (2.5), and it can be evaluated using the same methods as in Chapter 2. Using the scalar field propagator (2.7), we find in general that

$$W[J] = W[0] - \frac{1}{2} \int dx^4 dy^4 J(x)D(x-y)J(y).\tag{3.15}$$

Here  $W[0]$  is an (infinite) constant independent of  $J$  and so we will ignore it. All of the interesting physics is in the second term of the right-hand side, which is non-local.

We can now use the low energy expansion of the propagator (2.9) derived in the previous chapter:

$$D(x-y) = -\frac{\delta(x-y)}{m^2} + \frac{\partial^2\delta(x-y)}{m^4} + \dots\tag{3.16}$$

This gives us a local expansion of  $W[J]$  which is valid for large  $m^2$ . Notice in particular that as  $m^2 \rightarrow \infty$ ,  $W[J] \rightarrow 0$ , just as predicted by the decoupling theorem. Notice also that our expansion is a power series both in  $m^{-2}$  and in  $\partial^2$ . This can be verified by unit analysis. To  $O(m^{-4})$  we have

$$W[J] \approx \int dx^4 \frac{1}{2m^2} J(x)^2 - \frac{1}{2m^4} J(x)\partial^2 J(x).\tag{3.17}$$

By substituting  $J = -g\bar{N}N$  we can now derive the effective Lagrangian from the previous chapter.

However, our above expression remains valid for more general source  $J(x)$ , allowing us to generalise our model with ease. For instance, say we added to our Lagrangian a non-renormalisable term such as

$$\frac{\alpha}{\Lambda} \partial_\mu (\bar{N} \gamma^\mu N),$$

where  $\alpha$  is unitless. The term is manifestly non-renormalisable as it requires an inverse power of a cutoff  $\Lambda$ . We can quickly calculate the effective Lagrangian for the nucleons by

making the substitution

$$J(x) = -g\bar{N}(x)N(x) + \frac{\alpha}{\Lambda}\partial_\mu(\bar{N}(x)\gamma^\mu N(x)) \quad (3.18)$$

into  $W[J]$  in (3.17). With minimal effort we now find that

$$\Gamma[N, \bar{N}] = \int dx^4 \left( \bar{N}(i\not{\partial} - M)N + \frac{1}{2m^2} \left( g\bar{N}N - \frac{\alpha}{\Lambda}\partial_\mu(\bar{N}\gamma^\mu N) \right)^2 + O(m^{-4}) \right). \quad (3.19)$$

So far we have only discussed scalar mesons, but vector mesons such as the  $\omega$  and  $\rho$  are crucial for understanding nuclear forces. These mesons are governed by the Lagrangian

$$\mathcal{L} = -\frac{1}{4}(\partial^\mu A^\nu - \partial^\nu A^\mu)(\partial_\mu A_\nu - \partial_\nu A_\mu) + \frac{m^2}{2}A^\mu A_\mu + J^\mu A_\mu, \quad (3.20)$$

where  $A_\mu$  is a vector field of mass  $m$ . This again gives a Gaussian integral. To integrate out the vector bosons we can use the identity (for more details see Section 1.6 of [22])

$$\begin{aligned} W[J] &= -i \log \left( \int DA e^{i \int dx^4 \left( -\frac{1}{4}(\partial^\mu A^\nu - \partial^\nu A^\mu)(\partial_\mu A_\nu - \partial_\nu A_\mu) + \frac{m^2}{2}A^\mu A_\mu + J^\mu A_\mu \right)} \right) \\ &= W[0] - \frac{1}{2} \int dx^4 dy^4 J^\mu(x) D_{\mu\nu}(x-y) J^\nu(y). \end{aligned} \quad (3.21)$$

Again we can ignore  $W[0]$ . Here  $D_{\mu\nu}(x-y)$  is the propagator for a vector meson:

$$D_{\mu\nu}(x-y) = \int \frac{d^4k}{(2\pi)^4} e^{ik(x-y)} \frac{-g_{\mu\nu} + k_\mu k_\nu / m^2}{k^2 - m^2 + i\varepsilon}. \quad (3.22)$$

We can expand this in powers of  $m^{-1}$  just as we expanded the scalar propagator. We then find that

$$\begin{aligned} W[J] &= -\frac{1}{2} \int dx^4 dy^4 J^\mu(x) D_{\mu\nu}(x-y) J^\nu(y) \\ &= -\frac{1}{2} \int dx^4 \left( \frac{J^2}{m^2} + \sum_{n=1}^{\infty} \frac{(-1)^n}{m^{2n+2}} (J^\mu \partial^{2n} J_\mu - J^\mu \partial^{2n-2} \partial_\mu \partial_\nu J^\nu) \right) \\ &\approx \int dx^4 \left( -\frac{1}{2m^2} J(x)^2 + \frac{1}{2m^4} J^\mu \partial^2 J_\mu - \frac{1}{2m^4} J^\mu \partial_\mu \partial_\nu J^\nu \right). \end{aligned} \quad (3.23)$$

By using (3.17) and (3.23) we are able to integrate out any linear scalar or vector field from a theory. To order  $O(m^{-2})$  the scalar and vector expressions are identical up to a sign difference. As a result of this simple sign difference, we find that scalar mesons create attractive forces (as we saw in the previous chapter), whereas vector mesons generate repulsive forces between like particles. This general behaviour holds even in the massless limit, and the photon, a vector meson, induces a repulsion between like charged particles.

### 3.4 The Semiclassical Expansion

Now we will extend our results to non-linear theories, i.e., those with terms  $\sigma^n$  for  $n > 2$ . For instance, take the Lagrangian

$$\mathcal{L} = \frac{1}{2}(\partial\sigma)^2 - \frac{1}{2}m^2\sigma^2 - \frac{\mu}{3!}\sigma^3 - \frac{\lambda}{4!}\sigma^4 + J\sigma.$$

which contains both  $3\sigma$  and  $4\sigma$  vertices with coupling constants  $\mu$  and  $\lambda$  respectively. In general these interactions must be present. Even if we were to set  $\mu$  or  $\lambda$  to zero in the Lagrangian, we find that renormalisation requires including these terms [32]. These terms are important in many nuclear models, such as quantum hadrodynamics, where they are needed to accurately reproduce nuclear properties [33].

As shown in section 3.2, in order to derive an effective field theory we need to evaluate the path integral:

$$iW[J] = \log \left( \int D\sigma e^{i \int dx^4 \mathcal{L}[\sigma, J]} \right). \quad (3.24)$$

This is unfortunately impossible when the path integral is not a Gaussian. There are two main approaches we can use to systematically expand the integral, allowing us to derive effective field theories despite these difficulties. In this section we shall describe the semiclassical expansion, which we will then apply in the next section to a generalisation of the toy model in Chapter 2. The other expansion, using Feynman diagrams, will be discussed at the end of the chapter.

The semiclassical path integral expansion generalises and unifies a host of different techniques used in various fields of physics. In the context of nuclear physics, both relativistic mean-field theory and non-relativistic Hartree-Fock approaches can be understood as truncations of the semiclassical expansion. Moving further afield, these methods are heavily utilised in the study of spontaneous symmetry breaking [34], and also in the study of instantons [35].

The idea is simple: given a field theory

$$Z[J] = e^{iW[J]} = \int D\Phi e^{i \int dx^4 \mathcal{L}[\Phi, J]} = \int D\Phi e^{iS[\Phi, J]} \quad (3.25)$$

we would expect the most important contributions to the path integral to come from around the saddle point

$$\frac{\delta S[\Phi, J]}{\delta \Phi(x)} = 0. \quad (3.26)$$

The above equation is the Euler-Lagrange equation, which is solved by classical fields. Denoting the classical solution to the equation by  $\chi$ , we can approximate

$$Z[J] = \int D\Phi e^{iS[\Phi, J]} \sim e^{iS[\chi, J]}. \quad (3.27)$$

This is mean-field theory, and is particularly convenient to apply when  $\chi$  is easy to compute. For this reason it is mainly applied to the case where  $J(x) = J_0$  is constant, such as the case of infinite nuclear matter [33].

So how do we turn this into a systematic expansion? We can change variables in the path integral, defining  $\eta = \Phi - \chi$ , and then expand

$$\begin{aligned} Z[J] &= \int D\eta e^{iS[\chi+\eta, J]} \\ &= \int D\eta \exp \left[ iS[\chi, J] + \frac{i}{2} \int dx^4 dy^4 \eta(x) \eta(y) \left. \frac{\delta^2 S}{\delta \Phi(x) \delta \Phi(y)} \right|_{\Phi=\chi} + \dots \right]. \end{aligned} \quad (3.28)$$

The first order correction is zero by (3.26), and so the leading order correction is quadratic in  $\eta$ . This correction can be calculated as a functional determinant, which is the functional

generalisation of a matrix determinant (see page 287 of [21]). We then have the following expression for  $W[J]$ :

$$W[J] = \int dx^4 (\mathcal{L}[\chi, J]) - \frac{i}{2} \log \det \left[ -\frac{\delta^2 \mathcal{L}}{\delta \Phi(x) \delta \Phi(y)} \Big|_{\Phi=\chi} \right] + \dots \quad (3.29)$$

In general functional determinants are extremely difficult to compute. In fact, they can only be computed exactly for very special forms of  $J(x)$  [36]. If  $J(x)$  is small respect to  $m^2$ , a perturbative expansion exists in terms of the series of diagrams:

$$\log \det[\partial^2 + m^2 + J(x)] = \text{Diagram 1} + \text{Diagram 2} + \text{Diagram 3} + \text{Diagram 4} + \text{Diagram 5} + \dots \quad (3.30)$$

These diagrams are to be evaluated using the standard Feynman rules in position space, with each line representing a propagator  $D(x - y)$ , and each vertex a  $J(z)$  (more details can be found on page 304 of [21]). The  $n^{\text{th}}$  diagram in this sequence can be evaluated as

$$\frac{1}{n} \int J(x_1) D(x_1 - x_2) J(x_2) D(x_2 - x_3) \dots J(x_n) D(x_n - x_1), \quad (3.31)$$

where we integrate over each  $x_k$ .

So far we have shown how to calculate the classical limit and the first order quantum corrections. If we continue to Taylor expand the action, we will find

$$\begin{aligned} S[\chi + \eta] = & S[\chi] + \frac{1}{2} \int dx^4 dy^4 \eta(x) \eta(y) \frac{\delta^2 S}{\delta \Phi(x) \delta \Phi(y)} \Big|_{\Phi=\chi} \\ & + \frac{1}{6} \int dx^4 dy^4 dz^4 \eta(x) \eta(y) \eta(z) \frac{\delta^3 S}{\delta \Phi(x) \delta \Phi(y) \delta \Phi(z)} \Big|_{\Phi=\chi} + \dots \end{aligned} \quad (3.32)$$

The  $\eta^3$  and higher order terms can be included using standard Feynman diagram techniques, giving three-point and higher order vertices. A detailed discussion can be found in Chapter 5 of [37]; we merely note that calculations beyond leading order are quite difficult and rarely necessary.

### 3.5 Density Dependence in the Quark-Meson Coupling Model

We will now use the tools of the previous section to analyze another toy model. Let us take the Lagrangian

$$\mathcal{L}_\sigma = \frac{1}{2} (\partial\sigma)^2 - \frac{m^2}{2} \sigma^2 + g\sigma \bar{N}N - \frac{\lambda}{2M} \sigma^2 \bar{N}N. \quad (3.33)$$

This is the sigma sector of the Lagrangian in the simplest version of the quark-meson coupling (QMC) model [38]. The  $\lambda$ -term is a non-renormalisable term. In the QMC model it originates in structural changes in the nucleon due to the  $\sigma$  field, analogous to the polarisation of an atom in an electric field [39].

The QMC model has been used to derive density dependent energy density functionals [40, 41]. In particular nuclear saturation was demonstrated to occur in the model. We will present a novel derivation of these results, utilising the semiclassical expansion. The

advantage of our method is that it is more general and can be more clearly related to standard techniques in particles physics. Our derivation is novel, though it is heavily influenced by the computations used to study spontaneous symmetry breaking (a typical example of such a calculation is given in Chapter 11 of [21]).

We begin by introducing the two observables

$$J(x) = g\bar{N}(x)N(x), \quad K(x) = -\frac{\lambda}{M}\bar{N}(x)N(x), \quad (3.34)$$

so that we may simply write

$$\mathcal{L}_\sigma = \frac{1}{2}(\partial\sigma)^2 - \frac{m^2}{2}\sigma^2 + J\sigma + \frac{1}{2}K\sigma^2. \quad (3.35)$$

In order to remove the  $\sigma$  from our theory, we will need to perform the path integral

$$W[J, K] = -i \log \left( \int D\sigma e^{i \int dx^4 \left( \frac{1}{2}(\partial\sigma)^2 - \frac{1}{2}m^2\sigma^2 + J\sigma + \frac{1}{2}K\sigma^2 \right)} \right). \quad (3.36)$$

This we shall achieve via the semiclassical expansion. First we need to find that classical solution to the equation

$$\left. \frac{\delta S}{\delta\sigma(x)} \right|_{\sigma=\chi} = 0. \quad (3.37)$$

This gives the classical equation of motion

$$\partial^2\chi + m^2\chi = J + K\chi \quad (3.38)$$

where  $\chi$  denotes the classical solution to the equation. Once we calculate  $\chi$ , we can then use (3.32) to expand the action

$$S[\chi + \eta] = S[\chi] + \frac{1}{2} \int dx^4 dy^4 \eta(x)\eta(y) \left. \frac{\delta^2 S}{\delta\sigma(x)\delta\sigma(y)} \right|_{\sigma=\chi} + \dots \quad (3.39)$$

Because  $\mathcal{L}$  is quadratic in  $\sigma$ , we find that in general

$$\begin{aligned} \frac{\delta^2 S}{\delta\sigma(x)\delta\sigma(y)} &= -\partial^2\delta(x-y) - \delta(x-y)(m^2 - K(x)) = (-\partial^2 - m^2 + K(x))\delta(x-y) \\ \frac{\delta^n S}{\delta\sigma^n} &= 0 \text{ for } n > 2. \end{aligned} \quad (3.40)$$

Substituting this into (3.29), we can find an exact expression for  $W$  :

$$W[J, K] = \int dx^4 \left( \mathcal{L}[\chi] - \frac{i}{2} \log \det [\partial^2 + m^2 - K(x)] \right). \quad (3.41)$$

Notice that the second term does not depend on  $\chi$ .

We are interested in calculating  $W$  in the case where  $m$  is much larger than the typical variation in  $J$  and  $K$ . Rather than calculating an expansion in powers of  $m^{-1}$ , we shall instead expand in the number of derivatives of  $J$  and  $K$ . This is strictly better, as by dimensional analysis we see that any derivative must have a coefficient of  $m^{-1}$ . Furthermore it allows us to calculate infinite uniform nuclear matter properties to high

densities.

First we shall calculate  $\chi$ . To do this, introduce a constant  $a$  into the equation of motion

$$a\partial^2\chi + m^2\chi = J + K\chi. \quad (3.42)$$

Taking a power series expansion of  $\chi$ ,

$$\chi = \chi_0 + a\chi_1 + a^2\chi_2 + \dots, \quad (3.43)$$

it is straightforward to show that

$$\begin{aligned} \chi_0 &= \frac{J}{m^2 - K} \\ \chi_{k+1} &= \frac{-\partial^2\chi_k}{m^2 - K}. \end{aligned} \quad (3.44)$$

Therefore an expansion in  $a$  is equivalent to an expansion in derivatives of  $J$  and  $K$ . Substituting our series expression (3.44) for  $\chi$  into (3.35) and setting  $a = 1$ , we find that including up to second order derivative terms,

$$\begin{aligned} \mathcal{L}_\sigma[\chi] &\approx \mathcal{L}_\sigma[\chi_0 + \chi_1] \approx \frac{1}{2}(K - m^2)\chi_0^2 + J\chi_0 - \frac{1}{2}\chi_0\partial^2\chi_0 + (K - m^2)\chi_0\chi_1 + J\chi_1 \\ &= \frac{1}{2}\chi_0^2(m^2 - K) + \frac{1}{2}\chi_0\chi_1(m^2 - K) \\ &= \frac{J^2}{2(m^2 - K)} - \frac{J\partial^2 J}{2(m^2 - K)^2} - \frac{J^2\partial^2 K + 2J(\partial^\mu J)(\partial_\mu K)}{2(m^2 - K)^3} - \frac{2(\partial K)^2 J^2}{(m^2 - K)^4}. \end{aligned} \quad (3.45)$$

Substituting  $J$  and  $K$  using (3.34), we are to find an effective Lagrangian for the nucleon fields. In particular, the contribution of the first term in (3.50) to the effective action is

$$\int dx^4 \frac{J(x)^2}{2(m^2 - K(x))} = \int dx^4 \frac{g^2 (\overline{N}N)^2}{2(m^2 + \frac{\lambda}{M}\overline{N}N)}. \quad (3.46)$$

For infinite nuclear matter, this is the only contribution term. Following the procedure used in Chapter 2, we find that in the non-relativistic limit,

$$\int dx^4 \frac{g^2 (\overline{N}N)^2}{2(m^2 + \frac{\lambda}{M}\overline{N}N)} \rightarrow \int dx^4 \frac{g^2 \rho^2}{2(m^2 + \frac{\lambda}{M}\rho)}. \quad (3.47)$$

We can now calculate the energy density for infinite nuclear matter:

$$E = E_0 + E_{\text{int}} = \int dx^3 \left( \frac{C}{2M}\rho^{5/3} - \frac{g^2 \rho^2}{2(m^2 + \frac{\lambda}{M}\rho)} \right). \quad (3.48)$$

When  $\lambda = 0$  this reproduces (2.16), as we would expect. Unlike the model in Chapter 2 though, our current model provides a mechanism for nuclear saturation. For large  $\rho$  the second term is of order  $\rho$ , not  $\rho^2$  as in Chapter 2. Since the Fermi energy is  $\rho^{5/3}$ , at a sufficiently high density it will overcome the attraction and stabilise nuclear matter. In *Figure 3.1*, the energy density of nuclear matter is plotted as the ‘‘classical line’’, demonstrating nuclear saturation.

Our calculation is so far only a mean-field result. We know however that there will be quantum corrections to these results. They are difficult to calculate, and so we relegate

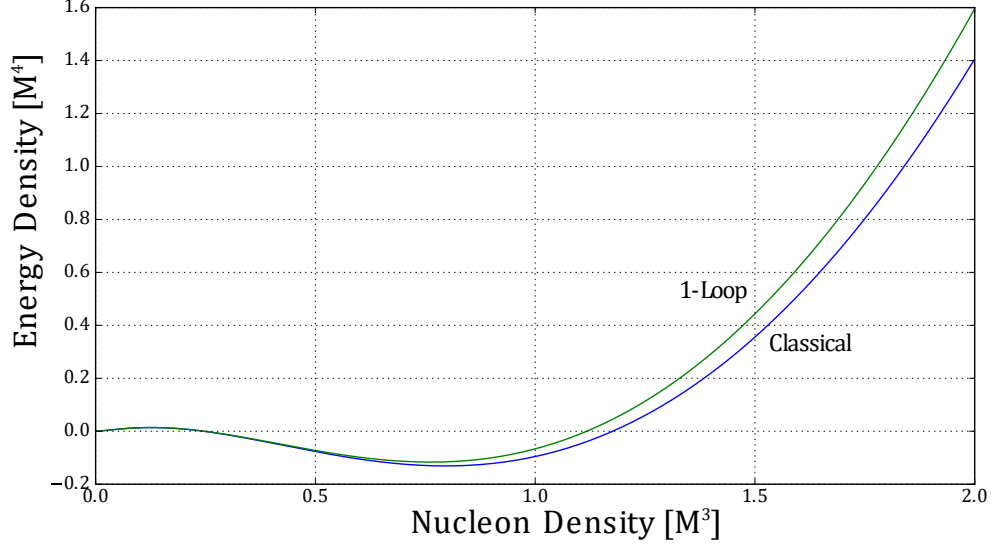


**Figure 3.1:** Energy density of infinite nuclear matter in the QMC model, for  $g = 2.8$ ,  $m = 700$  MeV and  $\lambda = 1$ . The nucleon density is in units of  $M^3$ , and the energy density  $M^4$ .

these calculations to Appendix B. In this appendix, we show that the one-loop corrections are

$$\begin{aligned} & \frac{i}{2} \log \det(\partial^2 + m^2 - K(x)) \\ &= \int dx^4 \frac{m^4}{8(2\pi)^2} \left( \frac{2K}{m^2} - \frac{3K^2}{m^4} + 2 \left( 1 - \frac{K}{m^2} \right)^2 \log \left( 1 - \frac{K}{m^2} \right) \right) + O(\partial^2) \end{aligned} \quad (3.49)$$

We can now combine all of the terms into one expansion

$$\begin{aligned} W[J, K] = \int dx^4 \left[ \frac{J^2}{2(m^2 - K)} - \frac{J\partial^2 J}{2(m^2 - K)^2} - \frac{J^2\partial^2 K + 2J\partial^\mu J\partial_\mu K}{2(m^2 - K)^3} - \frac{2(\partial K)^2 J^2}{(m^2 - K)^4} \right. \\ \left. - \frac{m^4}{8(2\pi)^2} \left( \frac{2K}{m^2} - \frac{3K^2}{m^4} + 2 \left( 1 - \frac{K}{m^2} \right)^2 \log \left( 1 - \frac{K}{m^2} \right) \right) + O(\partial^2) \right]. \end{aligned} \quad (3.50)$$

In *Figure 1*, we have also plotted the 1-loop corrections to the energy density. For infinite nuclear matter, the  $O(\partial^2)$  do not contribute. We see that the 1-loop result decreases the binding of nuclear matter, but that this effect is small at low nucleon density.

### 3.6 Feynman Diagrams for Effective Field Theories

In the previous two sections we saw that the semi-classical expansion provides a general non-perturbative framework in which calculations can be performed. Perturbation theory, utilising Feynman diagrams, provides a complimentary approach. Essentially we can think of the Feynman diagram method as the semi-classical method, but expanding around the solution  $\Phi = 0$  rather than  $\Phi = \Phi_{classical}$ . Conversely, the semi-classical expansion can be derived from Feynman diagrams by summing according to the number of loops in the

diagram. Diagrams without internal loops (‘tree’ diagrams) yield the classical result, and each internal loop adds a power of  $\hbar$ .

To illustrate the use of Feynman diagrams, take the Lagrangian

$$\mathcal{L} = \frac{1}{2}(\partial\Phi)^2 - \frac{1}{2}m^2\Phi^2 - \frac{\lambda}{4!}\Phi^4 + J\Phi, \quad (3.51)$$

where we have introduced a non-linear  $\lambda\Phi^4$  coupling. This Lagrangian is rather imaginatively known as “phi-4” theory in the literature. Note that this theory has a  $\mathbb{Z}_2$  symmetry given by the map  $\Phi \rightarrow -\Phi$ ,  $J \rightarrow -J$ .

Using Feynman diagrams, we can expand the effective action

$$i\Gamma[J] = \log \left( \int D\Phi e^{i \int dx^4 \mathcal{L}[\Phi, J]} \right) \quad (3.52)$$

in powers of  $\lambda$ . This is quite useful when  $\lambda$  is small, since the series will converge rapidly and so few terms will be needed. For our theory the Feynman rules are:

$$\begin{aligned} \text{---} &= iD(x-y) \\ \bullet\text{---} &= (-i) \int dx^4 J(x) \\ \times &= (-i)\lambda \int dx^4. \end{aligned} \quad (3.53)$$

The effective action is then given by

$$\begin{aligned} i\Gamma[J] &= \text{sum of connected, legless diagrams} \\ &= \bullet\text{---}\bullet + \text{---}\text{---} + \bullet\text{---}\bullet + \times + \dots \end{aligned}$$

Furthermore, we only care about terms in  $\Gamma[J]$  which depend on  $J$ . We can hence ignore any diagrams which have no  $J$  dependence, such as the second diagram above.

We are particularly interested in the low-energy form of  $\Gamma[J]$ . For some diagrams, such as tree-level diagrams, this is easy to calculate using the low-energy expansion of the propagator (2.9). For instance

$$\times = \frac{i\lambda}{24} \int dx^4 \left( \frac{1}{m^8} J(x)^4 - \frac{4}{m^{10}} J(x)^3 \partial^2 J(x) + \dots \right). \quad (3.54)$$

Unfortunately, it is much more difficult to evaluate loop diagrams. In the perturbative regime this is not a problem, since tree-level diagrams will give the most important contributions. However meson interactions are usually large and perturbation theory is not applicable.

Even with this limitation, Feynman diagrams provide a useful tool for analysing theories. They demonstrate that terms of the form  $J^{2n}$  will be generically included in our low energy effective field theory. Although in the non-perturbative case we cannot calculate the coefficient very easily, we can use unit analysis to estimate the size of the term. For

instance the general contributions to the effective Lagrangian must be of the form

$$\propto \frac{c_{n,k} J^n \partial^{2k} J}{m^{3n+2k-1}}$$

where  $c$  is unitless. Higher powers of  $J$  and derivative terms are both suppressed when  $m$  is large.

Furthermore, the effective field theory must have a  $\mathbb{Z}_2$  symmetry,  $J \rightarrow -J$ . This is induced by the  $\mathbb{Z}_2$  symmetry of the high-energy theory. From this we can deduce that  $c_{n,k} = 0$  if  $n$  is even.

Generically, to  $O(m^{-8})$  our effective action will have the form

$$\Gamma[J] = \int d^4x \left( \frac{a_0}{m^2} J^2 + \frac{a_1}{m^4} J \partial^2 J + \frac{a_2}{m^6} J \partial^4 J + \frac{a_2}{m^8} J \partial^6 J + \frac{b_0}{m^8} J^4 + \dots \right), \quad (3.55)$$

where the constants  $a_i$  and  $b_i$  are dimensionless. At low energies, the impact of high-energy physics is now completely contained within a handful of parameters. Unfortunately, unless our theory is perturbative it is impossible to calculate these parameters. Nevertheless, we could instead try to measure them experimentally. This brings us full circle back to the ideas discussed in Section 3.1: effective field theories can be used to make predictions at low energies if we fit our coupling constants to the low energy data.

We end this chapter with a rather abstract, but important, point. We will prove that

$$a_0 > 0. \quad (3.56)$$

Using (3.55), we can interpret this as implying that a massive scalar field will always be attractive at sufficiently low energies and densities, regardless of any interaction terms. The inequality (3.56) will be needed in Chapter 5.

To prove this result, we note that the  $J^2$  term in  $\Gamma[J]$  can be written in terms of the dressed propagator

$$-\frac{1}{2} \int d^4x d^4y J(x) G(x-y) J(y). \quad (3.57)$$

Here the propagator  $G(x-y)$  is the sum of the diagrams

$$G(x-y) = \text{---} + \text{---} \text{---} + \text{---} \text{---} + \text{---} \text{---} + \dots \quad (3.58)$$

and can be seen as the interacting generalisation of the Feynman propagator  $D(x-y)$ . Now invoke the Källén-Lehmann spectral representation of the propagator

$$G(x-y) = \int \frac{d^4p}{(2\pi)^4} e^{ip(x-y)} \int_0^\infty \frac{dX}{2\pi} \frac{\rho(X)}{p^2 - X}, \quad (3.59)$$

where  $\rho(X)$  is always non-negative. A derivation of this is found in Appendix B. We now Fourier transform  $G(x-y)$  and expand

$$\tilde{G}(p) = \int \frac{dX}{2\pi} \frac{\rho(p^2)}{p^2 - X} = - \int_0^\infty \frac{dX}{2\pi} \frac{\rho(X)}{X} + O(p^2). \quad (3.60)$$

Comparing to (3.55) and (3.57), we can now equate

$$a_0 = \frac{m^2}{2} \int_0^\infty \frac{dX}{2\pi} \frac{\rho(X)}{X} \geq 0 \quad (3.61)$$

as  $\rho(X)$  is always positive. This completes the proof. It is straightforward to generalise our result to vector mesons.

---

# The Non-Relativistic Limit

---

## 4.1 Overview

The previous chapter developed methods for removing heavy particles from field theories. In the context of nuclear models this allows us to replace a theory of nucleons and mesons with a theory of only nucleons. This is all we need to do in principle: all nuclear properties can be calculated from our effective field theory.

Yet as we noted when working with our toy model in Chapter 2, nucleons are actually quite heavy with respect to light mesons. Since our effective field theory is valid only at energies lower than the meson mass scale, our nucleons will be non-relativistic in this regime.

The aim of this chapter is to develop a general method for taking the non-relativistic limit of fermionic theories — such as theories containing only nucleons. What seems like a simple task is actually quite difficult, for a number of reasons.

The first reason is that the non-relativistic limit usually aims to produce a Galilean invariant theory, although higher-order relativistic corrections may be included and these break the Galilean symmetry. The standard name for this limit, ‘non-relativistic’, is hence rather confusing, since Galilean symmetry is a form of relativity. Galilean symmetry restricts the forms of these theories in much the same way that Lorentzian symmetry constrains traditional quantum field theories [42], but unfortunately our naming convention reflects a broader ignorance of the Galilean group. Unlike the Lorentz group, the Galilean group is not semi-simple, and hence has a far richer representation theory. There are ten vector representations of the group [43], which relate in non-trivial ways to Lorentz representations. As a result, the non-relativistic limit is often ambiguous: in electrodynamics for instance there are two distinct Galilean limits [44]. This thesis is not the place to discuss further the fascinating and often neglected subject of Galilean symmetry. We instead point the interested reader to the articles [42] and [46] which provide good introductions to the topic.

A second issue is that relativistic and non-relativistic theories are described using quite distinct frameworks. In relativistic theories, the full apparatus of quantum field theory is used, most often with a path integral formulations. On the other hand, non-relativistic theories usually start with classical particles, quantised through the use of wavefunctions. When we take the non-relativistic limit of a field theory, we will derive a non-relativistic field theory. Most nuclear models, however, do not utilise non-relativistic field theories. We will hence need to relate non-relativistic theories to more traditional approach using Skyrme energy density functionals. These are the inputs used in traditional nuclear many-body simulations [45].

To take the non-relativistic limit of a theory, we will essentially perform a Foldy-

Wouthuysen transformation [47]. This method has been applied to the case of relativistic mean-field theory in [48] and [49]. We will take our non-relativistic limit in the context of field theory, unlike traditional uses which aim to derive a single particle Schrödinger equation. We do this partly because it is more general, and partly because it is more suited to general field theories — unlike other approaches we are not constrained to use mean-field approximations<sup>1</sup>.

## 4.2 Schrödinger from Dirac

In this section we shall discuss the derivation of the Schrödinger Lagrangian from the Dirac equation. Nucleons are spin-1/2 fermions, and so when interactions are ignored, they are described by the Dirac equation

$$(i\gamma^\mu \partial_\mu - m)\psi = 0. \quad (4.1)$$

Since we are interested in the non-relativistic limit, the Dirac representation of the gamma matrices is the most convenient. In this representation,

$$\gamma^0 = \begin{pmatrix} I & 0 \\ 0 & -I \end{pmatrix}, \quad \gamma^i = \begin{pmatrix} 0 & \sigma^i \\ -\sigma^i & 0 \end{pmatrix}, \quad (4.2)$$

where  $I$  is the  $2 \times 2$  identity matrix, and  $\sigma^i$  are the pauli matrices. The other Dirac bilinears are given by

$$\gamma^5 = \begin{pmatrix} 0 & I \\ I & 0 \end{pmatrix}, \quad \sigma^{0i} = i \begin{pmatrix} 0 & \sigma^i \\ \sigma^i & 0 \end{pmatrix}, \quad \sigma^{ij} = \varepsilon^{ijk} \begin{pmatrix} \sigma^k & 0 \\ 0 & \sigma^k \end{pmatrix}. \quad (4.3)$$

Let us separate the Dirac spinor into two sets of two component vectors

$$\psi = \begin{pmatrix} \Psi \\ \chi \end{pmatrix}. \quad (4.4)$$

The Dirac equation then becomes

$$\begin{pmatrix} i\partial_0 - m & i\vec{\sigma} \cdot \nabla \\ -i\vec{\sigma} \cdot \nabla & -i\partial_0 - m \end{pmatrix} \begin{pmatrix} \Psi \\ \chi \end{pmatrix} = 0. \quad (4.5)$$

We use  $\nabla$  for spatial derivatives, using the non-relativistic metric so that

$$\nabla_i \nabla_i = \partial_x^2 + \partial_y^2 + \partial_z^2 = \Delta. \quad (4.6)$$

Consider stationary particles: these satisfy  $\nabla\psi = 0$ . In this case it is straightforward to solve the Dirac equation, and we find that the solutions are

$$e^{-imt} \begin{pmatrix} \Psi \\ 0 \end{pmatrix}, \quad e^{imt} \begin{pmatrix} 0 \\ \chi \end{pmatrix}. \quad (4.7)$$

---

<sup>1</sup>We note that recently a different approach to non-relativistic limits has been pursued in the context of point-coupling models [50, 51, 52]. In these papers it is noted that Galilean invariance will be lost upon including terms of  $O(v^2/c^2)$ . This leads to the development of a more general non-relativistic map, which can preserve Galilean invariance. On the other hand, the method is significantly more complicated, and furthermore the errors involved are unclear.

Bilinear	Scalar	Vector	Pseudovector	Pseudoscalar
$\bar{\psi}\psi$	$\bar{\psi}\psi$			
$\bar{\psi}\gamma^\mu\psi$	$\bar{\psi}\gamma^0\psi$	$\bar{\psi}\gamma^i\psi$		
$\bar{\psi}\sigma^{\mu\nu}\psi$		$\bar{\psi}\sigma^{0i}\psi$	$\varepsilon^{ijk}\bar{\psi}\sigma^{ij}\psi$	
$\bar{\psi}\gamma^5\gamma^\mu\psi$			$\bar{\psi}\gamma^5\gamma^i\psi$	$\bar{\psi}\gamma^5\gamma^0\psi$
$i\bar{\psi}\gamma^5\psi$				$i\bar{\psi}\gamma^5\psi$

**Table 4.1:** Dirac bilinears in the non-relativistic limit.

for constant  $\Psi$  and  $\chi$ . The first solution corresponds to particles and the second solution to antiparticles.

Naively we might try to use the particle solutions in (4.7) to derive the non-relativistic limit of the Dirac equation and Dirac bilinears. However, it is straightforward to verify that if this expression is substituted into the Dirac Lagrangian, this will not yield the Schrödinger Lagrangian as all time-dependence has been removed.

To derive the Schrödinger Lagrangian, we need a more sophisticated non-relativistic limit. Levy-Leblond [46] showed that

$$\psi = e^{-imt} \begin{pmatrix} \Psi \\ -\frac{i}{2m}\vec{\sigma} \cdot \nabla\Psi \end{pmatrix} \quad (4.8)$$

is Galilean-invariant. Substituting this into the Dirac Lagrangian and making the substitutions

$$\frac{\partial}{\partial t} \rightarrow \frac{1}{c} \frac{\partial}{\partial t}, \quad m \rightarrow mc, \quad (4.9)$$

we find that

$$\mathcal{L} = \bar{\psi}(i\not{\partial} - m)\psi = \frac{1}{c} \left( i\Psi^\dagger \frac{\partial\Psi}{\partial t} - \frac{1}{2m} \nabla\Psi^\dagger \nabla\Psi \right) + O(c^{-2}). \quad (4.10)$$

To leading order in  $c^{-1}$ , we obtain the Schrödinger Lagrangian.

### 4.3 Non-Relativistic Dirac Bilinears

In interactions, fermions interact through the 16 Dirac bilinears<sup>2</sup>

$$\bar{\psi}\psi, \quad \bar{\psi}\gamma^\mu\psi, \quad \bar{\psi}\sigma^{\mu\nu}\psi, \quad \bar{\psi}\gamma^5\gamma^\mu\psi, \quad i\bar{\psi}\gamma^5\psi, \quad (4.11)$$

To take the non-relativistic limit of an interacting theory, we need to calculate the non-relativistic limit of these bilinears.

First we should consider how the bilinears transform under rotations. This tells us how the bilinears will transform in the non-relativistic limit. For instance, the four-vector  $\bar{\psi}\gamma^\mu\psi$  in the non-relativistic limit splits into a scalar  $\bar{\psi}\gamma^0\psi$  and the vector  $\bar{\psi}\gamma^i\psi$ . In Table 4.1 this is generalised to the five sets of Dirac bilinears. Using this table, we shall define the (pseudo-)vectors

$$[\vec{\gamma}]^i = \gamma^i, \quad [\vec{\alpha}]^i = \sigma^{0i}, \quad [\vec{\beta}]^i = \varepsilon^{ijk}\sigma^{jk}.$$

<sup>2</sup>Each of these corresponds to a  $p$ -form, so that  $\sigma^{\mu\nu}$  is an antisymmetric tensor with 6 independent components.

Throughout the rest of the chapter, we shall use non-relativistic notation exclusively, so that  $a_i = a^{\mu=i}$ , and shall keep all indices lowered.

In taking the non-relativistic limit of the bilinears, we have a choice. If we use (4.8) to calculate our non-relativistic limit, then we shall obtain a Galilean invariant theory. Our bilinears will be correct to  $O(c^{-1})$ , and will include some but not all of the  $O(c^{-2})$  corrections. On the other hand, if we choose to sacrifice Galilean invariance, we can include the next-order corrections to (4.8). Our bilinears will then be correct to  $O(c^{-2})$ . The advantage of this is that the component of the spin-orbit interaction which originates in Thomas precession will be automatically included, along with a number of other corrections.

We shall expand to  $O(c^{-2})$  and sacrifice Galilean invariance. The easiest way to do this is to apply a boost to (4.7) and then expand to second order:

$$\begin{aligned} \psi &= e^{-\frac{i}{4}\omega_{\mu\nu}\sigma^{\mu\nu}} \begin{pmatrix} e^{-imt}\Psi \\ 0 \end{pmatrix} = e^{\frac{i}{2m}p_i\sigma_{0i}} \begin{pmatrix} e^{-imt}\Psi \\ 0 \end{pmatrix} \\ &= \left(1 + \frac{i}{2m}p_i\sigma_{0i} - \frac{1}{8m^2}p_i\sigma_{0i}p_j\sigma_{0j} + \dots\right) \begin{pmatrix} e^{-imt}\Psi \\ 0 \end{pmatrix} \\ &= \begin{pmatrix} e^{-imt}\Psi \\ 0 \end{pmatrix} - \frac{p_i}{2m} \begin{pmatrix} 0 & \sigma_i \\ \sigma_i & 0 \end{pmatrix} \begin{pmatrix} e^{-imt}\Psi \\ 0 \end{pmatrix} + \frac{p_i p_j}{8m^2} \begin{pmatrix} \sigma_i \sigma_j & 0 \\ 0 & \sigma_i \sigma_j \end{pmatrix} \begin{pmatrix} e^{-imt}\Psi \\ 0 \end{pmatrix} \end{aligned} \quad (4.12)$$

We now can relate the boost to the momentum of  $\Psi$ . The momentum operator is  $\vec{p} = -i\nabla$ , and so making this substitution, we find

$$\begin{aligned} \psi &= e^{-imt} \begin{pmatrix} \Psi \\ -\frac{i}{2m}\vec{\sigma} \cdot \nabla \Psi \end{pmatrix} - \frac{e^{-imt}\nabla_i \nabla_j}{8m^2} \begin{pmatrix} (\delta_{ij} + i\varepsilon_{ijk}\sigma_k)\Psi \\ 0 \end{pmatrix} \\ &= e^{-imt} \begin{pmatrix} \Psi - \frac{1}{8m^2}\nabla^2\Psi \\ -\frac{i}{2m}\vec{\sigma} \cdot \nabla \Psi \end{pmatrix}. \end{aligned} \quad (4.13)$$

Notice that the (4.8) is given by taking the first order boost, as we would expect. We could in principle now calculate the next order corrections to the Schrödinger Lagrangian in (4.10). We will however neglect such terms, as they contribute higher order spatial derivatives which can generally be neglected.

We now calculate the Dirac bilinears. Note that the relation

$$\vec{\sigma}(\vec{\sigma} \cdot \vec{a}) = I\vec{a} - i\vec{\sigma} \times \vec{a} \quad (4.14)$$

will be used many times below. First we calculate:

$$\bar{\psi} = \psi^\dagger \gamma^0 \approx e^{imt} \left( \Psi^\dagger - \frac{1}{8m^2} \nabla^2 \Psi^\dagger, \quad -\frac{i}{2m} \nabla \Psi^\dagger \cdot \vec{\sigma} \right). \quad (4.15)$$

Using this we can then calculate each of the bilinears:

$$\begin{aligned}
\bar{\psi}\psi &\approx \left(\Psi^\dagger - \frac{1}{8m^2}\nabla^2\Psi^\dagger\right)\left(\Psi - \frac{1}{8m^2}\nabla^2\Psi\right) - \frac{1}{4m^2}(\nabla\Psi^\dagger \cdot \vec{\sigma})(\vec{\sigma} \cdot \nabla\Psi) \\
&\approx |\Psi|^2 - \frac{1}{8m^2}\left(\Psi^\dagger\nabla^2\Psi + (\nabla^2\Psi^\dagger)\Psi\right) - \frac{1}{4m^2}\nabla\Psi^\dagger \cdot \nabla\Psi + \frac{i}{4m^2}\nabla\Psi^\dagger \cdot (\vec{\sigma} \times \nabla\Psi) \\
&= |\Psi|^2 - \frac{1}{8m^2}\nabla^2|\Psi|^2 + \frac{i}{4m^2}\nabla\Psi^\dagger \cdot (\vec{\sigma} \times \nabla\Psi), \\
\bar{\psi}\gamma^0\psi &\approx \left(\Psi^\dagger - \frac{1}{8m^2}\nabla^2\Psi^\dagger\right)\left(\Psi - \frac{1}{8m^2}\nabla^2\Psi\right) + \frac{1}{4m^2}(\nabla\Psi^\dagger \cdot \vec{\sigma})(\vec{\sigma} \cdot \nabla\Psi) \\
&\approx |\Psi|^2 - \frac{1}{8m^2}\left(\Psi^\dagger\nabla^2\Psi + (\nabla^2\Psi^\dagger)\Psi\right) + \frac{1}{4m^2}\nabla\Psi^\dagger \cdot \nabla\Psi - \frac{i}{4m^2}\nabla\Psi^\dagger \cdot (\vec{\sigma} \times \nabla\Psi) \\
&= |\Psi|^2 - \frac{1}{8m^2}\nabla^2|\Psi|^2 - \frac{i}{4m^2}\nabla\Psi^\dagger \cdot (\vec{\sigma} \times \nabla\Psi) + \frac{1}{2m^2}\nabla\Psi^\dagger \cdot \nabla\Psi, \\
\bar{\psi}\vec{\gamma}\psi &\approx -\frac{1}{2m}\left[i\left(\Psi^\dagger - \frac{1}{8m^2}\nabla^2\Psi^\dagger\right)\vec{\sigma}(\vec{\sigma} \cdot \nabla\Psi) + h.c.\right] \approx -\frac{1}{2m}\left[i\Psi^\dagger\vec{\sigma}(\vec{\sigma} \cdot \nabla\Psi) + h.c.\right] \\
&= -\frac{1}{2m}\left[i\Psi^\dagger\nabla\Psi - i(\nabla\Psi^\dagger)\Psi + \Psi^\dagger\vec{\sigma} \times \nabla\Psi - \nabla\Psi^\dagger \times \vec{\sigma}\Psi\right] \\
&= -\frac{1}{2m}\left[i\Psi^\dagger\nabla\Psi - i(\nabla\Psi^\dagger)\Psi - \nabla \times (\Psi^\dagger\vec{\sigma}\Psi)\right], \\
\bar{\psi}\vec{\alpha}\psi &\approx \frac{1}{2m}\left[\left(\Psi^\dagger - \frac{1}{8m^2}\nabla^2\Psi^\dagger\right)\vec{\sigma}(\vec{\sigma} \cdot \nabla\Psi) + h.c.\right] \approx \frac{1}{2m}\left[\Psi^\dagger\vec{\sigma}(\vec{\sigma} \cdot \nabla\Psi) + h.c.\right] \\
&= \frac{1}{2m}\left[\Psi^\dagger\nabla\Psi + (\nabla\Psi^\dagger)\Psi - i\Psi^\dagger\vec{\sigma} \times \nabla\Psi - i\nabla\Psi^\dagger \times \vec{\sigma}\Psi\right] \\
&= \frac{1}{2m}\left[\nabla(\Psi^\dagger\Psi) - i\Psi^\dagger\vec{\sigma} \times \nabla\Psi - i\nabla\Psi^\dagger \times \vec{\sigma}\Psi\right], \\
\bar{\psi}\vec{\beta}\psi &\approx \left[\left(\Psi^\dagger - \frac{1}{8m^2}\nabla^2\Psi^\dagger\right)\vec{\sigma}\left(\Psi - \frac{1}{8m^2}\nabla^2\Psi\right) - \frac{1}{4m^2}(\nabla\Psi^\dagger \cdot \vec{\sigma})\vec{\sigma}(\vec{\sigma} \cdot \nabla\Psi)\right] \\
&\approx \Psi^\dagger\vec{\sigma}\Psi - \frac{1}{8m^2}\left(\Psi^\dagger\vec{\sigma}\nabla^2\Psi + (\nabla^2\Psi^\dagger)\vec{\sigma}\Psi\right) - \frac{1}{4m^2}(\nabla\Psi^\dagger \cdot \vec{\sigma})(\nabla\Psi - i\vec{\sigma} \times \nabla\Psi) \\
&= \Psi^\dagger\vec{\sigma}\Psi - \frac{1}{8m^2}\nabla^2(\Psi^\dagger\vec{\sigma}\Psi) + \frac{1}{2m^2}\nabla^i\Psi^\dagger\vec{\sigma}\nabla_i\Psi \\
&\quad - \frac{1}{4m^2}\left[(\nabla\Psi^\dagger \cdot \vec{\sigma})\nabla\Psi + \nabla\Psi^\dagger(\vec{\sigma} \cdot \nabla\Psi) - i\nabla\Psi^\dagger \times \nabla\Psi\right], \\
\bar{\psi}\gamma^5\vec{\gamma}\psi &\approx \left[\left(\Psi^\dagger - \frac{1}{8m^2}\nabla^2\Psi^\dagger\right)\vec{\sigma}\left(\Psi - \frac{1}{8m^2}\nabla^2\Psi\right) + \frac{1}{4m^2}(\nabla\Psi^\dagger \cdot \vec{\sigma})\vec{\sigma}(\vec{\sigma} \cdot \nabla\Psi)\right] \\
&\approx \Psi^\dagger\vec{\sigma}\Psi - \frac{1}{8m^2}\left(\Psi^\dagger\vec{\sigma}\nabla^2\Psi + (\nabla^2\Psi^\dagger)\vec{\sigma}\Psi\right) + \frac{1}{4m^2}(\nabla\Psi^\dagger \cdot \vec{\sigma})(\nabla\Psi - i\vec{\sigma} \times \nabla\Psi) \\
&= \Psi^\dagger\vec{\sigma}\Psi - \frac{1}{8m^2}\nabla^2(\Psi^\dagger\vec{\sigma}\Psi) \\
&\quad + \frac{1}{4m^2}\left[(\nabla\Psi^\dagger \cdot \vec{\sigma})\nabla\Psi + \nabla\Psi^\dagger(\vec{\sigma} \cdot \nabla\Psi) - i\nabla\Psi^\dagger \times \nabla\Psi\right],
\end{aligned}
\tag{4.16}$$

$$\begin{aligned}
\bar{\psi}\gamma^5\gamma^0\psi &\approx -\frac{1}{2m} \left[ i \left( \Psi^\dagger - \frac{1}{8m^2} \nabla^2 \Psi^\dagger \right) \vec{\sigma} \cdot \nabla \Psi + h.c \right] \\
&\approx -\frac{i}{2m} \left[ \Psi^\dagger \vec{\sigma} \cdot \nabla \Psi - \nabla \Psi^\dagger \cdot \vec{\sigma} \Psi \right], \\
i\bar{\psi}\gamma^5\psi &\approx \frac{1}{2m} \left[ \left( \Psi^\dagger - \frac{1}{8m^2} \nabla^2 \Psi^\dagger \right) \vec{\sigma} \cdot \nabla \Psi + h.c \right] \\
&\approx \frac{1}{2m} \left[ \Psi^\dagger \vec{\sigma} \cdot \nabla \Psi + \nabla \Psi^\dagger \cdot \vec{\sigma} \Psi \right] \\
&= \frac{1}{2m} \nabla \cdot (\Psi^\dagger \vec{\sigma} \Psi).
\end{aligned} \tag{4.17}$$

So using the above expressions, we are able to calculate the non-relativistic limit of any theory of interacting Dirac fermions, along with the  $O(m^{-2})$  corrections.

Our expressions can be simplified if we introduce a series of local densities. This is common practise in nuclear physics. Rather than writing everything in terms of  $\Psi$ , we introduce invariant currents which are easier to work with and physically interpret. Following the conventions in [53], we introduce the seven quantities

$$\begin{aligned}
\rho &= \Psi^\dagger \Psi, & \tau &= \nabla \Psi^\dagger \cdot \nabla \Psi, & \vec{j} &= \frac{i}{2} \left( (\nabla \Psi^\dagger) \Psi - \Psi^\dagger \nabla \Psi \right), \\
\vec{s} &= \Psi^\dagger \vec{\sigma} \Psi, & \vec{\tau} &= \nabla^i \Psi^\dagger \vec{\sigma} \nabla_i \Psi, & J_{ij} &= \frac{i}{2} \left( (\nabla_j \Psi^\dagger) \sigma_i \Psi - \Psi^\dagger \sigma_i \nabla_j \Psi \right), \\
\vec{G} &= \frac{1}{2} (\nabla \Psi^\dagger \cdot \vec{\sigma}) \nabla \Psi + \frac{1}{2} \nabla \Psi^\dagger (\vec{\sigma} \cdot \nabla \Psi) - \frac{i}{2} \nabla \Psi^\dagger \times \nabla \Psi.
\end{aligned} \tag{4.18}$$

Reading from left to right, top to bottom, we have the density, the kinetic density and the current density, the spin density, the spin-kinetic density and the spin-current density, and the tensor-kinetic density. Our definition of  $\vec{G}$  differs from the tensor-kinetic density  $\vec{F}$  of [53] by an additional term:

$$\vec{G} = \vec{F} - \frac{i}{2} \nabla \Psi^\dagger \times \nabla \Psi,$$

which is not included in their definition.

The tensor  $J_{ij}$  can be decomposed into three quantities, a scalar, a pseudo-vector and a traceless symmetric tensor:

$$J_s = \delta_{ij} J_{ij}, \quad \vec{J}_v = \varepsilon_{ijk} J_{ij} \vec{e}_k = \frac{i}{2} \left( \Psi^\dagger \vec{\sigma} \times \nabla \Psi + \nabla \Psi^\dagger \times \vec{\sigma} \Psi \right), \quad \mathbf{J}_t = \frac{1}{2} (J_{ij} + J_{ji}) - \frac{1}{3} J_s$$

We are now able to write our Dirac bilinears in terms of these densities:

$$\begin{aligned}
\bar{\psi}\psi &\approx \rho - \frac{1}{8m^2} \nabla^2 \rho + \frac{1}{2m^2} \nabla \cdot \vec{J}_v, & \bar{\psi}\gamma^5\vec{\gamma}\psi &\approx \vec{s} - \frac{1}{8m^2} \nabla^2 \vec{s} + \frac{1}{2m^2} \vec{G}, \\
\bar{\psi}\gamma^0\psi &\approx \rho - \frac{1}{8m^2} \nabla^2 \rho - \frac{1}{2m^2} \nabla \cdot \vec{J}_v + \frac{1}{2m^2} \tau, & \bar{\psi}\vec{\beta}\psi &\approx \vec{s} - \frac{1}{8m^2} \nabla^2 \vec{s} - \frac{1}{2m^2} \vec{G} + \frac{1}{2m^2} \vec{\tau}, \\
\bar{\psi}\gamma^5\gamma^0\psi &\approx \frac{1}{m} J_s, & \bar{\psi}\vec{\tau}\psi &\approx \frac{1}{2m} \left( \nabla \times \vec{s} + 2\vec{j} \right), \\
i\bar{\psi}\gamma^5\psi &\approx \frac{1}{2m} \nabla \cdot \vec{s}, & \bar{\psi}\vec{\alpha}\psi &\approx \frac{1}{2m} \left( 2\vec{J}_v + \nabla \rho \right).
\end{aligned} \tag{4.19}$$

We conclude this section by concisely summarising the procedure we have developed

to take the non-relativistic limit.

1. Take a Lagrangian of the form

$$\mathcal{L} = \bar{\psi}(i\cancel{\partial} - m)\psi - V(\bar{\psi}\psi, \dots, i\psi\gamma^5\psi).$$

2. Replace the kinetic term  $\bar{\psi}(i\cancel{\partial} - m)\psi$  with the Schrödinger Lagrangian for a  $\frac{1}{2}$ -spinor

$$\bar{\psi}(i\cancel{\partial} - m)\psi \rightarrow \frac{1}{c} \left( i\Psi^\dagger \frac{\partial\Psi}{\partial t} - \frac{1}{2m} \nabla\Psi^\dagger \nabla\Psi \right).$$

3. In the interaction term  $V$ , replace each Dirac bilinear with their  $O(m^{-2})$  form given in (4.19).

4. Making the substitutions

$$\frac{\partial}{\partial t} \rightarrow \frac{1}{c} \frac{\partial}{\partial t}, \quad m \rightarrow mc,$$

write the interaction terms as

$$V = V_0 + \frac{1}{c} V_1 + \frac{1}{c^2} V_2 + \dots$$

5. In natural units (with  $c = 1$ ), the new Lagrangian is now

$$\tilde{\mathcal{L}} = \left( i\Psi^\dagger \frac{\partial\Psi}{\partial t} - \frac{1}{2m} \nabla\Psi^\dagger \nabla\Psi \right) - V_0 - V_1 - V_2.$$

## 4.4 Non-Relativistic Densities and Skyrme Functionals

Now that we have developed the tools to take non-relativistic limits, we should discuss how to interpret the results. In nuclear many-body calculations, the interaction is often described via an energy density functional (EDF).

To construct the EDF, the first step is to convert the Lagrangian to a Hamiltonian

$$\mathcal{H} = \dot{\Psi}\Pi - \mathcal{L}. \quad (4.20)$$

where  $\Pi$  is the conjugate momentum to  $\Psi$ . For a Schrödinger field, the conjugate momentum is given by

$$\Pi = \frac{\partial\mathcal{L}}{\partial\dot{\Psi}} = i\Psi^\dagger. \quad (4.21)$$

Given a Lagrangian of the form

$$\mathcal{L} = \left( i\Psi^\dagger \frac{\partial\Psi}{\partial t} - \frac{1}{2m} \nabla\Psi^\dagger \nabla\Psi \right) - V[\Psi^\dagger, \Psi] \quad (4.22)$$

we obtain the Hamiltonian

$$\mathcal{H} = \frac{1}{2m} \nabla\Psi^\dagger \nabla\Psi + V[\Psi^\dagger, \Psi]. \quad (4.23)$$

To convert the Hamiltonian to an EDF, we evaluate the expectation value of the Hamiltonian over the Slater determinant of single-nucleon wave-functions. We can calculate the

expectation value of the various densities of Section 4.3. For instance,

$$\rho = \langle \hat{\rho} \rangle = \langle \Psi^\dagger \Psi \rangle = \sum_{sq} \sum_{ij} \langle a_i^\dagger a_j \rangle \phi_i^{sq}(x)^* \phi_j(x)^{sq} = \sum_{sq} \sum_i |\phi_i^{sq}(x)|^2 \quad (4.24)$$

where  $a_i$  is the lowering operator for the  $i^{\text{th}}$  occupied state, and  $\phi_i(x)$  is the corresponding wavefunction. For simplicity, we shall assume that the one-body density matrix of our system is diagonal in spin and isospin. In this case, each particle is either a proton or a neutron, and is either spin up or spin down. We can then calculate the density of neutrons

$$\langle \hat{\rho}_N \rangle = \sum_{sq} \sum_{ij} \langle a_i^\dagger a_j \rangle \phi_i^{sq}(x)^* P_N \phi_j^{sq}(x) = \sum_s \sum_i |\phi_i^{sN}(x)|^2 \quad (4.25)$$

where  $P_N$  is the operator which projects onto neutron wavefunctions (the expression is identical for protons). More generally, we can introduce four operators,

$$\hat{\rho}_{N\uparrow}, \quad \hat{\rho}_{N\downarrow}, \quad \hat{\rho}_{P\uparrow}, \quad \hat{\rho}_{P\downarrow} \quad (4.26)$$

for each of the four different nucleon states.

In order to evaluate EDFs, we will need to calculate expectation values which are bilinear in these densities. As an example, let us calculate

$$\begin{aligned} \langle \hat{\rho}^2 \rangle &= \sum_{sq s' q'} \sum_{ijkl} \langle a_i^\dagger a_j a_k^\dagger a_l \rangle \phi_i^{sq}(x)^* \phi_j^{sq}(x) \phi_k^{s' q'}(x)^* \phi_l^{s' q'}(x) \\ &= \sum_{sq s' q'} \sum_{ijkl} (\delta_{ij} \delta_{kl} - \delta_{il} \delta_{jk}) \phi_i^{sq}(x)^* \phi_j^{sq}(x) \phi_k^{s' q'}(x)^* \phi_l^{s' q'}(x) \\ &= \rho^2 - \sum_{sq} \rho_{sq}^2. \end{aligned} \quad (4.27)$$

Here we see that  $\langle \hat{\rho}^2 \rangle \neq \langle \hat{\rho} \rangle^2$  because we need to take into account the fermionic nature of the nucleon. These corrections are known as the exchange terms. More complicated expectation values can be computed in an analogous fashion.

The Skyrme energy density functional is the most general non-relativistic energy density functional which is local, bilinear, involves derivatives only up to second order, and is compatible with the symmetries of nuclear physics, in particular Galilean invariance [54]. In terms of the densities given in (4.18), the functional is given by

$$\begin{aligned} \mathcal{E}_{\text{Skyrme}} &= \int dx^3 \sum_{t=0,1} \left( C_t^\rho \rho_t^2 + C_t^{\Delta\rho} \rho_t \Delta \rho_t + C_t^{s\bar{s}} \vec{s}_t^2 + C_t^{\Delta s} \vec{s}_t \Delta \vec{s}_t + C_t^\tau (\rho_t \tau_t - \vec{j}_t^2) \right. \\ &\quad \left. + C_t^{\nabla s} (\nabla \cdot \vec{s}_t)^2 + C_t^T (\vec{s}_t \cdot \vec{\tau}_t - J_{ij} J_{ij}) + C_t^F \left( \vec{s}_t \cdot \vec{F} - \frac{1}{2} (J_s^2 + J_{ij} J_{ij}) \right) \right) \\ &\quad \left. + C_t^{\nabla \cdot \vec{J}} (\rho_t \nabla \cdot \vec{J} + \vec{s} \cdot \nabla \times \vec{j}_t) \right). \end{aligned} \quad (4.28)$$

Each density can either be in an isoscalar  $t = 0$  or isovector  $t = 1$ , e.g.:

$$\rho_0^2 = \langle \hat{\rho} \rangle^2, \quad \rho_1^2 = \langle \hat{\rho}_a \rangle \langle \hat{\rho}_a \rangle = \langle \hat{\Psi}^\dagger \tau_a \hat{\Psi} \rangle \langle \hat{\Psi}^\dagger \tau_a \hat{\Psi} \rangle. \quad (4.29)$$

This gives a total of eighteen parameters. One way to physically interpret the terms is to relate the terms to two-nucleon forces, such as the zero-ranged Skyrme interaction [17, 55].

---

Roughly speaking, the first line of (4.28) corresponds to central terms, the second line to the tensor force, and the third to the spin-orbit interaction.

Another useful division of the terms is based on their symmetries. In time symmetric situations — such as nuclear ground-state properties — only the time-even densities will be non-zero. These densities are the  $\rho$ ,  $\tau$ , and  $\vec{J}$ . This simplifies calculations and reduces the number of undetermined parameters which need to be considered. Unfortunately, not all the time-odd coefficients in (4.28) can be constrained using time-even properties.



---

# Meson Models for Nuclear Forces

---

After two chapters of theoretical developments, we are now ready to confront our main goal: relating nuclear forces to higher energy physics. We will begin by describing relevant aspects of hadron phenomenology — in particular, we need to choose the relevant mesons for nuclear systems.

We begin with a review of the relevant aspects of quantum chromodynamics and the light hadron spectrum, placing our work in the broader context of subnuclear physics. Then, in Section 5.3, we discuss the low energy limits of linear meson theories. This is extended in Section 5.4 to include meson-meson interactions. In general, we show that it is very hard, if not impossible, to quantitatively determine nuclear forces in terms of higher energy physics. If, however, we rescale parameters, we can minimise the number of low energy parameters which need to be determined in order to make predictions. This is discussed in Section 5.5. We then suggest one remnant of high-energy physics that may survive at low energies — the relationship between the vector and tensor couplings of vector mesons.

The chapter ends with a discussion relating our results to other approaches to the nuclear force problem. We argue that details of mesonic physics are largely irrelevant for nuclear physics. Any theory satisfying a few physical properties will, with well-chosen parameters, be able to reproduce realistic nuclear forces at low energies. For this reason, even though phenomenological models may quantitatively perform well when describing nuclei, this does not necessarily validate their underlying physical assumptions.

## 5.1 Strong Quantum Chromodynamics

Quantum chromodynamics is a Yang-Mills theory with gauge group  $SU(3)$ . The gauge fields ('gluons') interact with quarks in the vector representation. We do not have space for a detailed discussion of the theory, and refer the reader to specialised literature such as [57] for elaboration on formal aspects of QCD and [58] for detailed applications to particle physics.

In principle we should begin with the QCD Lagrangian, and from that derive the properties of light mesons and baryons. A variety of methods have been developed to attack this problem, ranging from the large- $N_c$  limit [59] to QCD sum rules [57] to lattice QCD [60]. Phenomenological approaches, utilising bags [61], solitons [62], or point-like quark models [63], have also been extensively utilised to study light mesons and baryons. A detailed review of the successes and failures of these models is beyond the scope of this thesis, and we merely note that a detailed quantitative understanding of mesonic physics is still lacking. Lattice QCD is however rapidly progressing and calculations of light meson masses is now possible to within a few percent [64].

---

Symmetry	Group	Status
Baryon Number	$U(1)$	Exact
Isospin	$SU(2)$	Explicitly broken as $m_u \neq m_d$ . Broken by electroweak force.
Strangeness	$U(1)$	Broken by weak force.
Chiral Symmetry	$SU(2)$	Spontaneously broken. Explicitly broken as $m_{u,d} \neq 0$ Broken by weak force.
Space Parity (P) Time Reversal (T) Charge Parity(C)	$\mathbb{Z}_2$	Broken by weak force.

---

**Table 5.1:** Symmetries of QCD at low energies.

One aspect of QCD which can be clearly connected to low energy phenomenology is its exact and approximate symmetries. These symmetries are summarised in *Table 5.1*. Since symmetries manifest themselves in the meson spectrum, we shall discuss briefly their origins in QCD. A more detailed discussion can be found in [65].

The QCD scale is the energy scale at which the coupling constant formally becomes infinite. This is usually taken to be  $\Lambda_{QCD} \sim 1$  GeV, around the mass of the nucleon. At this energy scale, three quarks are relevant, the up, down and strange, with masses<sup>1</sup>:

$$m_u \sim 2.5 \text{ MeV}, \quad m_d \sim 5 \text{ MeV}, \quad m_s \sim 90 \text{ MeV}.$$

Since these are considerably smaller than the QCD scale, QCD poses a number of approximate symmetries. Most notably we have isospin symmetry relating the  $u$  and  $d$  quarks. It is this approximate symmetry which explains the small mass difference between the proton and the neutron: essentially the  $m_u - m_d$  mass difference is tiny compared to the  $O(\Lambda)$  contribution to the nucleon mass from non-perturbative QCD.

Another approximate symmetry is chiral symmetry. Unlike isospin symmetry this is not manifest in the QCD vacuum, but is spontaneously broken. The resulting Nambu-Goldstone bosons are the pions, the kaons, and the eta. But since chiral symmetry is also explicitly broken by the quark masses, these mesons are not massless, although they have masses which are much lower than other hadrons. In particular, the pion has a mass of around 140 MeV, compared to other mesons such as the  $\rho$  which has a mass of 775 MeV.

QCD has exact flavour symmetries. The number of  $u$ ,  $d$  and  $s$  quarks must be conserved independently in any reaction. These symmetries are broken in the Standard Model by the weak force, but this is much weaker than the strong force and so can often be ignored in hadronic physics. Finally, QCD has independent,  $P$ ,  $C$  and  $T$  symmetry, and again these are explicitly broken by the weak force.

## 5.2 Light Hadrons

In the absence of theoretical guidance, we turn instead to the experimentally observed spectrum of light hadrons. The light mesons are shown in *Table 5.2* and the light baryons are listed in *Table 5.3*, with data taken from the latest *Review of Particle Physics* [56].

---

<sup>1</sup>As free quarks do not exist, defining the quark masses is ambiguous. More details can be found in [56].

Hadron	$J^P$	Isospin	$S$	Mass (MeV)
$\pi$	$0^-$	1	0	135
$K$	$0^-$	1/2	1	494
$\eta$	$0^-$	0	0	548
$\eta'$	$0^-$	0	0	958
$\rho$	$1^-$	1	0	775
$\omega$	$1^-$	0	0	782
$K^*$	$1^-$	1/2	1	892
$\phi$	$1^-$	0	0	1019
$f_0(500)$	$0^+$	0	0	$\sim 500$
$f_0(980)$	$0^+$	0	0	980
$a_0(980)$	$0^+$	1	0	980

**Table 5.2:** Light mesons, listing their spin ( $S$ ), parity ( $P$ ), isospin, strangeness ( $S$ ), and mass. The data is taken from [56].

Hadron	$J$	Isospin	$S$	Mass (MeV)
$N$	1/2	1	0	938
$\Lambda$	1/2	0	1	1116
$\Sigma$	1/2	1	1	1189
$\Xi$	1/2	1/2	2	1315
$\Delta$	3/2	3/2	0	1232
$\Sigma^*$	3/2	1	1	1382
$N(1440)$	1/2	1	0	1440

**Table 5.3:** Light baryons, listing their spin ( $J$ ), isospin, strangeness ( $S$ ), and mass. The data is taken from [56].

All the mesons with a mass under 1100 MeV and all baryons under 1500 MeV are listed. Effective field theory suggests that these are the relevant degrees of freedom, and so we shall develop nuclear models using these light hadrons.

Many hadrons are listed in *Table 5.2* and *Table 5.3*. To have any hope of a predictive model, we need to choose only the most relevant. A few general principles allow us to cull. The isospin and strangeness flavour symmetries of QCD place tight restrictions on interactions. As strangeness is (approximately) conserved, we can ignore strange mesons when studying nuclei.

We can also ignore any sufficiently heavy hadron, as their contribution to the nucleon-nucleon interactions will be suppressed by an inverse power of the mass squared. A reasonable cut-off to take is  $\Lambda \sim 1$  GeV. This removes all of the baryons except the nucleon, and along with all but five of the mesons. We are left with the  $\pi$  and  $\eta$ , the  $\rho$  and  $\omega$ , and the  $f_0(500)$ . The  $\eta$  couples weakly to nuclei and is usually ignored [19].

The status of the  $f_0(500)$  is complicated. Most meson models need a scalar-isoscalar particle to explain nuclear attraction, and so usually include a scalar-isoscalar  $\sigma$  meson. However, the identity of the  $f_0(500)$  is not well-understood (it does not fit easily into traditional  $\bar{q}q$  meson models) [66], and its connection to the  $\sigma$  is not straightforward. In chiral perturbation theory the attractive force between nucleons can be generated by  $\pi\pi$ -exchange, and this can mimic  $\sigma$  exchange [67]. We can instead think of the  $\sigma$  as an effective way to simulate more complicated underlying pion dynamics [3], rather than as the field associated with the  $f_0(500)$ .

Now that we have determined our particle content (the  $\pi, \sigma, \omega, \rho$  and the nucleon  $N$ ), we need to add interactions. In an effective field theory, we need to include all possible interactions compatible with symmetries. The non-renormalisable interactions will however be suppressed by a factor of the cut-off,  $\Lambda$ , which (for simplicity) we shall take to be about the nucleon mass  $M = 940$  GeV.

Even if we were restricted only to renormalisable interactions, we would find that there are over 20 parameters. Furthermore, the meson-meson interactions could potentially be strong. As discussed in Chapter 2, non-perturbative theories are theoretically very challenging to study. We shall instead begin by studying linear theories, and only afterwards will extend our results to the general non-linear case.

## 5.3 Meson-Nucleon Interactions

### 5.3.1 The Sigma

We will begin by describing possible sigma-nucleon interactions. There is only one renormalisable term for this interaction

$$\mathcal{L}_0 = g_0 \sigma \bar{N} N. \quad (5.1)$$

The first non-renormalisable interactions, suppressed by a power of  $\Lambda^{-1} = M^{-1}$ , are given by

$$\mathcal{L}_1 = -\frac{g_1}{2M} \sigma^2 \bar{N} N + \frac{g_2}{M} \sigma \partial_\mu (\bar{N} \gamma^\mu N). \quad (5.2)$$

If we set

$$J = g_0 \bar{N} N + \frac{g_2}{M} \partial_\mu (\bar{N} \gamma^\mu N), \quad K = -\frac{g_1}{M} \bar{N} N, \quad (5.3)$$

then we find that the full Lagrangian for our theory is

$$\mathcal{L} = \bar{N} (i\cancel{\partial} - M) N + \frac{1}{2} (\partial\sigma)^2 - \frac{1}{2} m_\sigma^2 \sigma^2 + J\sigma + \frac{1}{2} K\sigma^2. \quad (5.4)$$

The  $\sigma$  meson can be integrated out using the results of section 3.5. We found that

$$\mathcal{L}_{\text{eff}} = \bar{N} (i\cancel{\partial} - M) N + W[J, K] \quad (5.5)$$

where

$$W[J, K] = \int dx^4 \left( \frac{J^2}{2(m^2 - K)} - \frac{J\partial^2 J}{2(m^2 - K)^2} - \frac{J^2\partial^2 K + 2J\partial^\mu J\partial_\mu K}{2(m^2 - K)^3} - \frac{2(\partial K)^2 J^2}{(m^2 - K)^4} \right. \\ \left. - \frac{m^4}{8(2\pi)^2} \left( \frac{2K}{m^2} - \frac{3K^2}{m^4} + 2 \left( 1 - \frac{K}{m^2} \right)^2 \log \left( 1 - \frac{K}{m^2} \right) \right) + O(\partial^2) \right). \quad (5.6)$$

We are now able to calculate the non-relativistic limit of theory using the results of Chapter 4. To simplify our calculations, we will keep only the most important terms in  $W$ :

$$W[J, K] \approx \int dx^4 \left( \frac{J(x)^2}{2(m_\sigma^2 - K(x))} - \frac{J(x)\partial^2 J(x)}{2(m_\sigma^2 - K(x))^2} \right). \quad (5.7)$$

All other terms in  $W$  are suppressed by a factor of  $m^6$  or larger. We then find that

$$\begin{aligned} \mathcal{L}_{\text{NR}} = & i\Psi^\dagger \frac{\partial \Psi}{\partial t} - \frac{1}{2m} \nabla \Psi^\dagger \nabla \Psi + \frac{g_0^2 \rho^2}{2(m_\sigma^2 + g_1 \rho/M)} + \rho \nabla \cdot \vec{J}_v \left[ \frac{g_0^2}{2M^2(m_\sigma^2 + g_1 \rho/M)} \right] \\ & + \rho \Delta \rho \left[ -\frac{g_0^2}{8M^2(m_\sigma^2 + g_1 \rho/M)} + \frac{g_0^2}{2(m_\sigma^2 + g_1 \rho/M)^2} \right]. \end{aligned} \quad (5.8)$$

Notice that the dependence on  $g_2$  completely drops out. From the above Lagrangian, we can see that the  $\sigma$  meson contributes to an attractive central force (the  $\rho$  and  $\rho \Delta \rho$  terms), along with an isoscalar contribution to the spin-orbit ( $\rho \nabla \cdot \vec{J}_v$ ) interaction. The  $g_1$  term results in a non-trivial density dependence. Setting  $g_1 = 0$  removes this, and this yields the simpler Lagrangian

$$\mathcal{L}_{\text{NR}} = i\Psi^\dagger \frac{\partial \Psi}{\partial t} - \frac{1}{2m} \nabla \Psi^\dagger \nabla \Psi + \frac{g_0^2 \rho^2}{2m_\sigma^2} + \rho \nabla \cdot \vec{J}_v \frac{g_0^2}{2M^2 m_\sigma^2} + \rho \Delta \rho \left[ -\frac{g_0^2}{8M^2 m_\sigma^2} + \frac{g_0^2}{2m_\sigma^4} \right]. \quad (5.9)$$

We will use this simpler Lagrangian in the rest of this section, and will discuss more complicated density dependence in the next section.

### 5.3.2 The Pion

A proper treatment of the pion is difficult for two reasons. The first reason is quite simple: the pion is very light  $\sim 140$  MeV and so the errors associated with truncating it in an effective field theory are more severe than for the heavier mesons. The second is that the pion is a pseudo-Nambu Goldstone boson of the spontaneously broken chiral symmetry. This provides tight constraints on pion interactions [68]. For the moment we shall ignore these issues, and will return to them later in the chapter.

We shall use the field  $\pi_a(x)$  for the pion field — confusion with the mathematical constant  $\pi$  is avoided because of the isospin index of the pion field. The only renormalisable interaction which preserves parity symmetry is

$$\mathcal{L}_0 = -\alpha_0 \pi_a i \bar{N} \gamma^5 \tau_a N \quad (5.10)$$

where  $\tau_a$  is a Pauli matrix in isospin space. We will also consider a single non-renormalisable term,

$$\mathcal{L}_1 = -\frac{\alpha_1}{M} \pi_a \partial_\mu \bar{N} \gamma^5 \gamma^\mu \tau_a N. \quad (5.11)$$

Chiral symmetry requires that  $\alpha_0 = 0$  and so  $\mathcal{L}_1$  is actually the lowest-order contribution to the  $\pi N$  interaction (see Section 19.5 of [69]). If we introduce the current

$$J_a(x) = \alpha_0 i \bar{N} \gamma^5 \tau_a N + \frac{\alpha_1}{M} \partial_\mu \bar{N} \gamma^5 \gamma^\mu \tau_a N, \quad (5.12)$$

then our full Lagrangian is

$$\mathcal{L} = \bar{N}(i\not{\partial} - M)N + \frac{1}{2}(\partial^\mu \pi_a)(\partial_\mu \pi_a) - \frac{1}{2}m_\pi^2 \pi_a \pi_a - \pi_a J_a. \quad (5.13)$$

The  $\pi_a$  field can be integrated out using the results of Chapter 3.3. Indeed, we can simply modify (3.19) to use isovector-pseudoscalar rather than isoscalar-scalar couplings, and

with this we find that

$$\mathcal{L}_{\text{eff}} = \bar{N}(i\not{\partial} - M)N + \frac{1}{2m_\pi^2} \left( i\alpha_0 \bar{N} \gamma^5 \tau_a N + \frac{\alpha_1}{M} \partial_\mu (\bar{N} \gamma^5 \gamma^\mu \tau_a N) \right)^2 + O(m_\pi^{-4}). \quad (5.14)$$

We can take the non-relativistic limit of this expression using the methods of Chapter 4. Before doing this however, we note the following non-relativistic limits:

$$\begin{aligned} i\bar{N} \gamma^5 \tau_a N &\rightarrow \frac{1}{2M} \nabla \cdot \vec{s}_a \\ \frac{1}{M} \partial_\mu (\bar{N} \gamma^5 \gamma^\mu \tau_a N) &\rightarrow -\frac{1}{2M} \nabla \cdot \vec{s}_a. \end{aligned} \quad (5.15)$$

From this we notice two things. First, in the non-relativistic limit, both couplings contribute to the same term! This caused much confusion historically, as using a pseudoscalar coupling will coincidentally give the correct answer to lowest order, but will be completely wrong at higher orders [19].

The second thing to note is that both terms are suppressed by a power of  $M^{-1}$  in the non-relativistic limit, so the leading-order corrections from pion exchange is  $O(M^{-2})$ . In the non-relativistic limit, the effective Lagrangian is therefore

$$\mathcal{L}_{\text{NR}} = i\Psi^\dagger \frac{\partial \Psi}{\partial t} - \frac{1}{2m} \nabla \Psi^\dagger \nabla \Psi + \frac{(\alpha_0 - \alpha_1)^2}{8m_\pi^2 M^2} (\nabla \cdot \vec{s}_a)^2. \quad (5.16)$$

### 5.3.3 The Omega and the Rho

The case of the omega and the rho are identical, except for the additional isospin dependence from the rho. We will start with the omega, as it is simpler.

The only renormalisable omega-nucleon interaction is

$$\mathcal{L}_0 = \lambda_0 \omega_\mu \bar{N} \gamma^\mu N. \quad (5.17)$$

The first non-renormalisable interactions, suppressed by a power of  $\Lambda^{-1} = M^{-1}$ , are given by

$$\mathcal{L}_1 = \frac{\lambda_1}{M} \omega_\mu \partial_\nu \bar{N} \sigma^{\mu\nu} N + \frac{\lambda_2}{M} \omega_\mu \partial^\mu (\bar{N} N). \quad (5.18)$$

We ignore the  $\omega^2 \bar{N} N$  term which gives the complicated density dependence analogous to the  $\sigma$ , and will instead discuss this in the next section. If we introduce the current

$$J^\mu(x) = \lambda_0 \bar{N} \gamma^\mu N + \frac{\lambda_1}{M} \partial_\nu \bar{N} \sigma^{\mu\nu} N + \frac{\lambda_2}{M} \partial^\mu (\bar{N} N) \quad (5.19)$$

then our Lagrangian is

$$\mathcal{L} = \bar{N}(i\not{\partial} - M)N - \frac{1}{4} (\partial^\mu \omega^\nu - \partial^\nu \omega^\mu) (\partial_\mu \omega_\nu - \partial_\nu \omega_\mu) - \frac{1}{2} m_\omega^2 \omega^2 + \omega_\mu J^\mu. \quad (5.20)$$

The  $\omega$  field can be integrated out using the results of Chapter 3.3.

$$\mathcal{L}_{\text{eff}} \approx \bar{N}(i\not{\partial} - M)N - \frac{1}{2m^2} J^2 + \frac{1}{2m^4} J^\mu \partial^2 J_\mu - \frac{1}{2m^4} J^\mu \partial_\mu \partial_\nu J^\nu. \quad (5.21)$$

Taking the non-relativistic limit,  $J^\mu$  will split into a scalar  $J^0$  and a vector  $\vec{J}$ . Using the

results of Chapter 4, we find that the relativistic currents translate to:

$$\begin{aligned}
 \bar{N}\gamma^0 N &\rightarrow \rho - \frac{1}{8M^2}\Delta\rho - \frac{1}{2M^2}\nabla \cdot \vec{J}_v + \frac{1}{2M^2}\tau \\
 \nabla \cdot (\bar{N}\vec{\alpha}N) &\rightarrow \frac{1}{2M^2}(2\nabla \cdot \vec{J}_v + \Delta\rho) \\
 \bar{N}\vec{\gamma}N &\rightarrow \frac{1}{2M}(\nabla \times \vec{s} + 2\vec{j}) \\
 \nabla \times (\bar{N}\vec{\beta}N) &\rightarrow \nabla \times \vec{s} \\
 \nabla(\bar{N}N) &\rightarrow \nabla\rho.
 \end{aligned} \tag{5.22}$$

Our non-relativistic Lagrangian is therefore

$$\begin{aligned}
 \mathcal{L}_{\text{NR}} = &i\Psi^\dagger \frac{\partial\Psi}{\partial t} - \frac{1}{2m}\nabla\Psi^\dagger\nabla\Psi - \frac{\lambda_0^2\rho^2}{2m_\omega^2} \\
 &- \frac{\rho\Delta\rho}{2m_\omega^2} \left( \frac{\lambda_0^2}{m_\omega^2} - \frac{1}{M^2} \left( \lambda_0\lambda_1 + \frac{\lambda_0^2}{4} - \lambda_2^2 \right) \right) + \frac{\lambda_0^2}{2m_\omega^2 M^2}(\rho\tau - \vec{j}^2) \\
 &+ \frac{\lambda_0^2 - \lambda_0\lambda_1}{m_\omega^2 M^2}(\rho\nabla \cdot \vec{J}_v + \vec{s} \cdot \nabla \times \vec{j}) - \frac{\lambda_0^2}{2m_\omega^2 M^2}\rho\nabla \cdot \vec{J}_v + \frac{(2\lambda_1 - \lambda_0)^2}{8m_\omega^2 M^2}(\nabla \times \vec{s})^2.
 \end{aligned} \tag{5.23}$$

The term  $(\nabla \times \vec{s})^2$  is not a standard term in the Skyrme functional, but using vector identities and partial integral can be shown to be equal to

$$\int dx^3 (\nabla \times \vec{s})^2 = - \int dx^3 (\vec{s}\Delta\vec{s} + (\nabla \cdot \vec{s})^2). \tag{5.24}$$

Of all the mesons considered, the  $\omega$  gives the most complicated contribution to the Lagrangian. The  $\omega$  contributes to the central force, to the spin-orbit interaction, and to the tensor force via the  $(\nabla \times \vec{s})^2$  term.

The  $\rho$  meson has an identical effective Lagrangian, except that each density is isovector rather than isoscalar. We will denote the couplings constants as  $\mu_0$ ,  $\mu_1$  and  $\mu_2$  in analogy to the  $\omega$  couplings,  $\lambda_0$ ,  $\lambda_1$  and  $\lambda_2$  respectively.

### 5.3.4 Summary of Results

We have calculated the low energy effective field theories resulting from linear meson fields. In a theory with all four mesons, the effective Lagrangian will simply be the sum of the individual effective Lagrangians calculated in the above three sections. The properties of this Lagrangian are summarised in *Table 5.4*. The results have been terms which are very similar to those that appear in the Skyrme EDF (4.28). We should be careful not to confuse the Lagrangian we just derived with an EDF. On the other hand, just as the Skyrme EDF is the most general non-relativistic EDF which is local, bilinear, has derivatives only up to second order, the Lagrangian with interactions identical to (4.28) will be the most general Lagrangian with these properties. We could dub this the ‘Skyrme Lagrangian’, noting that the EDF derived from this will be the Skyrme EDF (though there is not necessarily a one-to-one correspondence between terms in the two).

We will begin with the central component of the nuclear force. In a theory with all

four mesons, we will find that the contribution to the central force is given by

$$\begin{aligned} \mathcal{L}_C = & \rho^2 \left[ \frac{g_0^2}{2m_\sigma^2} - \frac{\lambda_0^2}{2m_\omega^2} \right] - \frac{\mu_0^2 \rho_a^2}{2m_\omega^2} + \frac{\lambda_0^2}{2m_\omega^2 M^2} (\rho\tau - \vec{j}^2) + \frac{\mu_0^2}{2m_\rho^2 M^2} (\rho_a \tau_a - \vec{j}_a^2) \\ & - \frac{\rho \Delta \rho}{2m_\omega^2} \left( \frac{\lambda_0^2}{m_\omega^2} - \frac{1}{M^2} \left( \lambda_0 \lambda_1 + \frac{\lambda_0^2}{4} - \lambda_2^2 \right) \right) + \rho \Delta \rho \left[ -\frac{g_0^2}{8M^2 m_\sigma^2} + \frac{g_0^2}{2m_\sigma^4} \right] \\ & - \frac{\rho_a \Delta \rho_a}{2m_\rho^2} \left( \frac{\mu_0^2}{m_\rho^2} - \frac{1}{M^2} \left( \mu_0 \mu_1 + \frac{\mu_0^2}{4} - \mu_2^2 \right) \right). \end{aligned} \quad (5.25)$$

The  $\sigma$  gives an attractive force and the  $\omega$  a repulsive shorter ranged force. This partial cancellation is critical: it is responsible for keeping the binding per nucleon in nuclei around 8 MeV, much smaller than would be expected purely from dimensional analysis [3]. The  $\rho$  is also generally repulsive but is isospin dependent. Nuclear matter with an equal number of protons and neutrons is energetically favoured as a result. Our findings are in agreement with both meson-exchange models [19] and relativistic mean-field theory [70].

Next we turn to the spin-spin terms:

$$\mathcal{L}_{SS} = \frac{(\alpha_0 - \alpha_1)^2}{8m_\pi^2 M^2} (\nabla \cdot \vec{s}_a)^2 + \frac{(2\lambda_1 - \lambda_0)^2}{8m_\omega^2 M^2} (\nabla \times \vec{s})^2 + \frac{(2\mu_1 - \mu_0)^2}{8m_\rho^2 M^2} (\nabla \times \vec{s}_a)^2. \quad (5.26)$$

Notice we do not have a  $(\vec{s})^2$  term. Later we will discuss possible origins of this term. For now we simply note that its absence suggests that the term is less relevant to nuclear physics than might naively be expected. Furthermore notice that  $\mathcal{L}_{SS}$  is strictly positive, and hence the spin-spin terms will always increase the binding energy of nuclei. This is in agreement with relativistic mean-field calculations [71].

In traditional Skyrme parametrisations, the spin-spin terms are written in terms of the densities  $(\nabla \cdot \vec{s})^2$  and  $\vec{s} \Delta \vec{s}$ . As we discussed in the previous section, it is possible to rewrite the  $(\nabla \times \vec{s})^2$  in terms of these. In the isoscalar channel, this gives a relationship between the coefficients of the spin-gradient terms — the coefficients of the  $(\nabla \cdot \vec{s})^2$  and  $\vec{s} \nabla \vec{s}$  terms should be equal. This is our first non-trivial implication of meson physics.

We now turn to the spin-orbit terms

$$\begin{aligned} \mathcal{L}_{SO} = & \frac{\lambda_0^2 - \lambda_0 \lambda_1}{m_\omega^2 M^2} (\rho \nabla \cdot \vec{J}_v + \vec{s} \cdot \nabla \times \vec{j}) + \frac{\mu_0^2 - \mu_0 \mu_1}{m_\rho^2 M^2} (\rho_a \nabla \cdot \vec{J}_{va} + \vec{s}_a \cdot \nabla \times \vec{j}_a) \\ & + \rho \nabla \cdot \vec{J}_v \left[ \frac{g_0^2}{2M^2 m_\sigma^2} - \frac{\lambda_0^2}{2m_\omega^2 M^2} \right] - \rho_a \nabla \cdot \vec{J}_{va} \frac{\mu_0^2}{2m_\rho^2 M^2} \end{aligned} \quad (5.27)$$

Unlike the central terms, where the  $\sigma$  and the  $\omega$  acted in opposition, in the spin-orbit terms the  $\sigma$  and  $\omega$  add together — note the  $\omega$  contributes to two different spin-orbit terms and these both need to be considered. As a result we expect that the spin-orbit splittings in nuclei should be large even though the binding energy per nucleon is low, in agreement with the nuclear shell model phenomenology [72]. This is a generic feature of relativistic approaches to nuclear forces, but is difficult to explain in non-relativistic potential models [73].

The spin-orbit contribution is not Galilean invariant, as we find  $\rho \nabla \cdot \vec{J}_v$  terms without the attending  $\vec{s} \cdot \nabla \times \vec{j}$  term needed to ensure Galilean invariance. This should not be surprising — our non-relativistic limit was taken to second-order in  $M$ , explicitly breaking Galilean invariance. It is curious however that this is the only term that breaks Galilean

Type	Lagrangian Term	Isoscalar Origin	Isvector Origin
Central	$\rho^2$	$\sigma, \omega$	$\rho$
	$\rho\Delta\rho$	$\sigma, \omega$	$\rho$
	$\rho\tau - \vec{j}^2$	$\omega$	$\rho$
Spin-Spin	$\vec{s}^2$	None	None
	$\vec{s}\Delta\vec{s}$	$\omega$	$\rho$
	$(\nabla \cdot \vec{s})^2$	$\omega$	$\rho, \pi$
Spin-Orbit	$\rho\nabla \cdot \vec{J}_v + \vec{s} \cdot \nabla \times \vec{j}$	$\omega$	$\rho$
	$\rho\nabla \cdot \vec{J}_v$	$\sigma, \omega$	$\rho$
Tensor	$\vec{s} \cdot \vec{\tau} - J_{ij}J_{ij}$	None	None
	$\vec{s} \cdot \vec{F} - \frac{1}{2}(J_s^2 + J_{ij}J_{ji})$	None	None

**Table 5.4:** Origin of the Lagrangian Terms.

invariance in our final Lagrangian. Physically we can interpret the non-invariant terms as the Thomas precession. This effect can usually be derived by treating the nucleons classically (for instance see [74]), but here we can see the effect emerge from field theory. In a Galilean invariant theory these non-invariant parts should be dropped, and so in this sense the Thomas precession is a relativistic correction. However, the vector mesons also contribute to a Galilean invariant spin-orbit interaction, and this contribution should not be seen as a relativistic correction.

Finally we turn to the tensor components of the force. Like the  $(\vec{s})^2$  term, these two terms are absent in the Lagrangian, and we will discuss their origin later.

We have shown that theories with linear mesons can reproduce most, but not all, of the terms found in the Skyrme energy density functional. This has allowed us to relate Skyrme terms to meson phenomenology in an efficient manner. It is now logical to ask whether we can constrain Skyrme EDFs without any restrictions on the coupling constants. If we take the  $m_\omega$  and  $m_\rho$  masses to be set by experiments, then in the isoscalar channel we have six terms, to be determined by six parameters. In the isovector channel we again have six terms, but these are determined by four parameters. Hence our Lagrangian is not strongly constrained. We will defer a more in-depth treatment of the problem for the moment, and will return once we have studied the effect of meson-meson interactions.

## 5.4 Meson-Meson Interactions

We will start with the case of the  $\omega$  field. Non-linear behaviour can be introduced via the Lagrangian

$$\mathcal{L} = \bar{N}(i\not{\partial} - M)N - \frac{1}{4}(\partial^\mu\omega^\nu - \partial^\nu\omega^\mu)(\partial_\mu\omega_\nu - \partial_\nu\omega_\mu) + \frac{1}{2}m_\omega^2\omega^2 - \frac{1}{24}\zeta(\omega^2)^2 + \omega_\mu J^\mu, \quad (5.28)$$

where the source  $J^\mu$  is written in terms of  $N$  in (5.20). As our theory is an effective one, we should in principle include further non-renormalisable terms such as a  $(\omega^2)^3$  term, but for simplicity we will temporarily ignore this. In order to calculate the low-energy meson-less effective field theory, we need to evaluate the path-integral

$$W[J] = \int D\omega e^{i \int dx^4 \left( -\frac{1}{4}(\partial^\mu\omega^\nu - \partial^\nu\omega^\mu)(\partial_\mu\omega_\nu - \partial_\nu\omega_\mu) + \frac{1}{2}m_\omega^2\omega^2 - \frac{1}{24}\zeta(\omega^2)^2 + \omega_\mu J^\mu \right)}, \quad (5.29)$$

The parameter  $\zeta$  is undetermined. Comparing to quantum hadrodynamical models, which fit these parameters to nuclear properties using relativistic mean-field theory, we find that this parameter is not necessarily small. It is however under-constrained by nuclear data [20]. This is not surprising in light of the results of the previous section, which showed that even a simple linear meson model does not provide strong constraints on a Skyrme functional. Introducing new non-linear couplings can only worsen the predictive power of our theory.

As we discussed in Section 3.6, it is difficult to evaluate  $W[J]$  in the non-perturbative regime. Analogous to (3.55), we can expand

$$W[J] = \int dx^4 \left( \frac{a_0}{m_\omega^2} J^2 + \frac{a_1}{m_\omega^4} J^\mu \partial^2 J_\mu + \frac{a_2}{m_\omega^4} (\partial^\mu J_\mu)^2 + \dots + \frac{b_0}{m_\omega^8} (J^2)^2 + \dots \right) \quad (5.30)$$

where the coefficients  $a_i$  and  $b_i$  are dimensionless functions of  $\lambda$ . In the perturbative regime we can expand

$$a_0 = -\frac{1}{2} + O(\lambda^2), \quad a_1 = \frac{1}{2} + O(\lambda^2), \quad a_2 = -\frac{1}{2} + O(\lambda^2), \quad b_0 = \lambda + O(\lambda^2). \quad (5.31)$$

Setting  $\lambda = 0$  will then yield the Gaussian result (3.23) as expected.

In general though, the Gaussian result must be modified. This, in turn, will modify the effective Lagrangian (5.23). In particular, we expect there to be higher-order density dependence such as the  $(J^2)^2$  term. In the non-relativistic limit, the leading order contribution of this will be a  $\rho^4$  term. More generally, each term in (5.23) will become density dependent.

The situation becomes more complicated when we consider interactions between the  $\sigma$ ,  $\omega$  and  $\rho$  mesons (we will discuss the pion later). With these three mesons we have the following nine renormalisable interactions:

$$\sigma^3, \quad \sigma^4, \quad \sigma\omega^2, \quad \sigma^2\omega^2, \quad \sigma\rho^2, \quad \sigma^2\rho^2, \quad (\omega^2)^2, \quad (\rho^2)^2, \quad \omega^2\rho^2. \quad (5.32)$$

We also can introduce non-renormalisable interactions such as

$$\sigma^2\bar{N}N, \quad \omega^2\bar{N}N, \quad \sigma^5, \quad \sigma(\partial\sigma)^2, \quad \dots \quad (5.33)$$

Even enumerating all non-renormalisable terms up to a given order is difficult. Field redefinitions can partially help — for instance the  $\sigma^2\bar{N}N$  term which we used in Section 3.5 can actually be removed in this way [75]. Nevertheless, the brute force approach of including as many terms as possible is clearly not feasible. Whilst these terms will all generically be present in any meson model, they are impossible to constrain. The simplest approach is to use the results of Section 3.6 to generalise (5.30). In general our effective Lagrangian should involve all possible combinations of the sources (5.3) and (5.19):

$$\begin{aligned} J_\sigma &= g_0\bar{N}N + \frac{g_2}{M}\partial_\mu(\bar{N}\gamma^\mu N), \\ J_\omega^\mu &= \lambda_0\bar{N}\gamma^\mu N + \frac{\lambda_1}{M}\partial_\nu\bar{N}\sigma^{\mu\nu}N + \frac{\lambda_2}{M}\partial^\mu(\bar{N}N), \\ J_{\rho a}^\mu &= \mu_0\bar{N}\gamma^\mu\tau_a N + \frac{\mu_1}{M}\partial_\nu\bar{N}\sigma^{\mu\nu}\tau_a N + \frac{\mu_2}{M}\partial^\mu(\bar{N}\tau_a N). \end{aligned} \quad (5.34)$$

We can expand  $W[J]$  in inverse powers of the meson mass scale,  $m \sim 700$  GeV:

$$W[J] = \left( \frac{1}{m^2} W_2[J] + \frac{1}{m^4} W_4[J] + \frac{1}{m^5} W_5[J] + \dots \right). \quad (5.35)$$

The lowest-order contribution is given by

$$W_2[J] = \int dx^4 (C_1 J_\sigma^2 + C_2 (J_\omega)^2 + C_3 (J_{\rho a})^2) \quad (5.36)$$

followed by the fourth-order contribution

$$W_4[J] = \int dx^4 (D_1 J \partial^2 J + D_2 J_\omega^\mu \partial^2 J_{\mu\omega} + D_3 (\partial_\mu J_\omega)^2 + D_4 J_{\rho a}^\mu \partial^2 J_{\mu\rho a} + D_5 (\partial_\mu J_{\rho a})^2) \quad (5.37)$$

and the fifth-order

$$W_5[J] = \int dx^4 J_\sigma (E_1 J_\sigma^2 + E_2 (J_\omega)^2 + E_3 (J_{\rho a})^2). \quad (5.38)$$

The coupling constants  $C_i, D_i$ , and  $E_i$  are dimensionless. The two lowest-order contributions are a simple generalisation of the linear meson case. Indeed, we can recover the linear case (with  $g_1 = 0$ ) via the substitutions

$$\begin{aligned} C_1 &= \frac{m^2}{2m_\sigma^2}, & C_2 &= -\frac{m^2}{2m_\omega^2}, & C_3 &= -\frac{m^2}{2m_\rho^2}, \\ D_1 &= \frac{m^4}{2m_\sigma^4}, & D_2 &= -\frac{m^4}{2m_\omega^4}, & D_3 &= -\frac{m^4}{2m_\rho^4}, & D_4 &= -\frac{m^4}{2m_\rho^4}, & D_5 &= -\frac{m^4}{2m_\rho^4}. \end{aligned} \quad (5.39)$$

The terms in  $W_5[J]$  will result in density-dependent Skyrme terms. Higher order terms in  $W[J]$  will involve more complicated density-dependence and higher-order derivatives. These are however suppressed by powers of  $M$ , and so the terms  $W_2, W_3$  and  $W_5$  are the most important at low energies. As a result, generalising to non-linear meson theories does not significantly change the low-energy limit. This may seem surprising at first but is a direct consequence of effective field theory — details of meson interaction should not be relevant for low energy nuclear physics. Notice also that  $W_5[J]$  will include a  $\rho^3$  term, which, if repulsive, can counteract the effect of the  $\rho^2$  and therefore allow for nuclear saturation. Hence we can see that nuclear saturation is an effect that can generically occur in any meson model — postulating a specific mechanism for it, whether that be relativistic effects [76] or nucleon polarisation via the sigma [39] ignores the complexity of meson physics.

Next we should ask, will an interacting theory generate the tensor terms and the  $\vec{s}^2$  term which were conspicuously absent in the previous section? A quick look at (5.34) combined with the results of Section 4.3 can confirm that they will not appear even in an interacting theory. The only Dirac bilinears that yield a density  $\vec{s}$  in the non-relativistic limit are the tensor and the pseudovector coupling. Our Lagrangian would therefore need to include at least one of the following terms

$$\bar{N} \sigma^{\mu\nu} N \bar{N} \sigma_{\mu\nu} N, \quad \bar{N} \gamma^\mu \gamma^5 N \bar{N} \gamma_\mu \gamma^5 N, \quad (5.40)$$

once the meson fields are integrated out. There are two ways to achieve this. The first

would be to couple the nucleons to a tensor meson or a pseudovector meson. This seems a little implausible, as the necessary mesons do not appear in *Table 5.2* and therefore must be quite heavy. Since we are working in an effective field theory however, the terms in (5.40) will also generically appear, suppressed by powers of the cut-off  $M$ . Since the nucleon is a composite particle, these terms do not need to be associated with meson exchange but could result from more complicated dynamics, such as nucleon excitations. That we do not see the  $\vec{s}^2$  terms and the tensor terms in our simple meson exchange model suggests that in the Skyrme energy density functional, these terms originate primarily as Fock terms.

### 5.4.1 Relationship to Relativistic Mean-Field Theory

Although our primary focus is on Skyrme interactions, it is worth considering for a moment the relationship of our methods to relativistic mean-field (RMF) theory. The starting point of relativistic mean-field is a Lagrangian with both mesons and nucleons. In the RMF approach, the meson fields are treated classically and solved self-consistently. Meson interactions can be included in this approach, and indeed they are critical in reproducing the experimentally observed properties of nuclear matter.

Observe that the RMF approach is effectively a type of semiclassical expansion. This simple fact is unfortunately obscured by the language traditionally used in RMF.

Once the meson fields are treated classically, it is trivial to integrate them out of a theory. If we can calculate the meson fields analytically, then (3.27) gives the partition function. In general this is not possible though, and Feynman diagrams provide the simplest tool to derive the low-energy theory. If  $\hbar$  is not set to 1, then each loop in a Feynman diagram contributes a factor of  $\hbar$  [22]. The classical result is then just the sum of tree-level diagrams, which do not include any loops. For the  $\omega$  theory from the previous section, with Lagrangian (5.28), we find that

$$W_{\text{RMF}}[J] = \text{---} + \text{X} + \text{Y} + \dots \quad (5.41)$$

We can then take the low-energy limit of this functional by considering the low-energy expansion of the propagator (3.23). The first term will reproduce the linear results of Section 5.3.3, and the second term will introduce a density dependent term  $\zeta\rho^4$ . So RMF theory extends the results of linear meson theories by including density dependent terms, but it will not modify the terms originating in the linear case.

It is straightforward to see how this generalises. Any interaction term will be represented by intersection of three or more points in a Feynman diagram. If there are no loops in the diagram, the diagram necessarily involves at least three sources. Hence the contribution of the diagram will be at least cubic in  $J$  and so will not modify the quadratic terms.

We have found that RMF occupies a middle ground between linear theories and general interacting theories — density-dependent terms are added, but the quadratic terms are not modified. Nevertheless, it is impossible to justify in the context of strong coupling constants, since in this regime loop corrections could be important. This issue is mitigated by fitting coupling constants to low-energy nuclear data, although this sacrifices any ability to extrapolate calculations beyond known regions of the nuclear chart with any certainty.

### 5.4.2 Expanding around Nuclear Saturation Density

We have so far expanded around the vacuum,  $\rho = 0$ . In nuclear calculations however, we are most interested in expanding around nuclear saturation density,

$$\rho_C \approx 0.16 \text{ fm}^{-3} \approx 107^3 \text{ MeV}^3 \approx (0.15m)^3. \quad (5.42)$$

For instance, if we wished to incorporate the effects of  $W_5[J]$  most efficiently, we can rewrite

$$\begin{aligned} W_2[J] + W_5[J] &= \int dx^4 \frac{1}{m^2} \left( C_1 J_\sigma^2 + C_2 (J_\omega)^2 + C_3 (J_{\rho a})^2 + \frac{J_\sigma}{m^3} (E_1 J_\sigma^2 + E_2 (J_\omega)^2 + E_3 (J_{\rho a})^2) \right) \\ &= \frac{1}{m^2} \int dx^4 \left[ \left( C_1 + \frac{E_1 \rho_C^3}{m^3} \right) J_\sigma^2 + \left( C_2 + \frac{E_2 \rho_C^3}{m^3} \right) (J_\omega)^2 + \left( C_3 + \frac{E_3 \rho_C^3}{m^3} \right) (J_{\rho a})^2 \right. \\ &\quad \left. + \left( \frac{J_\sigma - \rho_C^3}{m^3} \right) (E_1 J_\sigma^2 + E_2 (J_\omega)^2 + E_3 (J_{\rho a})^2) \right]. \end{aligned} \quad (5.43)$$

We can generalise this rearrangement to include higher powers of  $J$ . We can now define the ‘in-medium’ coupling constants

$$c_1 = C_1 + \frac{E_1 \rho_C}{m^3} + O\left(\frac{\rho_C^2}{m^6}\right), \quad c_2 = C_2 + \frac{E_2 \rho_C}{m^3} + O\left(\frac{\rho_C^2}{m^6}\right), \quad c_3 = C_3 + \frac{E_3 \rho_C}{m^3} + O\left(\frac{\rho_C^2}{m^6}\right). \quad (5.44)$$

These are the constants which are most relevant for many-body calculations, as they automatically incorporate the ‘in-medium’ effects.

## 5.5 Rescaling Parameters

We now return to the question posed in Section 5.3: Can we use our results to predict the value of Skyrme parameters from higher energy physics? There are really two parts to this question. We need both to know whether parameters such as  $g_i$ ,  $\lambda_i$  and  $\mu_i$  can be measured experimentally or derived theoretically, and we then need to know if these values lead to predictions in the Skyrme interaction. In light of the results of the previous section, it may seem like we have an impossible task, as we were forced to introduce a series of constants  $c_i$ ,  $d_i$  and  $e_i$ , along with the generic prediction that all terms should be density-dependent. But as we shall see, this is overly pessimistic.

First note that we have the freedom to rescale our parameters. By rescaling the parameters  $g_i$ ,  $\lambda_i$ , and  $\mu_i$ , we are able to set  $c_i$  to their linear values as given in (5.39). Notice that rescaling (say)  $g_i$  by a factor of  $R$  is equivalent to rescaling by a factor of  $1/R^2$ . So we are only able to rescale  $c_i$  to their linear values if the coefficients in the interacting theory have the same sign as the coefficients in the linear theory. From our proof of (3.56) at the end of Section 3.6, we know that the rescaling is justified for the bare parameters  $C_i$ . Since  $c_i$  are related to  $C_i$  by a small perturbation ( $\rho_C = (0.15m)^3$ ), as long as the constants  $E_i$  are not unnaturally large, we should expect  $c_i$  to also have the correct signs to enable the rescaling.

It is most convenient to rescale so that

$$c_1 = 1, \quad c_2 = -1, \quad c_3 = -1, \quad (5.45)$$

allowing us to use a single mass scale  $m$  in our Lagrangian. We will denote the rescaled

mass parameters by  $\tilde{g}_i$ ,  $\tilde{\lambda}_i$  and  $\tilde{\mu}_i$ . With this rescaling, we find that  $W_2[J]$  in the non-relativistic limit will produce a result very close to that of Section 5.3.4:

$$\begin{aligned}
W_2^{\text{NR}}[J] = & \int dx^4 \frac{1}{m^2} \left( (\tilde{g}_0^2 - \tilde{\lambda}_0^2) \rho^2 - \tilde{\mu}_0^2 \rho_a^2 + \frac{1}{M^2} (\tilde{\lambda}_0^2 (\rho \tau - \vec{j}^2) + \tilde{\mu}_0^2 (\rho_a \tau_a - \vec{j}_a^2)) \right. \\
& + \frac{1}{4M^2} \left( \tilde{\alpha}^2 (\nabla \cdot \vec{s}_a)^2 + (2\tilde{\lambda}_1 - \tilde{\lambda}_0)^2 (\nabla \times \vec{s})^2 + (2\tilde{\mu}_1 - \tilde{\mu}_0)^2 (\nabla \times \vec{s}_a)^2 \right) \\
& + \frac{1}{M^2} \left( (\tilde{\lambda}_0^2 - \tilde{\lambda}_0 \tilde{\lambda}_1) (\rho \nabla \cdot \vec{J}_v + \vec{s} \cdot \nabla \times \vec{j}) + (\tilde{\mu}_0^2 - \tilde{\mu}_0 \tilde{\mu}_1)^2 (\rho \nabla \cdot \vec{J}_v + \vec{s} \cdot \nabla \times \vec{j}) \right) \\
& \left. + \frac{1}{2M^2} \left( \rho_a \nabla \cdot \vec{J}_{va} (\tilde{g}_0^2 - \tilde{\lambda}_0^2) - \tilde{\mu}_0^2 \rho_a \nabla \cdot \vec{J}_{va} \right) + \rho_a \Delta \rho_a \text{ terms} \right)
\end{aligned} \tag{5.46}$$

The  $\tilde{\alpha}^2$  term contains the rescaled contribution from the pion. Since the  $\rho \Delta \rho$  terms will receive contributions from  $W_4[J]$  which cannot be constrained, there is little point in writing out the contribution for these terms from  $W_2[J]$ . It is simplest to instead introduce rescaled coefficients  $\tilde{d}_1$  and  $\tilde{d}_2$ , so that

$$W_2^{\text{NR}}[J] + W_4^{\text{NR}}[J] = \int dx^4 \frac{1}{m^4} \left( \tilde{d}_1 \rho \Delta \rho + \tilde{d}_2 \rho_a \Delta \rho_a \right) + \text{other terms} \tag{5.47}$$

After these rescalings, calculating or measuring the parameters  $\tilde{g}_i$ ,  $\tilde{\lambda}_i$ , and  $\tilde{\mu}_i$  will be even more difficult than previously. But their ratios are unchanged by this procedure. Utilising this we can still make predictions.

## 5.6 Vector and Tensor Couplings

Staring at (5.46), we note that there are two pairs of parameters we may hope to relate —  $\tilde{\lambda}_0$  to  $\tilde{\lambda}_1$ , and  $\tilde{\mu}_0$  to  $\tilde{\mu}_1$ . The two parameters govern, respectively, the vector and the tensor couplings of the nucleon to the vector boson. Though both quantities have been rescaled, we can consider their ratios:

$$\frac{\tilde{\lambda}_1}{\tilde{\lambda}_0} = \frac{\lambda_1}{\lambda_0} = \frac{1}{2} \kappa_\omega = \frac{\mu_\omega - 1}{2}, \quad \frac{\tilde{\mu}_1}{\tilde{\mu}_0} = \frac{\mu_1}{\mu_0} = \frac{1}{2} \kappa_\rho = \frac{\mu_\rho - 1}{2}. \tag{5.48}$$

To understand these ratios, we should consider a third vector boson, whose coupling to the nucleon is experimentally accessible — the photon. Because the nucleon is not a point-like particle, both protons and neutrons have magnetic moments which differ from the Dirac prediction. These have been measured to an extremely high precision experimentally [56]:

$$\mu_P = 2.792847356 \pm 0.000000023, \quad \mu_N = -1.91304272 \pm 0.000000045. \tag{5.49}$$

The photon does not respect isospin invariance, and so it is useful to introduce the isoscalar and isovector anomalous magnetic moments

$$\mu_s = \mu_P + \mu_N = 0.88, \quad \mu_v = \mu_n - \mu_p = 4.71. \tag{5.50}$$

Two different phenomenological models, the vector dominance model (VDM) due to Sakurai [77] and the quark-meson coupling (QMC) model due to Guichon [78], make the pre-

diction that

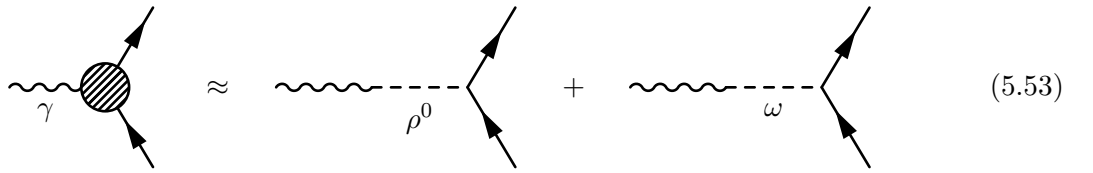
$$\mu_\rho = \mu_s, \quad \mu_\omega = \mu_v, \quad (5.51)$$

although the justification for this result differs. Using (5.50), we have the predictions

$$\kappa_\rho = 3.71, \quad \kappa_\omega = -0.12. \quad (5.52)$$

The tensor coupling of the  $\rho$  is therefore much more important than that of the  $\omega$ , in agreement with the prediction of traditional meson phenomenology [19].

In the VDM, the interaction of the photon with the nucleon is assumed to be dominated by the neutral vector bosons, the  $\omega$  and the  $\rho^0$ . Since these bosons have the same quantum numbers as the photon, mixing can occur. Diagrammatically, we can understand the VDM model as



$$\gamma \text{ vertex} \approx \rho^0 \text{ vertex} + \omega \text{ vertex} \quad (5.53)$$

so that the form factor  $\gamma NN$  is dominated by a virtual vector meson exchange. We would then expect that the magnetic moments of the nucleon to be dominated by the tensor couplings of these vector mesons, and so we can derive (5.51). More details can be found in [79, 80].

The QMC model is a generalisation of the MIT bag model, where not only the photon but also general mesons interact directly with point-like quarks confined within a spherical cavity. In the MIT bag model, the electroweak properties can be calculated directly from the quark wavefunctions [81]. This yields predictions which are reasonably close to the experimental values (see Chapter 12 of [58]) for both the octet and decuplet baryons, and this agreement is improved through the inclusion of pionic corrections [82].

In the QMC model the vector mesons couple directly to quarks in a manner completely analogous to the photon. Therefore the tensor couplings of the rho and omega are generated by the quark structure of the nucleon [39], and so (5.51) should be satisfied.

How well does the prediction (5.51) hold experimentally? Dispersion analysis of  $NN$  and  $N\pi$  scattering have been used to yield values of  $\kappa_\rho = 6.6 \pm 1$  [83],  $6.1 \pm 0.6$  [84], and  $6.1 \pm 0.2$  [85]. A value of 5.9 was found in [86] using an effective  $\rho$  mass of 0.63 GeV. These values are about 40% greater than the prediction of (5.52).

Similarly, the value of  $\kappa_\omega$  was found to be  $-0.17$  in [88] and  $-0.16 \pm 0.01$  in [85], a  $\sim 25\%$  increase in magnitude from the prediction of (5.52). Overall this suggests that we should use values around

$$\mu_\rho = 7.1 \pm 0.2, \quad \mu_\omega = 0.84 \pm 0.01, \quad (5.54)$$

leading to

$$\kappa_\rho = 6.1 \pm 0.2, \quad \kappa_\omega = -0.16 \pm 0.01, \quad (5.55)$$

rather than the values of (5.52).

Various theoretical arguments have been suggested to explain this discrepancy — a summary can be found in [87]. Whilst the specifics vary, the inclusion of pions is critical in all of these models.

## 5.7 Discussion

We have shown that under general conditions, the lowest-order contributions to nuclear interactions will be given by a Skyrme-like Lagrangian, with higher-order contributions responsible for density dependence of the coupling constants. Although we began by considering the relevant mesons and other aspects of strong QCD, we have steadily stripped our theory of any direct link with this high energy physics. We should now consider what physics is important in order to reproduce a realistic form of the nuclear force.

The most obvious piece of physics that has remained relevant throughout are the symmetries associated with QCD. Isospin symmetry allows us to treat the nucleon as a single species, so that proton-proton, neutron-neutron, and proton-neutron forces are all facets of the same underlying force. Space-time symmetries are critical in determining the allowed interactions, both relativistically and non-relativistically. As we saw in Chapter 4, different terms in a non-relativistic theory are often related relativistically. This is manifest in our expression for  $W_2^{\text{NR}}$  (5.46), where a handful of relativistic coupling constants are able to relate numerous non-relativistic terms.

One symmetry which has not featured prominently has been chiral symmetry. Unlike the other three mesons, we found that the pion only contributes a measly  $(\nabla \cdot \vec{s}_a)^2$ , triply suppressed in many-body physics as the square of a time-odd, derivative, isovector term. Since chiral symmetry is spontaneously broken, with the pion being the pseudo-Nambu Goldstone boson, the irrelevance of chiral symmetry to nuclei can be related to the relative unimportance of pions.

This situation contrasts with the critical role that pions play in scattering. Since the pion is much lighter than any other meson, for nucleon-nucleon scattering the pion is the most important particle. Unlike many-body nuclear forces, in the last two decades a systematic understanding of nucleon scattering has been developed, using chiral perturbation theory ( $\chi$ PT) [89]. A detailed discussion of  $\chi$ PT would be to far afield from our current discussion, but we shall return to this subject in the conclusion.

The critical physical inputs to our theory were the energy scales of the higher-energy physics. These scales were the light meson energy scale  $m \sim 700$  MeV, and the QCD scale  $\Lambda \sim 1$  GeV. On the other hand, the specific masses of the sigma, omega, and rho meson are not actually that relevant, as we saw that through non-linearities and rescaling they could be removed. It is an unfortunate weakness of our models that the light (non-pseudo Nambu Goldstone) mesons are not much lighter than the QCD scale, and for this reason it is difficult to draw strong conclusions from the absence of various terms (such as the tensor terms) in our theories.

Another important input is that we need to know how the nucleon couples to higher energy physics. This is given in terms of the sources (5.34), and we found that the relevant channels are the scalar-isoscalar, vector-isoscalar, and vector-isovector channels. In a meson model these channels correspond to the sigma, omega and rho mesons respectively. Notice however that any details of the mesons are actually irrelevant at low energies. For instance, the conclusions of Section 5.4 would be unchanged if there were three omega mesons rather than one, or if the self-couplings of the mesons were shuffled around. All that matters is their transformation properties under spin and isospin symmetries.

Finally, in order to reproduce realistic nuclear forces, it is necessary to include non-linear interactions. These interactions are needed in order to reproduce the observed properties of nuclear matter, such as nuclear saturation. However, as we discussed in Section 5.4 the actual details of these interactions are impossible to constrain, so whilst some

---

non-linearities are needed (and all should be included in principle), various combinations will give indistinguishable behaviour at low energies.

To concisely summarise, the four ingredients which are necessary to reproduce a realistic nuclear force are:

1. Symmetries — isospin, Lorentzian, and parity.
2. A meson energy scale  $m$  and QCD energy scale  $\Lambda$ .
3. The interaction channels — scalar-isoscalar, vector-isoscalar, and vector-isovector.
4. Non-linearities to achieve nuclear saturation, though the details are not important.

Since any theory with these properties will reproduce a Skyrme-like Lagrangian at low energies, any theory with such properties will be able to reproduce realistic nuclear forces if the parameters are fitted to nuclear data.

Our results explain how a plethora of models are all able to reproduce the properties of nuclei. At heart, the problem of determining the correct higher energy physics is simply very under-constrained. The successful reproduction of experimental results is often used to justify that a model is ‘correct’ in that the physics involved is the most relevant and the model should remain valid when extrapolated to new regimes. Our work shows that this cannot be considered a sufficient criteria for judging validity. To justify a model, either compelling theoretical evidence or connections to experimental data outside of many-body nuclear physics (such as scattering data) should be required.

Furthermore, the logic of effective field theory suggests that no simple theory of nuclear forces can exist. At high energies there are many competing theoretical processes which can explain any given feature of low energy nuclear phenomenology. Effective field theory suggests that all of these processes should be considered and all will likely be relevant. Developing complicated phenomenological models will not lead to progress, but rather a proliferation of unconstrained parameters.

We will return to the question of how we can further our understanding of nuclear forces in the conclusion. In the next chapter, we shall quantitatively study the Lagrangian derived in this chapter, and will compare to existing Skyrme parametrisations.



---

# The Energy Density Functional for Time-Even Systems

---

In the previous chapter we derived a universal form of the low-energy nuclear force in (5.46) and (5.47), using eight parameters. We also discussed how the vector and tensor coupling constants could be related, reducing the total number of parameters to only six. This is much less than the number of parameters used in traditional Skyrme functionals.

In this chapter we will study quantitatively the predictions of (5.46) and (5.47) for systems exhibiting symmetry under time reversal (time-even systems). This is the case most commonly considered in nuclear simulations, and most Skyrme parametrisations in the literature have been constrained for time-even systems only.

## 6.1 The Time-Even EDF

In order to compare our Lagrangians to Skyrme EDFs, we will need to derive the energy density functional. We can use the methods discussed in Section 4.4. Under time reversal, spin up nucleons are mapped to spin down nucleons. For a time-even system, this means that

$$\rho_{N\uparrow} = \rho_{N\downarrow}, \quad \rho_{P\uparrow} = \rho_{P\downarrow} \quad (6.1)$$

so that we only need to keep track of the neutron and proton mean-fields. This greatly simplifies our calculations.

Using the methods of Section 4.4, we are able to now calculate the expectation values of the various operators in (5.46) and (5.47). The calculations are contained in *Appendix C*. It is then straightforward to calculate the time-even EDF from (5.46) and (5.47). To simplify notation, in this chapter and the next we shall make the replacements

$$\begin{aligned} \tilde{g}_0 &\rightarrow g, & \tilde{\lambda}_0 &\rightarrow \lambda, & \tilde{\mu}_0 &\rightarrow \mu \\ \tilde{\alpha} &\rightarrow \alpha, & \tilde{d}_1 &\rightarrow d_1, & \tilde{d}_2 &\rightarrow d_2 \end{aligned} \quad (6.2)$$

in order to remove now redundant tildes and subscripts. With this substitution, the time-

even EDF is now given by

$$\begin{aligned}
\mathcal{E} = & \frac{1}{4m^2} \int dx^4 \left[ \rho^2(-3g^2 + 3\lambda^2 - 3\mu^2) + \rho_a^2(g^2 - \lambda^2 + 5\mu^2) \right. \\
& + \frac{1}{2M^2} (-5g^2 + 5\lambda^2(1 - 2\mu_\omega) + 3\mu^2(1 - 2\mu_\rho)) \rho \nabla \cdot \vec{J}_v \\
& + \frac{1}{2M^2} (-g^2 + \lambda^2(1 - 2\mu_\omega) + 3\mu^2(1 - 2\mu_\rho)) \rho_a \nabla \cdot \vec{J}_{va} \\
& + \frac{1}{16m^2} \left( -56d_1 + 24d_2 - \frac{m^2}{M^2} (6\alpha^2 + (\mu_\omega^2 - 4\mu_\omega + 8)\lambda^2 + 3(\mu_\rho^2 - 4\mu_\rho + 8)\mu^2) \right) \rho \Delta \rho \\
& + \frac{1}{16m^2} \left( 8d_1 - 72d_2 + \frac{m^2}{M^2} (2\alpha^2 - (\mu_\omega^2 - 4\mu_\omega + 8)\lambda^2 + (\mu_\rho^2 - 4\mu_\rho + 8)\mu^2) \right) \rho_a \Delta \rho_a \\
& + \frac{1}{4M^2} \left( (\mu_\omega^2 - 4\mu_\omega - 12)\lambda^2 + 3(\mu_\rho - 2)^2 \mu^2 + 6\alpha^2 - \frac{8M^2}{m^2} (d_1 + 3d_2) \right) \rho \tau \\
& + \frac{1}{4M^2} \left( (\mu_\omega - 2)^2 \lambda^2 - (\mu_\rho^2 - 4\mu_\rho - 20)\mu^2 - 2\alpha^2 - \frac{8M^2}{m^2} (d_1 - d_2) \right) \rho_a \tau_a \\
& + \frac{1}{4M^2} \left( \frac{8M^2}{m^2} (d_1 + 3d_2) + 6\alpha^2 - \lambda^2(5\mu_\omega^2 - 20\mu_\omega + 16) - 3\mu^2(5\mu_\rho^2 - 20\mu_\rho + 16) \right) J_{ij} J_{ij} \\
& + \frac{1}{4M^2} \left( \frac{8M^2}{m^2} (d_1 - d_2) - 2\alpha^2 - \lambda^2(5\mu_\omega^2 - 20\mu_\omega + 16) + \mu^2(5\mu_\rho^2 - 20\mu_\rho + 16) \right) J_{ija} J_{ija} \\
& + \frac{1}{8M^2} (6\alpha^2 - 3\lambda^2(\mu_\omega - 2)^2 - 9\mu^2(\mu_\rho - 2)^2) (J_{ij} J_{ji} + J_s^2) \\
& \left. + \frac{1}{8M^2} (-2\alpha^2 - 3\lambda^2(\mu_\omega - 2)^2 + 3\mu^2(\mu_\rho - 2)^2) (J_{ija} J_{jia} + (J_{sa})^2) \right]. \tag{6.3}
\end{aligned}$$

Comparing to (4.28), the various coefficients  $C_i^A$  can be read off the EDF. We find that these coefficients are linear combinations of  $g^2$ ,  $\lambda^2$ ,  $\mu^2$ ,  $\alpha^2$ ,  $d_1$  and  $d_2$ . As there are twelve Skyrme coefficients, we have reduced the number of degrees of freedom in the Skyrme functional by six.

The rest of this chapter will examine the implications of (6.3). By comparing to existing Skyrme parametrisations, we shall be able to test whether the Skyrme parametrisations are compatible with our EDF. As more Skyrme parameters exist than input parameters, we shall be able to relate Skyrme parameters to each other.

Another potential use of (6.3) is to take parameters from relativistic mean-field theory. As discussed in Section 5.4.1, RMF gives values of  $g^2$ ,  $\lambda^2$ ,  $\mu^2$ , and so (6.3) allows us to efficiently calculate the low energy behaviour of the theory. Difficulties emerge in this approach when attempting to account for density-dependent terms, and so in this thesis we will focus on non-relativistic Skyrme parametrisations. Nevertheless, comparing Skyrme and RMF using (6.3) is an interesting possibility that should be pursued in future work.

## 6.2 Skyrme Parametrisations

### 6.2.1 Parametrisations Used

Numerous Skyrme parametrisations exist in the literature. For instance, [8] presents a comparison of 240 distinct sets of parameters. We can only take a small subset of these parameters, listed in *Table 6.1*. These parametrisations were chosen as they are commonly

Name	Paper	$\gamma$	Isvector Spin-Orbit	Tensor
UNEDF0	[90]	0.322 (Fitted)	Fixed	No
UNEDF1	[91]	0.270 (Fitted)	Fitted	No
UNEDF2	[92]	0.377 (Fitted)	Fitted	Yes (Spherical)
SLy4	[93]	1/6 (Fixed)	Fixed	No
SLy6	[93]	1/6 (Fixed)	Fixed	No
SLy10	[93]	1/6 (Fixed)	Fitted	No
SkM*	[94]	1/6 (Fixed)	Fixed	No
SkI4	[95]	1/4 (Fixed)	Fixed	No
BSk1	[96]	1/3 (Fixed)	Fixed	No

**Table 6.1:** Skyrme parametrisations considered in this thesis.

used in mean-field calculations.

There are several ways to parametrise a Skyrme EDF. We will use the parametrisation

$$\mathcal{E}_{\text{Skyrme}} = \int dx^3 \left[ \sum_{t=0,1} \frac{C_t^\rho[\rho]}{m^2} \rho_t^2 + \frac{C_t^{\Delta\rho}}{m^4} \rho_t \Delta \rho_t + \frac{C_t^\tau}{m^2 M^2} \rho_t \tau_t + \frac{C_t^{SO}}{m^2 M^2} \rho_t \nabla \cdot \vec{J}_{vt} - \frac{C_t^T}{m^2 M^2} J_{ij} J_{ij} - \frac{C_t^F}{2m^2 M^2} (J_{ij} J^{ji} + J_s^2) \right] \quad (6.4)$$

where  $t = 0$  denotes an isoscalar and  $t = 1$  an isovector. We have included factors of  $m$  and  $M$  so that the parameters are unitless. Because density dependent terms are needed to reproduce nuclear saturation, the coefficient  $C_t^\rho$  is not constant, but instead is given by

$$C_t^\rho[\rho] = C_{t0}^\rho + \frac{C_{tD}^\rho}{m^{3\gamma}} \rho^\gamma. \quad (6.5)$$

We are most concerned with the value of this parameter around nuclear saturation density  $\rho_C$ , and so for brevity will define

$$C_t^\rho \equiv C_t^\rho[\rho_C]. \quad (6.6)$$

This form of density dependence is purely phenomenological. Often  $\gamma$  is fixed ( $\gamma = 1/6$  is particularly common), though in the UNEDF parametrisations,  $\gamma$  was fitted. Similarly, the isovector component of the spin-orbit term is often fixed to a third of the isoscalar coupling. This is also included in *Table 6.1*.

Few Skyrme parametrisations include tensor terms, fixing

$$C_t^T = C_t^F = 0. \quad (6.7)$$

Of the Skyrme forces considered, only UNEDF2 includes some of the tensor terms. Even UNEDF2 fits the tensor only for spherically symmetric systems — this allows the coefficients

$$C_t^J = \frac{C_t^F}{2} - C_t^T \quad (6.8)$$

to be constrained.

### 6.2.2 Fitting Parameters and Uncertainties

The physical content of Skyrme parametrisations is strongly linked to the methodology used to fit their parameters. Some parameters are far better constrained than others.

Symmetric infinite nuclear-matter (SNM) provides an important idealisation, and its properties can be approximated by studying the bulk properties of heavy nuclei. In this idealisation, the proton and neutron densities are equal and there are no Coulomb forces, so the only terms which contribute are the isoscalar  $C_0^\rho[\rho]\rho^2$  and effective mass term  $C_0^\tau\rho\tau$ .

The saturation density  $\rho_C$  and energy per nucleon  $E_A^{NM}$  are the most straightforward terms to extrapolate from experimental data [97]:

$$\rho_C \approx 0.16 \text{ fm}^{-3}, \quad E_A^{NM} = -16 \text{ MeV.} \quad (6.9)$$

In order to relate these quantities to  $C_0^\rho$  and  $C_0^\tau$  we also need to know the isoscalar effective mass  $M_s^*[\rho_C]/M$ . The value of  $M_s^*[\rho_C]/M$  is not well constrained [98], but values around unity are consistent with experimental single-particle energies [99]. The coefficients  $C_0^\rho$  and  $C_0^\tau$  are then given by

$$\begin{aligned} \frac{C_0^\tau}{m^2 M^2} &= \frac{1}{\rho_C} \left( \frac{1}{2M_s^*[\rho_C]} - \frac{1}{2M} \right), \\ \frac{C_0^\rho}{m^2} &= \frac{E_A^{NM}}{\rho_C} - \frac{1}{2M_s^*[\rho_C]} \frac{C_k}{\rho_C^{1/3}} \end{aligned} \quad (6.10)$$

where  $C_k = \frac{3}{5} \left( \frac{3\pi^2}{2} \right)^{2/3}$ . A derivation can be found in [100].

By considering asymmetric infinite nuclear-matter, the isovector terms  $C_1^\rho$  and  $C_1^\tau$  can similarly be expressed in terms of nuclear-matter properties. They are related to the symmetry energy  $a_A^{NM}$  and to the isovector mass  $M_v^*[\rho_C]$ . The value of  $a_A^{NM}$  is around 30 MeV. On the other hand,  $M_v^*[\rho_C]$  is even harder to constrain than  $M_s^*[\rho_C]$ . In the SLy family of Skyrme parametrisations, the value was fitted to the neutron-matter equation of state, which yielded  $M/M_v^*[\rho_C] = 1.249$  [93], and this value was adopted in the UNEDF family of parametrisations as well [90]. The  $C_1^\rho$  and  $C_1^\tau$  are given by

$$\begin{aligned} \frac{C_1^\tau}{m^2 M^2} &= \frac{C_0^\tau}{m^2 M^2} - \frac{1}{\rho_C} \left( \frac{1}{2M_v^*[\rho_C]} - \frac{1}{2M} \right), \\ \frac{C_1^\rho}{m^2} &= \frac{a^{NM}}{\rho_C} - \frac{5C_k}{9\rho_C^{1/3}} \left( \frac{\rho_C(C_0^\tau + 3C_1^\tau)}{m^2 M^2} - \frac{1}{2M} \right). \end{aligned} \quad (6.11)$$

Again a derivation can be found in [100].

Skyrme coefficients are also constrained using experimental data, such as the masses and charge radii of selected nuclei. Specific information on the fit procedure for each Skyrme parametrisation can be found in the relevant papers cited in *Table 6.1*.

Unlike other Skyrme parametrisations, the UNEDF family includes calculations of uncertainties in their parameters. For UNEDF1 these uncertainties are shown in *Table 6.2*. From the table, we can see that  $C_0^\rho$  and  $C_0^{SO}$  are constrained to less than 10%. The relative error for  $C_1^{SO}$  on the other hand is 65%. Although  $C_0^\tau$  has a relative error of 1550%, this is a symptom of the fact that  $M_s^*[\rho_C]$  is very close to 1 for UNEDF1. As a general rule, isoscalar terms are better constrained than isovector terms, and non-derivative terms are better constrained than derivative terms.

Term	Value	Abs.	Rel. (%)	Term	Value	Abs.	Rel. (%)
$C_0^\rho$	-15.12	1.09	7.2	$C_1^\rho$	10.60	>2.43	>23
$C_0^\tau$	-1.440	23.3	1620	$C_1^\tau$	-48.81	>23.3	>48
$C_0^{\Delta\rho}$	-36.53	4.42	12	$C_1^{\Delta\rho}$	-117.6	42.2	36
$C_0^{SO}$	-107.8	7.33	6.8	$C_1^{SO}$	-51.93	33.71	65

**Table 6.2:** Absolute and relative uncertainties in the UNEDF1 parametrisations.

As we noted above, UNEDF1 does not fit  $M_v^*[\rho_C]$ , but instead constrains it to  $M_v^*[\rho_C] = 1.249$ . Because of this, the uncertainties for  $C_1^\rho$  and  $C_1^\tau$  can only be given lower bounds.

### 6.3 Relating the Central and Spin-Orbit Terms

We will begin our discussion with the  $C_t^\rho$  and the spin-orbit terms. These four terms depend only on the three parameters  $g^2$ ,  $\lambda^2$  and  $\mu^2$ , and so we use this fact to relate the terms.

Begin with the  $\rho^2$  terms. These two terms are linearly related to the parameters  $g^2 - \lambda^2$ , and  $\mu^2$  by

$$\begin{aligned} C_0^\rho &= \frac{3}{4}(\lambda^2 - g^2) - \frac{3}{4}\mu^2, \\ C_1^\rho &= -\frac{1}{4}(\lambda^2 - g^2) + \frac{5}{4}\mu^2, \end{aligned} \quad (6.12)$$

as can be read directly from (6.3). Inverting this equation allows us to determine  $\mu^2$  and  $g^2 - \lambda^2$  from any Skyrme parametrisation:

$$\begin{aligned} \mu^2 &= \frac{1}{3}C_0^\rho + C_1^\rho, \\ \lambda^2 - g^2 &= \frac{5}{3}C_0^\rho + C_1^\rho. \end{aligned} \quad (6.13)$$

The spin-orbit terms depend only on the parameters  $\mu^2(1 - 2\mu_\rho)$  and  $(g^2 - \lambda^2)(1 - 2\mu_\omega)$

$$\begin{aligned} C_0^{SO} &= -\frac{5}{8}(g^2 - \lambda^2(1 - 2\mu_\omega)) + \frac{3}{8}\mu^2(1 - 2\mu_\rho), \\ C_1^{SO} &= -\frac{1}{8}(g^2 - \lambda^2(1 - 2\mu_\omega)) + \frac{3}{8}\mu^2(1 - 2\mu_\rho). \end{aligned} \quad (6.14)$$

Again we can invert these expressions:

$$\begin{aligned} \mu^2(1 - 2\mu_\rho) &= -\frac{2}{3}C_0^{SO} + \frac{10}{3}C_1^{SO}, \\ g^2 - \lambda^2(1 - 2\mu_\omega) &= -\frac{1}{2}C_0^{SO} + \frac{1}{2}C_1^{SO}. \end{aligned} \quad (6.15)$$

#### 6.3.1 Inequalities

We will now use the equations (6.13) and (6.15) to derive inequalities between Skyrme parameters. This allows us to make general statements about Skyrme parameters without specific reference to the coefficients  $g$ ,  $\lambda$  and  $\mu$ .

As a simple example, as  $\mu^2$  must be positive, we can use (6.13) to deduce that

$$C_1^\rho \geq -\frac{1}{3}C_0^\rho. \quad (6.16)$$

Nuclear saturation requires that  $C_0^\rho < 0$ , and so (6.16) acts as a lower bound on the size of  $C_1^\rho$ . In particular,  $C_1^\rho$  is necessarily positive.

Similar inequalities for the spin-orbit terms require conditions on  $\mu_\omega$  and  $\mu_\rho$ . For the experimental values of these couplings, we have the inequalities

$$\mu_{\rho,\omega} > \frac{1}{2} \implies (1 - 2\mu_{\rho,\omega}) < 0. \quad (6.17)$$

These inequalities also hold for the VMD predictions and we postulate that (6.17) will hold for any reasonable values of the tensor couplings. If we assume (6.17), then using (6.15) we derive the inequalities

$$5C_1^{SO} - C_0^{SO} \leq 0, \quad (6.18a)$$

$$C_1^{SO} - C_0^{SO} \geq 0. \quad (6.18b)$$

These inequalities can be combined into a single inequality

$$C_0^{SO} \leq C_1^{SO} \leq \frac{1}{5}C_0^{SO} \leq 0, \quad (6.19)$$

implying in particular that both spin-orbit coefficients must be negative.

Lastly, we can derive inequalities relating the  $\rho^2$  to the spin-orbit terms. Assuming that (6.17) holds, we can use (6.13) to write

$$\left| \frac{5}{3}C_0^\rho + C_1^\rho \right| = |g^2 - \lambda^2| < g^2 - \lambda^2(1 - 2\mu_\omega). \quad (6.20)$$

Combining this inequality with (6.15),

$$C_0^{SO} \leq -\frac{5}{8} \left| \frac{3}{5}C_0^\rho + C_1^\rho \right| + \frac{3}{8}(1 - 2\mu_\rho) \left( \frac{1}{3}C_0^\rho + C_1^\rho \right), \quad (6.21a)$$

$$C_1^{SO} \leq -\frac{1}{8} \left| \frac{3}{5}C_0^\rho + C_1^\rho \right| + \frac{3}{8}(1 - 2\mu_\rho) \left( \frac{1}{3}C_0^\rho + C_1^\rho \right). \quad (6.21b)$$

We can now test our five inequalities, (6.16), (6.18a), (6.18b), (6.21a) and (6.21b) against our Skyrme parametrisations. The results are shown in *Table 6.3*. UNEDF1 and UNEDF2, SkM\* and BSk1 satisfy all five inequalities. The SLy family passes all but the first inequality. A plausible cause of this is the unusually small values of  $C_1^\rho$  of this family. SkI4 likewise has a very small value of  $C_1^\rho$ . Both UNEDF0 and SkI4 fail a number of inequalities, and these can be traced to the fact that in both,  $C_1^{SO}$  is positive.

### 6.3.2 The Isovector Dependence of the Spin-Orbit Term

Because the four coefficients  $C_t^\rho$  and  $C_t^{SO}$  depend on only three parameters  $g^2$ ,  $\lambda^2$  and  $\mu^2$ , we can predict the value of one coefficient given the other three. In practice, it is most useful to relate the isovector spin-orbit term to the other three terms, as this term is the

Name	(6.16)	(6.18a)	(6.18b)	(6.21a)	(6.21b)
UNEDF2	✓	✓	✓	✓	✓
UNEDF1	✓	✓	✓	✓	✓
UNEDF0	✓	X	✓	✓	X
SLy4	X	✓	✓	✓	✓
SLy6	X	✓	✓	✓	✓
SLy10	X	✓	✓	✓	✓
SkM*	✓	✓	✓	✓	✓
Bsk1	✓	✓	✓	✓	✓
SkI4	X	X	✓	✓	X

**Table 6.3:** Testing Skyrme parameters against the our derived inequalities.

most under-constrained of the four. Using (6.13) and (6.15), we can derive

$$C_1^{SO} = \frac{1}{5}C_0^{SO} + \left( \frac{1}{10}C_0^\rho + \frac{3}{10}C_1^\rho \right) (1 - 2\mu_\rho) \quad (6.22)$$

and so the ratio of the isovector to isoscalar spin-orbit is given by

$$S = \frac{C_1^{SO}}{C_0^{SO}} = \frac{1}{5} + \frac{C_0^\rho + 3C_1^\rho}{10C_0^{SO}}(1 - 2\mu_\rho) = \frac{1}{5} + \frac{4}{5 - 25\frac{g^2 - \lambda^2(1 - 2\mu_\omega)}{3(1 - 2\mu_\rho)\mu^2}}. \quad (6.23)$$

The inequality (6.19) bounds  $S$  to satisfy

$$\frac{1}{5} \leq S \leq 1. \quad (6.24)$$

We can now use (6.23) to understand the origin of these extremal values. The ratio  $S = \frac{1}{5}$  holds when  $\mu = 0$ , whereas  $S = 1$  holds when  $g^2 - \lambda^2(1 - 2\mu_\omega) = 0$ . Hence  $S$  measures the relative importance of the isoscalar and isovector contributions to the spin-orbit term — the larger  $S$  is, the more important the isovector contribution is.

In Skyrme parametrisations,  $S$  is often fixed to  $\frac{1}{3}$ , chosen primarily for convenience. As  $1/3$  is the harmonic mean of the extremal allowed values of  $S$ , (6.24) provides a justification of this value as a reasonable first guess.

We can attempt to calculate the value of  $S$  in two different ways. For the Skyrme parametrisations where  $C_1^{SO}$  is fitted independently of  $C_0^{SO}$ , we can calculate the ratio directly. These parametrisations are UNEDF1, UNEDF2, SLy10 and SkI4. Of these, SkI4 has a  $C_1^{SO}$  value which is unrealistically large and positive.

The other option is to indirectly calculate  $C_1^{SO}$ , using (6.22). This procedure will yield sensible results if the relevant inequalities (6.16) and (6.21a) are satisfied. Five parametrisations satisfy these inequalities — UNEDF0, UNEDF1, UNEDF2, SkM\*, and Bsk1.

In *Figure 6.1*, values of  $S$  are calculated both from fitted and calculated values of  $C_1^{SO}$ . For the UNEDF family of parametrisations, uncertainties are calculated for  $S$ . As discussed in Section 6.2.2, the uncertainties in  $C_1^\rho$  are likely underestimated and hence so are the uncertainties of the calculated values of  $S$ .

Fitted values of  $S$  suggest a value of  $S$  somewhat larger than  $\frac{1}{3}$ . The uncertainties though are quite large — for instance, UNEDF2 has a value of  $S = 0.60 \pm 0.25$ .

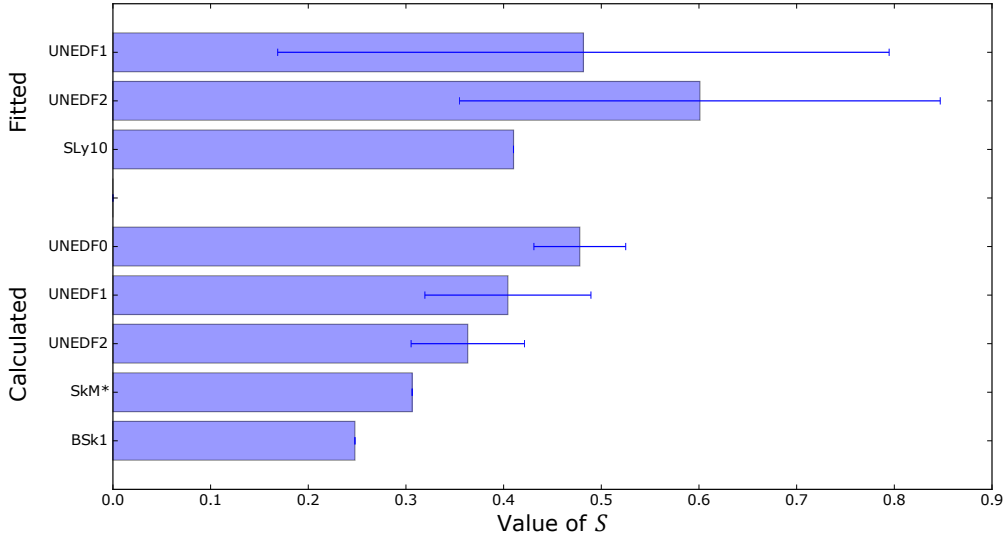


**Figure 6.1:** Isospin dependence of the spin-orbit term, using the fitted values (top), or calculated using (6.23) (bottom). Uncertainties are shown only for the UNEDF parametrizations.

The calculated values of  $S$  are consistent with, though somewhat smaller than, the fitted values. More interestingly, the calculated uncertainties are much smaller than those for the fitted values. This results from the fact that the  $\rho^2$  and isoscalar spin-orbit terms are much better constrained than the isovector terms. For UNEDF2, the calculated value of  $S$  was  $0.36 \pm 0.06$ . As we have noted, the uncertainties in  $C_1^\rho$  are underestimated, and a more detailed understanding of these uncertainties should be pursued before drawing conclusions. Once this is achieved though, using (6.22) could potentially give yield a more precise value of  $S$  than directly fitting  $C_1^{SO}$ .

### 6.3.3 Calculating $\mu^2$

We now have two different methods of calculating  $\mu^2$ , using (6.13) and (6.15) respectively:

$$\begin{aligned} \mu^2 &= \frac{1}{3}C_0^\rho + C_1^\rho, \\ \mu^2 &= \frac{1}{1 - 2\mu_\rho} (-2C_0^{SO} + 10C_1^{SO}). \end{aligned} \quad (6.25)$$

The two equations involve separate coefficients, and so give independent values of  $\mu^2$ .

Using the UNEDF1 and UNEDF2 parametrizations, we can compare the values of  $\mu^2$  gained using both methods. Since UNEDF1 and UNEDF2 include uncertainties on their parameters, we can also calculate the uncertainties in the values. As can be expected, the first equation yields the most precise value of  $\mu^2$ ,  $5.56 \pm 2.46$  for UNEDF1 and  $3.86 \pm 1.05$  for UNEDF2. Using (6.15) gives values of  $\mu^2$  which are consistent with these values, though with relative uncertainties which are greater than 60%.

Overall, our calculations yield values of  $\mu^2$  which are consistent with each other. By comparing both methods for calculating the same quantity, we can see the importance of choosing well-constrained parameters in calculations. Uncertainties in Skyrme parameters can quickly lead to very large errors.

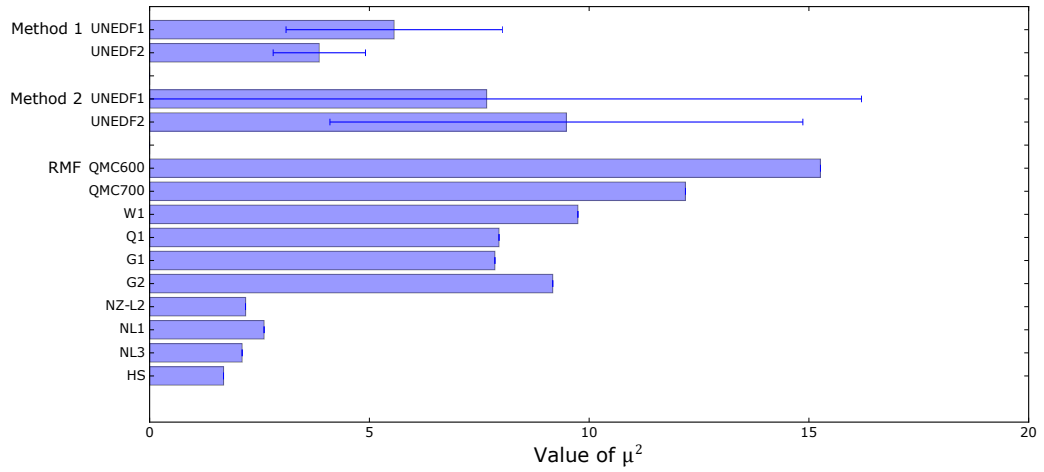


**Figure 6.2:** Comparison of  $\mu^2$  calculated using (6.13) (Method 1) and (6.15) (Method 2) with values of  $\mu^2$  used in relativistic mean-field theories.

Name	Paper	Name	Paper
QMC600	[41]	W1	[20]
QMC700	[41]	Q1	[20]
NL1	[101]	G1	[20]
NL3	[101]	G2	[20]
NL-Z2	[102]	HS	[3]

**Table 6.4:** Relativistic mean-field parametrisations used in *Figure 6.2*.

We discussed in Section 6.1 the possibility of comparing Skyrme parametrisations with relativistic mean-field theory. The value of  $\mu^2$  allows a simple comparison, since in most RMFs there is no density-dependent isovector term. In *Figure 6.2*, a comparison is given between the values of  $\mu^2$  calculated with (6.13) and (6.15), and values of  $\mu^2$  extracted from RMF parametrisations. The RMF parametrisations used, along with the relevant papers, are given in *Table 6.4*.

*Figure 6.2* shows that there is significant variations in the values of  $\mu^2$  given by different RMF values. Nevertheless, our calculations with Skyrme parametrisations have yielded values of  $\mu^2$  which are compatible with those given in RMF, suggesting that a more detailed comparison of Skyrme forces with RMF may be fruitful.

## 6.4 Gradient and Effective Mass Terms

We now turn to the gradient and effective mass terms. These four terms are linearly related to five parameters,  $d_1$ ,  $d_2$ ,  $\mu^2$ ,  $\lambda^2$  and  $\alpha^2$ :

$$\begin{aligned}
C_0^{\Delta\rho} &= \frac{1}{64} \left( -56d_1 + 24d_2 - \frac{m^2}{M^2} (6\alpha^2 + (\mu_\omega^2 - 4\mu_\omega + 8)\lambda^2 + 3(\mu_\rho^2 - 4\mu_\rho + 8)\mu^2) \right), \\
C_1^{\Delta\rho} &= \frac{1}{64} \left( 8d_1 - 72d_2 + \frac{m^2}{M^2} (2\alpha^2 - (\mu_\omega^2 - 4\mu_\omega + 8)\lambda^2 + (\mu_\rho^2 - 4\mu_\rho + 8)\mu^2) \right), \\
C_0^\tau &= \frac{1}{16} \left( (\mu_\omega^2 - 4\mu_\omega - 12)\lambda^2 + 3(\mu_\rho - 2)^2\mu^2 + 6\alpha^2 - \frac{8M^2}{m^2} (d_1 + 3d_2) \right), \\
C_1^\tau &= \frac{1}{16} \left( (\mu_\omega - 2)^2\lambda^2 - (\mu_\rho^2 - 4\mu_\rho - 20)\mu^2 - 2\alpha^2 - \frac{8M^2}{m^2} (d_1 - d_2) \right).
\end{aligned} \tag{6.26}$$

It is hence impossible to relate the coefficients to each other. Nevertheless, using the results of the previous section, we can calculate  $\lambda^2$  and  $\mu^2$  from  $C_{0,1}^\rho$  and  $C_0^{SO}$ . We can then define

$$\begin{aligned}
\tilde{C}_0^{\Delta\rho} &= C_0^{\Delta\rho} + \frac{m^2}{64M^2} ((\mu_\omega^2 - 4\mu_\omega + 8)\lambda^2 + 3(\mu_\rho^2 - 4\mu_\rho + 8)\mu^2) = -\frac{7}{8}d_1 + \frac{3}{8}d_2 - \frac{3\alpha^2 m^2}{32M^2}, \\
\tilde{C}_1^{\Delta\rho} &= C_1^{\Delta\rho} + \frac{m^2}{64M^2} ((\mu_\omega^2 - 4\mu_\omega + 8)\lambda^2 - (\mu_\rho^2 - 4\mu_\rho + 8)\mu^2) = \frac{1}{8}d_1 - \frac{9}{8}d_2 + \frac{\alpha^2 m^2}{32M^2}, \\
\tilde{C}_0^\tau &= C_0^\tau - \frac{1}{16} ((\mu_\omega^2 - 4\mu_\omega - 12)\lambda^2 + 3(\mu_\rho - 2)^2\mu^2) = \frac{3}{8}\alpha^2 - \frac{M^2}{2m^2} (d_1 + 3d_2), \\
\tilde{C}_1^\tau &= C_1^\tau - \frac{1}{16} ((\mu_\omega - 2)^2\lambda^2 - (\mu_\rho^2 - 4\mu_\rho - 20)\mu^2) = -\frac{1}{8}\alpha^2 - \frac{M^2}{2m^2} (d_1 - d_2).
\end{aligned} \tag{6.27}$$

Choosing any three of the four above equations and inverting, we are able to calculate  $\alpha^2$ ,  $d_1$  and  $d_2$ .

### 6.4.1 The Pion Contribution

The parameter  $\alpha^2$  controls the pseudo-scalar isovector interaction channel, which in meson models is associated with the pion. Using the first three equations of (6.27), we can derive

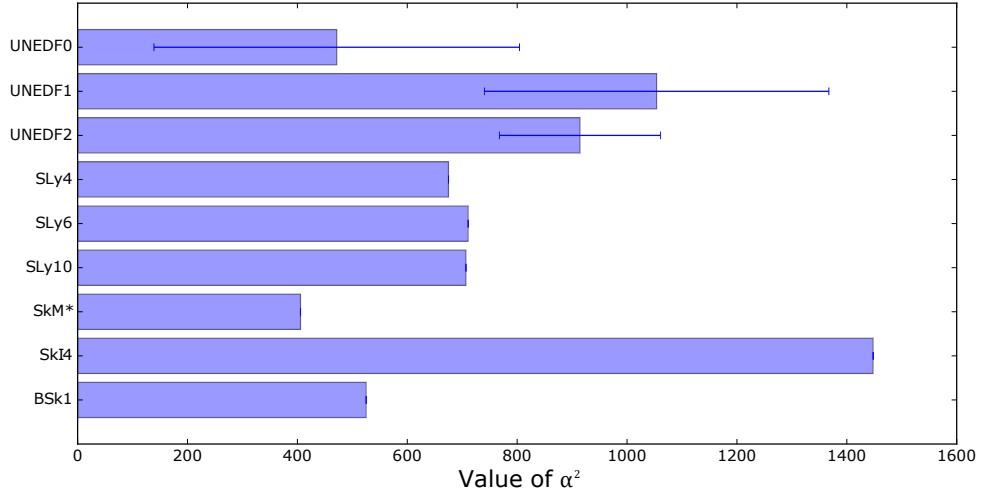


**Figure 6.3:** Values of  $\alpha^2$  calculated from Skyrme parametrizations using (6.28).

the expression

$$\alpha^2 = -\frac{M^2}{m^2} \left( 2\tilde{C}_0^{\Delta\rho} + 4\tilde{C}_1^{\Delta\rho} - \frac{5}{4}\tilde{C}_0^\tau \right). \quad (6.28)$$

Since we expect  $\alpha^2$  to be positive, this yields an inequality

$$5\tilde{C}_0^\tau - 8\tilde{C}_0^{\Delta\rho} - 16\tilde{C}_1^{\Delta\rho} \geq 0, \quad (6.29)$$

which we expect to hold in general.

The results of (6.28) are shown in *Figure 6.3*. Uncertainties are shown for the UNEDF parametrizations. Although there is considerable variability in the value of  $\alpha^2$ , each Skyrme parametrization yields a positive value of  $\alpha^2$  and hence satisfies (6.29).

Our calculated values of  $\alpha^2 \sim 10^3$  are large compared to the values of  $\mu^2 \sim 10$  found in Section 6.3.3. Similar calculations for  $g^2$  and  $\lambda^2$  yields values of  $\sim 10^2$ , so that  $\alpha^2$  is at least an order of magnitude larger than the other coupling constants. A possible explanation for this is that the pion is much lighter than the other mesons:  $m_\pi \sim 140$  MeV. We would then expect the pionic contribution to be magnified by a factor of  $m^2/m_\pi^2 \sim 25$  compared to the other mesons. This provides evidence that the pion plays an important role in nuclei, and although it is a pseudo-scalar, it will still contribute to time-even systems through Fock terms.

#### 6.4.2 Calculating the Isovector Effective Mass Term

The coefficient  $C_1^\tau$  is poorly constrained. By using the coefficients  $C_{0,1}^\rho$ ,  $C_{0,1}^{\Delta\rho}$ ,  $C_0^{SO}$  and  $C_0^\tau$ , we are able to calculate  $\alpha^2$ ,  $\lambda^2$ ,  $\mu^2$ ,  $d_1$  and  $d_2$ . We can then use (6.26) to calculate  $C_1^\tau$ . The results are shown in *Figure 6.4*. Error bars for the UNEDF parametrizations have been included.

Our calculated values of  $C_1^\tau$  are consistent across most of the Skyrme parametrizations — UNEDF2 yields  $-51.52 \pm 25.74$ . Although the error bars are large, our calculations favour a negative values of  $C_1^\tau$ . For comparison, the values of  $C_1^\tau$  obtained by the authors from their fit protocol are also shown in *Figure 6.4*. There is a much greater variation in

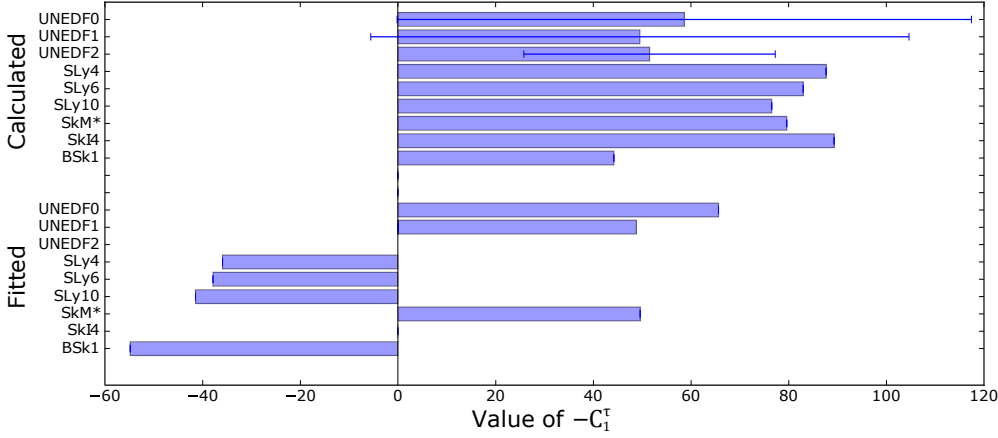


**Figure 6.4:** Calculated and fitted values of  $-C_1^\tau$ .

these fitted values than in the calculated values. For instance, UNDEF1 favours  $C_1^\tau = -65.6$  where as SLy10 has  $C_1^\tau = 41.1$ . Again we see that indirect calculations of Skyrme parameters may yield more precise values than a direct fit to nuclear data.

### 6.4.3 The Tensor Terms

The coefficients of the tensor terms can be calculated as a function  $\alpha^2$ ,  $\lambda^2$ ,  $\mu^2$ ,  $d_1$  and  $d_2$ :

$$\begin{aligned}
 C_0^T &= \frac{1}{16} \left( \frac{8M^2}{m^2} (d_1 + 3d_2) + 6\alpha^2 - \lambda^2 (5\mu_\omega^2 - 20\mu_\omega + 16) - 3\mu^2 (5\mu_\rho^2 - 20\mu_\rho + 16) \right), \\
 C_1^T &= \frac{1}{16} \left( \frac{8M^2}{m^2} (d_1 - d_2) - 2\alpha^2 - \lambda^2 (5\mu_\omega^2 - 20\mu_\omega + 16) + \mu^2 (5\mu_\rho^2 - 20\mu_\rho + 16) \right), \\
 C_0^F &= \frac{1}{32} (6\alpha^2 - 3\lambda^2 (\mu_\omega - 2)^2 - 9\mu^2 (\mu_\rho - 2)^2), \\
 C_1^F &= \frac{1}{32} (-2\alpha^2 - 3\lambda^2 (\mu_\omega - 2)^2 + 3\mu^2 (\mu_\rho - 2)^2).
 \end{aligned} \tag{6.30}$$

The tensor terms are poorly constrained but are of immense interest in nuclear structure studies of exotic nuclei [53] as well as in reactions studies [103]. Of the Skyrme parametrizations considered here, only UNEDF2 contains any of the tensor terms — and then only for spherical cases.

Similar to the isovector effective mass term, we are able to calculate the tensor terms using  $C_{0,1}^\rho$ ,  $C_{0,1}^{\Delta\rho}$ ,  $C_0^{SO}$  and  $C_0^\tau$ . As the tensor terms are poorly understood, interpreting the results of such a calculation is non-trivial. For this reason, we shall not delve further into this topic in this thesis. Future work on this topic will be forthcoming.

---

# Conclusion

---

Even after almost a century of nuclear physics, the nuclear forces — the microscopic foundation of all nuclear phenomenology — are poorly understood. In nuclear modelling, we are forced to utilise phenomenologically fitted forces, which are not clearly linked to the underlying physics involved, and are difficult to utilise in new regimes where experimental data is not abundant.

In this thesis, we aimed to relate non-relativistic nuclear forces to higher energy physics systematically and efficiently. It was hoped that this could then be used to constrain low-energy nuclear forces, and more specifically to constrain the form of the Skyrme energy density functional. To this end, we investigated effective field theory in Chapter 3, and the non-relativistic limit in Chapter 4. These tools allowed us to efficiently extract the low-energy limit of any given mesonic model.

We showed in Chapter 5 that the lowest order contributions to nuclear forces will be a Skyrme-like Lagrangian. These conclusions were generally, relying only on a few pieces of mesonic physics: the QCD symmetries, the QCD energy scales, the predominant interaction channels, and the presence of non-linearity. Any theory with these properties will be able to reproduce a realistic nuclear force. Low energy observables will therefore not allow us to distinguish between different models.

Connecting the low-energy nuclear forces to ultraviolet physics is further complicated by both the non-perturbative nature of mesonic physics, and the presence of density-dependent terms in medium, each of which were reabsorbed into a handful of coupling constants. These coupling constants cannot be linked in a straightforward manner to mesonic observables, and so must be fitted to nuclear properties in a manner akin to traditional Skyrme parametrisations. Nevertheless, we suggest that the ratio of the vector and tensor couplings of the nucleon may be preserved through these rescalings, and this may be observable in low-energy nuclear phenomenology.

In spite of these conclusions, we were able to place constraints on the form of low-energy nuclear forces. Chapter 6 applied these results to time-even systems. We related twelve Skyrme coefficients to only six underlying parameters. This enabled us to derive a series of six inequalities which should be satisfied by any Skyrme parametrisation. We then analysed the isospin dependence of the spin-orbit and effective mass terms, measuring these coefficients to greater precision than that which can be achieved through traditional fitting methods.

## Future Work

There are two primary avenues for future study, corresponding to extensions of either Chapter 5 or Chapter 6. We will begin with the latter, for which the future directions to

take are more straightforward.

## Energy Density Functional

In Chapter 6, we considered only time-even systems, and we considered only Skyrme parametrisations. Both these restrictions should be removed in future work. The results of Section 5.4.1 and Section 6.1 set up the necessary foundations to allow Skyrme parametrisations to be compared to relativistic mean-field theories. We gave an example of such a comparison in Section 6.4.3 in the context of the  $\mu^2$  parameter — in future work we should present a systematic comparison across all interaction channels. This work should enable cross-pollination between these two distinct yet complimentary approaches to the nuclear many-body problem.

Lifting the requirement of time-reversal symmetry will allow us to study time-odd and tensor terms. These terms are poorly constrained by experimental data. Nevertheless, these terms are critical to understanding nuclear structure and reactions [53, 104, 105]. Perhaps most dramatically, isovector-tensor terms can result in the appearance of new magic numbers in exotic nuclei [106]. By further investigating the predictions of our EDF, we may be able to provide quantitative constraints on the time-odd and tensor terms. The significance of these constraints to the structure of exotic nuclei can then be investigated.

In Chapter 6 we related various Skyrme parameters to each other in non-trivial ways. We should hence consider fitting our energy density functional to nuclear data directly, rather than using pre-existing Skyrme parametrisations. This would create a Skyrme interaction with all our constraints inbuilt, and would hence give a more precise determination of both coefficients, and of the underlying parameters which constrain these coefficients.

## Relating Skyrme Forces to Higher Energy Physics

We now turn to Chapter 5. In this, we concluded that the ultraviolet models were under-constrained by observable nuclear properties. Given these conclusions, how can we progress towards a quantitative understanding of the relationship between nuclear forces and high-energy physics? What we need in order to progress is a better handle of the parameters involved in the high energy physics. There are two main routes to which we can achieve this: through theory and through experiment.

We will start with the experimental front. Most traditional Skyrme interactions are fitted to the observed properties of nuclei. As neutron-rich and super-heavy nuclei become more experimentally accessible, our ability to constrain Skyrme parameters, particularly the isospin dependent parameters, will be improved. More exotically, observational properties of neutron stars can provide constraints at densities which are inaccessible on Earth [8]. We could also search for better ways to constrain Skyrme terms using current data. For instance, UNEDF2 utilised spin-orbit level splittings in doubly magic nuclei in order to constrain spin-orbit and tensor couplings [92]. This approach has many limitations however — relying on experimental data makes it difficult to extrapolate to regimes where experimental data is scarce. Furthermore, the Hartree-Fock method used in the fitting procedure is only an approximation, and this introduces systematic errors that complicate the fitting of Skyrme forces to experimental data [107]. Finally, the Skyrme functional is itself an approximation and so is limited in how well it can reproduce the experimental data. In [108], it is shown that root mean square deviations from single-particle energies are at best of the order of 1.1 MeV for a time-even Skyrme functional.

---

Scattering presents another possible source of experimental data. Nucleon-nucleon and nucleon-pion scattering is well understood both theoretically and experimentally [109, 110]. On the other hand, the rho and omega are extremely unstable, and the sigma is fictitious, so it is difficult to constrain their couplings with nucleons through scattering. Even more problematically, in section 5.4 we showed that non-linear meson fields will result in density-dependent couplings. The meson-nucleon couplings, and even the meson masses, will be different in-medium [38], and scattering data cannot constrain this.

Having discussed the experimental options, let us now turn to theory. Our difficulties lie not in developing models that fit the experimental data, but rather in choosing amongst the plethora of models which can be made to fit the data. For this reason, we should not focus on model building, but rather on systematically relating QCD to nuclear physics.

Chiral perturbation theory provides an example framework. Originating in work of Weinberg [111, 112, 113], chiral perturbation theory is an effective field theory of pions and nucleons grounded in chiral symmetry breaking. Nucleon-nucleon and nucleon-pion scattering can be described using a series of low-energy constants, which must be determined experimentally [110]. Nuclear many-body forces are more difficult to handle in this approach, though *ab initio* calculations of light nuclear structure is rapidly advancing [89]. Future work is needed on the topic of connecting chiral perturbation theory to traditional Skyrme approaches.

Other tools used to study QCD may also provide insight into the problem, especially in conjunction with chiral perturbation theory. For instance, QCD sum rules have been utilised to constrain the properties of nuclear matter [114]. Lattice QCD will enable quantitative study of non-perturbative aspects of QCD, and may allow the calculations of constants which are difficult to assess experimentally [115]. Though much work needs to be done, a detailed understanding of the quantitative connections between QCD and nuclear phenomenology may eventually be achieved.



---

# Quark-Meson Coupling to One-Loop

---

In this appendix, we will show that (3.49) holds:

$$\begin{aligned} & \frac{i}{2} \log \det(\partial^2 + m^2 - K(x)) \\ &= \int dx^4 \frac{m^4}{8(2\pi)^2} \left( \frac{2K}{m^2} - \frac{3K^2}{m^4} + 2 \left( 1 - \frac{K}{m^2} \right)^2 \log \left( 1 - \frac{K}{m^2} \right) \right) + O(\partial^2) \end{aligned} \quad (\text{A.1})$$

As we discussed in Section 3.4, functional determinants cannot be evaluated except either for special cases or through the use of Feynman diagrams. The case of constant  $K(x) = K_0$  can be evaluated explicitly (for a derivation see page 374 of [21]):

$$\frac{i}{2} \log \det [\partial^2 + m^2 - K_0] = \frac{i}{2} (VT) \int \frac{dk^4}{(2\pi)^4} \log(k^2 - m^2 + K_0). \quad (\text{A.2})$$

Here  $(VT)$  is a four-dimensional volume, equivalent to the integral in (A.1). Our expression is divergent, so we introduce a high-energy cut-off  $\Lambda$ , and then calculate

$$L(K_0) = \frac{i}{2} \int^\Lambda \frac{dk^4}{(2\pi)^4} \log(k^2 - m^2 + K_0) = a\Lambda^4 + b\Lambda^2 K_0 + cK_0^2 \log \Lambda + \text{finite terms}. \quad (\text{A.3})$$

For the moment assume that we have counter-terms to remove the divergence. To evaluate the finite part we calculate

$$\frac{d^3 L}{dK_0^3} = \int^\Lambda \frac{dk^4}{(2\pi)^4} \frac{i}{(k^2 - m^2 + K_0)^3} \xrightarrow{\Lambda \rightarrow \infty} \frac{1}{2(2\pi)^2(m^2 - K_0)}. \quad (\text{A.4})$$

By integrating thrice, we find that

$$L(K_0) = \frac{m^4}{4(2\pi)^2} \left( 1 - \frac{K_0}{m^2} \right)^2 \log \left( 1 - \frac{K_0}{m^2} \right) + A + BK_0 + CK_0^2, \quad (\text{A.5})$$

where  $A, B$  and  $C$  are arbitrary constants. We can always set  $A$  to zero. For simplicity we shall renormalise around the vacuum, setting

$$L(0) = L'(0) = L''(0) = 0. \quad (\text{A.6})$$

This then leads to the equation

$$L = \frac{m^4}{8(2\pi)^2} \left( \frac{2K_0}{m^2} - \frac{3K_0^2}{m^4} + 2 \left( 1 - \frac{K_0}{m^2} \right)^2 \log \left( 1 - \frac{K_0}{m^2} \right) \right). \quad (\text{A.7})$$

Evaluating the dependence of the functional determinant on derivative terms such as  $K\partial^2 K$  is much more difficult. The only method I know of which allows these calculations is the Feynman diagram approach. Using this it is possible, though difficult, to evaluate terms such as  $K^n\partial^2 K$  using (3.31). This is however of limited use as the series obtained is asymptotic (there exist methods to sum such divergent sequences [116], but for our current purposes this is overkill). Here we will simply note that, by evaluating the two vertex diagram, in (3.30), we can calculate the  $K\partial^2 K$  term:

$$\begin{array}{c} \circ \\ \bullet \quad \bullet \end{array} = \dots - \frac{1}{24(2\pi)^2 m^2} \int dx^4 K(x) \partial^2 K(x) + \dots \quad (\text{A.8})$$

---

# The Källén-Lehmann Spectral Representation

---

In Section 3.6, we invoked the Källén-Lehmann representation of the 2-point function

$$G(x - y) = \int \frac{d^4 p}{(2\pi)^4} e^{ip(x-y)} \int_0^\infty \frac{dX}{2\pi} \frac{\rho(X)}{p^2 - X}, \quad (\text{B.1})$$

where  $\rho(X)$  is positive. This representation was discovered independently by Källén [117] and Lehmann [118]. We will provide a proof of this result. Further details can be found in [119].

Begin by writing the propagator  $G(x - y)$  in terms of field operators:

$$G(x - y) = \langle \Omega | \Phi(x) \Phi^\dagger(y) | \Omega \rangle, \quad (\text{B.2})$$

where  $|\Omega\rangle$  is the vacuum state. We will expand this function by inserting a complete set of states between  $\Phi(x)$  and  $\Phi(y)$ . Let  $|\lambda_0\rangle$  be an eigenstate of the Hamiltonian  $H$ , with eigenvalue  $E_\lambda$  and zero momentum:

$$\vec{P}|\lambda_0\rangle = 0. \quad (\text{B.3})$$

Since  $\vec{P}$  and  $H$  commute, we can boost  $|\lambda_0\rangle$ , and the result  $|\lambda_p\rangle$  will also be an eigenstate of  $H$ . The completion relation for the Hilbert space is then given by

$$1 = \sum_\lambda \int \frac{d^3 p}{(2\pi)^3} \frac{1}{2\sqrt{p^2 + E_\lambda^2}} |\lambda_p\rangle \langle \lambda_p|, \quad (\text{B.4})$$

where the sum of  $\lambda$  occurs over all eigenstates of  $H$  with zero momentum. Inserting this into (B.2), we find that

$$G(x - y) = \sum_\lambda \int \frac{d^3 p}{(2\pi)^3} \frac{1}{2\sqrt{p^2 + E_\lambda^2}} \langle \Omega | \Phi(x) | \lambda_p \rangle \langle \lambda_p | \Phi^\dagger(y) | \Omega \rangle. \quad (\text{B.5})$$

Now we can manipulate the expression

$$\begin{aligned} \langle \Omega | \Phi(x) | \lambda_p \rangle &= \langle \Omega | e^{-iPx} \Phi(0) e^{iPx} | \lambda_p \rangle \\ &= e^{ipx} \langle \Omega | \Phi(0) | \lambda_p \rangle_{p^0=E_\lambda} = e^{ipx} |_{p^0=E_\lambda} \langle \Omega | \Phi(0) | \lambda_0 \rangle. \end{aligned} \quad (\text{B.6})$$

The last equality uses the fact that both  $\langle \Omega |$  and  $\Phi(0)$  are Lorentz invariant. For this

reason, a boost can be inserted shifting  $|\lambda_p\rangle$  to  $|\lambda_0\rangle$ . We now find that

$$\begin{aligned} G(x-y) &= \sum_{\lambda} \int \frac{d^3p}{(2\pi)^3} \frac{1}{2\sqrt{p^2 + E_{\lambda}^2}} e^{ip(x-y)} \Big|_{p^0=E_{\lambda}} |\langle \Omega | \Phi(0) | \lambda_0 \rangle|^2 \\ &= \sum_{\lambda} \int \frac{d^4p}{(2\pi)^4} \frac{1}{p^2 - E_{\lambda}^2 + i\epsilon} |\langle \Omega | \Phi(0) | \lambda_0 \rangle|^2 \end{aligned} \quad (\text{B.7})$$

Defining the positive spectral density function

$$\rho(X) = \sum_{\lambda} 2\pi \delta(X - E_{\lambda}^2) |\langle \Omega | \Phi(0) | \lambda_0 \rangle|^2 \geq 0, \quad (\text{B.8})$$

we can write

$$G(x-y) = \int \frac{d^4p}{(2\pi)^4} e^{ip(x-y)} \int_0^{\infty} \frac{dX}{2\pi} \frac{\rho(X)}{p^2 - X}. \quad (\text{B.9})$$

This completes the derivation.

---

# Expectation Values of Time-Even Densities

---

In this appendix we shall calculate the expectation values of various operators for time-even systems. For simplicity, we shall assume that the one-body density matrix of our system is diagonal in spin and isospin — this restricts our scope to the case of spin-saturated matter. For systems which possess time-reversal symmetry but are not diagonal in spin, our results should still be correct, with the exception of the spin-orbit and possibly the tensor terms. Work is currently being done to generalise to this case.

## C.1 Time-Even Densities

If the one-body density matrix is diagonal in spin and isospin, this means that the nucleon wavefunctions are of the form

$$\begin{pmatrix} \psi_i \\ 0 \\ 0 \\ 0 \end{pmatrix}, \quad \begin{pmatrix} 0 \\ -\psi_i^* \\ 0 \\ 0 \end{pmatrix}, \quad \begin{pmatrix} 0 \\ 0 \\ \phi_i \\ 0 \end{pmatrix}, \quad \begin{pmatrix} 0 \\ 0 \\ 0 \\ -\phi_i^* \end{pmatrix}. \quad (\text{C.1})$$

Here we take the top two components to be proton wavefunctions, and the bottom two components are neutron wavefunctions.

For time-even systems, the only non-zero local densities are  $\rho$ ,  $\tau$  and  $J_{ij}$ . We are able to calculate both the isoscalar and isovector expectation values of the corresponding bilinears:

$$\begin{aligned} \langle \hat{\rho} \rangle &= 2 \sum_i |\psi_i|^2 + 2 \sum_j |\phi_j|^2, & \langle (\hat{\rho}_1)_3 \rangle &= 2 \sum_i |\psi_i|^2 - 2 \sum_j |\phi_j|^2, \\ \langle \hat{\tau} \rangle &= 2 \sum_i |\nabla \psi_i|^2 + 2 \sum_j |\nabla \phi_j|^2, & \langle (\hat{\tau}_1)_3 \rangle &= 2 \sum_i |\nabla \psi_i|^2 - 2 \sum_j |\nabla \phi_j|^2, \\ \langle \hat{J}^{1j} \rangle &= \langle \hat{J}^{2j} \rangle = 0, & \langle (\hat{J}^{1j})_3 \rangle &= \langle (\hat{J}^{2j})_3 \rangle = 0 \\ \langle \hat{J}^{3j} \rangle &= i \begin{pmatrix} \psi_i \nabla_x \psi_i^* + \phi_i \nabla_x \phi_i^* \\ \psi_i \nabla_y \psi_i^* + \phi_i \nabla_y \phi_i^* \\ \psi_i \nabla_z \psi_i^* + \phi_i \nabla_z \phi_i^* \end{pmatrix}_j + H.C., & \langle (\hat{J}^{3j})_3 \rangle &= i \begin{pmatrix} \psi_i \nabla_x \psi_i^* - \phi_i \nabla_x \phi_i^* \\ \psi_i \nabla_y \psi_i^* - \phi_i \nabla_y \phi_i^* \\ \psi_i \nabla_z \psi_i^* - \phi_i \nabla_z \phi_i^* \end{pmatrix}_j + H.C. \end{aligned} \quad (\text{C.2})$$

Our notation is such that  $\langle (\hat{\rho}_1)_3 \rangle$  denotes the third isovector component of  $\langle \hat{\rho}_1 \rangle$ . We will

adopt the notation  $A = \langle \hat{A} \rangle$ . In particular, we find that the tensor terms have the form:

$$J_{ij}J_{ij} = -(\psi_k \nabla \psi_k^* - \psi_k^* \nabla \psi_k + \phi_k \nabla \phi_k^* - \phi_k^* \nabla \phi_k)^2. \quad (\text{C.3})$$

$$\frac{1}{2} (J_{ij}J_{ji} + J_s^2) = -(\psi_k \nabla_z \psi_k^* - \psi_k^* \nabla_z \psi_k + \phi_k \nabla_z \phi_k^* - \phi_k^* \nabla_z \phi_k)^2. \quad (\text{C.4})$$

We can also derive the useful relationships

$$\sum_i 4\psi_i \nabla^i \psi_i^* = \nabla^i \rho - i2J^{3i}, \quad \sum_i 2\psi_i^* \Delta \psi_i + 2\psi_i \Delta \psi_i^* = \Delta \rho + 2\tau. \quad (\text{C.5})$$

## C.2 Evaluating Bilinears

Single-particle operators have the general form

$$A = A_{ij} a_i^\dagger a_j, \quad (\text{C.6})$$

so that their expectation value is

$$\langle A \rangle = A_{ii} = \text{tr}(A). \quad (\text{C.7})$$

For the product of two single-particle operators, we find that

$$\langle AB \rangle = A_{ii} B_{jj} - A_{ij} B_{ji} = \text{tr}(A)\text{tr}(B) - \text{tr}(AB) \quad (\text{C.8})$$

Evaluating bilinears is straightforward but tedious. It will be convenient to index wavefunctions by their spin and isospin,  $\psi_{iqs}$ , so that

$$\psi_{i00} = \begin{pmatrix} \psi_i \\ 0 \\ 0 \\ 0 \end{pmatrix}, \quad \psi_{i01} = \begin{pmatrix} 0 \\ -\psi_i^* \\ 0 \\ 0 \end{pmatrix}, \quad \psi_{i10} = \begin{pmatrix} 0 \\ 0 \\ \phi_i \\ 0 \end{pmatrix}, \quad \psi_{i11} = \begin{pmatrix} 0 \\ 0 \\ 0 \\ -\phi_i^* \end{pmatrix}, \quad (\text{C.9})$$

where  $q = 0$  for protons and 1 for neutrons. Similarly,  $s = 0$  is a spin-up nucleon and  $s = 1$  is a spin-down nucleon.

We will start with the scalar-isoscalar densities:

$$\begin{aligned}
 \langle \rho^2 \rangle &= \rho^2 - \sum_{ijsqs'q'} \psi_{iqs}^* \psi_{jq's'} \psi_{jq's'}^* \psi_{iqs} = \rho^2 - \sum_q \rho_q^2 = \frac{3}{4} \rho^2 - \frac{1}{4} \rho_a^2 \\
 \langle \rho\tau \rangle &= \rho\tau - \sum_q (2\psi_{iq}^* \psi_{jq} \nabla \psi_{jq}^* \cdot \nabla \psi_{iq}) = \rho\tau - \frac{1}{8} \sum_q |\nabla^i \rho_q + 2iJ_{3iq}|^2 \\
 &= \rho\tau + \sum_q \left( \frac{1}{8} \rho_q \Delta \rho_q - \frac{1}{2} J_{ijq} J_{ijq} \right) = \rho\tau + \frac{1}{16} (\rho \Delta \rho + \rho_a \Delta \rho_a) - \frac{1}{4} (J_{ij} J_{ij} + J_{ija} J_{ija}) \\
 \langle \rho \Delta \rho \rangle &= \rho \Delta \rho - \sum_q 2\psi_{iq}^* \psi_{jq} \Delta \psi_{jq}^* \psi_{iq} \\
 &= \rho \Delta \rho - \sum_q 2|\psi_{iq}|^2 (\psi_{jq} \Delta \psi_{jq}^* + \psi_{jq}^* \Delta \psi_{jq}) + 4\psi_{iq}^* \nabla \psi_{iq} \cdot \psi_{jq} \nabla \psi_{jq}^* \\
 &= \rho \Delta \rho + \sum_q \left( -\frac{1}{2} \rho_q \Delta \rho_q + \rho_q \tau_q + \frac{1}{4} \rho_q \Delta \rho_q - J_{ijq} J_{ijq} \right) \\
 &= \frac{7}{8} \rho \Delta \rho - \frac{1}{8} \rho_a \Delta \rho_a - \frac{1}{2} (J_{ij} J_{ij} + J_{ija} J_{ija} - \rho\tau - \rho_a \tau_a)
 \end{aligned} \tag{C.10}$$

Next we calculate the scalar-isovector densities. These can be quickly calculated from the scalar-isoscalar densities if the following relationship is noted:

$$\begin{aligned}
 \sum_{qq'} A_q \tau_a B_{q'} C_{q'} \tau_a D_q &= \sum_{qq'} (1 - \delta_{qq'}) 2A_q B_{q'} C_{q'} D_q + \delta_{qq'} A_q B_q C_q D_q \\
 &= \frac{3}{2} (AD)(BC) - \frac{1}{2} (AD)_a (BC)_a.
 \end{aligned} \tag{C.11}$$

We can now calculate:

$$\begin{aligned}
 \langle \rho_a^2 \rangle &= \rho_a^2 - \frac{1}{2} (\rho_P^2 + \rho_N^2 + 4\rho_P \rho_N) = -\frac{3}{4} \rho^2 + \frac{5}{4} \rho_a^2 \\
 \langle \rho_a \tau_a \rangle &= \rho_a \tau_a - \sum_{qq'} 2\psi_{iq}^* \tau_a \psi_{jq'} \nabla \psi_{jq'}^* \tau_a \cdot \nabla \psi_{iq} \\
 &= \rho_a \tau_a - \frac{1}{8} \left( \frac{3}{2} |\nabla^i \rho + 2iJ^{3i}|^2 - \frac{1}{2} |\nabla^i \rho_a + 2iJ_a^{3i}|^2 \right) \\
 &= \rho_a \tau_a - \frac{1}{16} (-3\rho \Delta \rho + 12J_{ij} J_{ij} + \rho_a \Delta \rho_a - 4J_a^{ij} J_{ija})
 \end{aligned} \tag{C.12}$$

$$\begin{aligned}
 \langle \rho_a \Delta \rho_a \rangle &= \rho_a \Delta \rho_a - \sum_q 2\psi_i^* \tau_a \psi_j \Delta \psi_j^* \tau_a \psi_i \\
 &= \rho_a \Delta \rho_a - \frac{3}{2} \left( \frac{1}{4} \rho \Delta \rho + J_{ij} J_{ij} - \rho\tau \right) + \frac{1}{2} \left( \frac{1}{4} \rho_a \Delta \rho_a + J_{ija} J_{ija} - \rho\tau \right) \\
 &= \frac{9}{8} \rho_a \Delta \rho_a - \frac{3}{8} \rho \Delta \rho + \frac{3}{2} \rho\tau - \frac{1}{2} \rho_a \tau_a - \frac{3}{2} J_{ij} J_{ij} + \frac{1}{2} J_{ija} J_{ija}.
 \end{aligned} \tag{C.13}$$

Finally we turn to the densities which involve spin. These can be evaluated by using

the relationship

$$\begin{aligned} \sum_{ss'} A_s \sigma_a B_{s'} C_{s'} \sigma_a D_s &= \sum_{ss'} (1 - \delta_{ss'}) 2A_s B_{s'} C_{s'} D_s + \delta_{ss'} A_s B_s C_s D_s \\ &= \frac{3}{2} (AD)(BC) - \frac{1}{2} (AD)_i (BC)_i = \frac{3}{2} \text{Re}(AD) \text{Re}(BC) - \frac{1}{2} \text{Im}(AD) \text{Im}(BC). \end{aligned} \quad (\text{C.14})$$

From this, we are now able to calculate

$$\begin{aligned} \langle \vec{s} \Delta \vec{s} \rangle &= - \sum_q \left( \frac{3}{2} \left( \frac{1}{4} \rho_q \Delta \rho_q + J_{ijq} J_{ijq} - \rho_q \tau_q \right) + \frac{1}{4} (J_{ijq} J_{jiq} + J_{sq}^2) \right) \\ &= - \frac{3}{16} (\rho \Delta \rho + \rho_a \Delta \rho_a) - \frac{3}{4} (J_{ij} J_{ij} + J_a^{ij} J_{ija}) \\ &\quad + \frac{3}{4} (\rho \tau + \rho_a \tau_a) + \frac{1}{8} (J_{ij} J_{ji} + J_s^2 + J_{ija} J_{jia} + (J_{sa})^2) \\ \langle \vec{s}_a \Delta \vec{s}_a \rangle &= \frac{9}{4} \left( -\frac{1}{4} \rho \Delta \rho - J_{ij} J_{ij} + \rho \tau \right) + \frac{3}{8} (J_{ij} J_{ji} + J_s^2) \\ &\quad - \frac{3}{4} \left( -\frac{1}{4} \rho_a \Delta \rho_a - J_{ija} J_{ija} + \rho_a \tau_a \right) - \frac{1}{8} (J_{ija} J_{jia} + (J_{sa})^2) \end{aligned} \quad (\text{C.15})$$

$$\begin{aligned} \langle (\nabla \cdot \vec{s})^2 \rangle &= - \sum_{sqis'q'j} (\nabla \cdot (\psi_{isq}^* \vec{\sigma} \psi_{js'q'})) (\nabla \cdot (\psi_{js'q'}^* \vec{\sigma} \psi_{isq})) \\ &= - \sum_{qij} 2 |\partial_z (\psi_{iq}^* \psi_{jq})|^2 + 2 |\partial_x (\psi_{iq}^* \psi_{jq}^*)|^2 + 2 |\partial_y (\psi_{iq}^* \psi_{jq}^*)|^2 \\ &= - \sum_q \rho_q \tau_q - 2 \sum_q \frac{1}{16} ((\partial_z \rho_q + i2J_{33q})^2 + (\partial_y \rho_q - i2J_{32q})^2) \\ &\quad - 2 \sum_q \frac{1}{8} |\partial_x \rho_q + i2J_{3iq}|^2 + \frac{1}{8} |\partial_y \rho_q + i2J_{31q}|^2 \\ &= - \sum_q \rho_q \tau_q - \frac{1}{4} \sum_q (\nabla \rho_q)^2 - 4(J_{33q})^2 + 4(J_{31q})^2 + 4(J_{32q})^2 \\ &= - \frac{1}{2} (\rho \tau + \rho_a \tau_a) + \frac{1}{8} (\rho \Delta \rho + \rho_a \Delta \rho_a + 4(J_{ij} J_{ji} + J_s^2) \\ &\quad + 4(J_{ija} J_{jia} + J_s^2) - 4J_{ij} J_{ij} - 4J_{ija} J_{ija}) \\ \langle (\nabla \cdot \vec{s}_a)^2 \rangle &= - \frac{1}{2} (3\rho \tau - \rho_a \tau_a) + \frac{1}{8} (3\rho \Delta \rho - \rho_a \Delta \rho_a) \\ &\quad + \frac{1}{2} (3J_{ij} J_{ji} - J_{ija} J_{jia} + 3J_s^2 - (J_{sa})^2 - 3J_{ij} J_{ij} + J_{ij} J_{ij}) \end{aligned} \quad (\text{C.16})$$

The calculation of spin-orbit terms is a much more difficult task. Furthermore, we would not obtain the correct results under the assumption of a spin-saturated system [120]. For this reason, we used the expectation values of these terms calculated in [41]:

$$\begin{aligned} \langle \rho \nabla \cdot \vec{J}_v \rangle &= \frac{5}{4} \rho \nabla \cdot \vec{J}_v + \frac{1}{4} \rho_a \nabla \cdot \vec{J}_{va} \\ \langle \rho_a \nabla \cdot \vec{J}_v^a \rangle &= \frac{3}{4} \rho \nabla \cdot \vec{J}_v + \frac{3}{4} \rho_a \nabla \cdot \vec{J}_{va}. \end{aligned} \quad (\text{C.17})$$

---

# Bibliography

---

- [1] D. Rowe. *Nuclear Collective Motion: Models and Theory*. World Scientific, 1970.
- [2] M. Bender, P. Heenen, P. Reinhard. *Reviews of Modern Physics* 75:121, 2003.
- [3] P. Ring. *Progress in Particle and Nuclear Physics* 37:193, 1996.
- [4] P. Ring, P. Schuck. *The Nuclear Many-Body Problem*. Springer-Verlag, 1980.
- [5] T. Skyrme. *Philosophical Magazine* 1:1403, 1956.
- [6] D. Vautherin, D. Brink. *Physical Review C* 5:626, 1972.
- [7] J. Dechargé, D. Gogny. *Physical Review C* 21:1568, 1980.
- [8] M. Dutra *et al.* *Physical Review C* 85:035201, 2012.
- [9] Y. Oganessian, V. Utyonkov. *Reports on Progress in Physics* 78:03601, 2013.
- [10] M. Bender, P. Heenen. *Journal of Physics: Conference Series* 420:1, 2013.
- [11] J. Hamilton, S. Hofmann, Y. Oganessian. *Annual Review of Nuclear and Particle Science* 63:383, 2013.
- [12] M. Mumpower *et al.* *Progress in Particle and Nuclear Physics* 86:86, 2016.
- [13] J. Lattimer. *Annual Review of Nuclear and Particle Science* 63:485, 2012.
- [14] J. Erler *et al.* *Nature* 486:509, 2012.
- [15] K. Langanke, M. Wiescher. *Reports on Progress in Physics* 64:1657, 2001.
- [16] T. Bürvenich *et al.* *Physical Review C* 69:014307, 2004.
- [17] M. Bender *et al.* *Physical Review C* 65:054322, 2002.
- [18] H. Yukawa. *Proceedings of the Physico-Mathematical Society of Japan* 17:48, 1935.
- [19] R. Machleidt. *Advanced in Nuclear Physics* 19:189, 1989.
- [20] B. Serot, J. Walecka. *International Journal of Modern Physics E* 06:515, 1997.
- [21] M. Peskin, D. Schroeder, *An Introduction to Quantum Field Theory*. Westview Press, 1995.
- [22] A. Zee. *Quantum Field Theory in a Nutshell*. Princeton University Press, 2003.
- [23] D. Schroeder. *An Introduction to Thermal Physics*. Addison Wesley, 1999.
- [24] S. Weinberg, *The Quantum Theory of Fields, Volume 1*. Cambridge University Press, 1995.

- [25] M. Kaku, *Quantum Field Theory: A Modern Introduction*. Oxford University Press, 1993.
- [26] K. Wilson. *Reviews of Modern Physics* 55:583, 1983.
- [27] A. Dobada *et al.* *Effective Lagrangian for the Standard Model*. Springer, 1997.
- [28] C. Burgess. *Living Reviews in Relativity* 7, 2004.
- [29] R. Mohapatra, A. Smirnov. *Annual Review of Nuclear and Particle Physics* 56:549, 2006.
- [30] S. Weinberg. *Physica* 96A, 1979.
- [31] T. Appelquist, J. Carazzone. *Physical Review D* 11:2856, 1975.
- [32] K. Wilson, J. Kogut. *Physics Reports* 12:75, 1974.
- [33] B. Serot, J. Walecka. *Advanced in Nuclear Physics* 16:1, 1986.
- [34] E. Weinberg. *Radiative Corrections as the Origin of Spontaneous Symmetry Breaking* 1973. arXiv:hep-th/0507214.
- [35] T. Morris, D. Ross, C. Sachrajda. *Nuclear Physics B* 255:115, 1985.
- [36] G. Dunne. *Journal of Physics A* 41:304006, 2008.
- [37] R. Rivers. *Path integral methods in quantum field theory*. Cambridge University Press, 1987.
- [38] K. Saito, K. Tsushima, A. Thomas. *Progress in Particle and Nuclear Physics* 58:1 2007.
- [39] P. Guichon *et al.* *Nuclear Physics A* 601:349, 1996.
- [40] P. Guichon, A. Thomas. *Physical Review Letters* 93:132502, 2004.
- [41] P. Guichon *et al.* *Nuclear Physics A* 772:1, 2006.
- [42] J. Lévy-Leblond. *Chapter 5 of Group Theory and its Applications* Volume 2, edited by E. Loeb. Academic Press, 1971.
- [43] M. Montigny, J. Niederle, A. Nikitin. *Journal of Physics A* 39:9365, 2006.
- [44] G. Rousseaux. *The European Physical Journal Plus* 128:81, 2013.
- [45] C. Simenel. *The European Physical Journal A* 48:125, 2012.
- [46] J. Lévy-Leblond. *Communications in Mathematical Physics* 6:286, 1967.
- [47] L. Foldy, S. Wouthuysen. *Physical Review* 78:29, 1950.
- [48] M. Thies. *Physics Letters B* 166:23, 1986.
- [49] P. Reinhard. *Reports on Progress in Physics* 52:439, 1989.
- [50] A. Sulaksono *et al.* *Annals of Physics* 308:354, 2003.

- 
- [51] A. Sulaksono *et al.* *Physical Review Letters* 98:262501, 2007.
- [52] A. Sulaksono *et al.* *International Journal of Modern Physics E* 20:139, 2011.
- [53] T. Lensinski *et al.* *Physical Review C* 76:014312, 2007.
- [54] J. Dobaczewski and J. Dudek. *Acta Physica Polonica B* 27:45 (1996).
- [55] T. Skyrme. *Nuclear Physics* 9:615, 1959.
- [56] K. Olive *et al.* *Review of Particle Physics (2014)*.
- [57] A. Smilga. *Lectures on Quantum Chromodynamics*. World Scientific, 2001.
- [58] J. Donogoe, E. Golowich, B. Holstein. *Dynamics of the Standard Model*. Cambridge University Press, 1992.
- [59] A. Manohar. *Large N QCD* (1998) arXiv:hep-ph/9802419.
- [60] A. Kronfeld. *Annual Review of Nuclear and Particle Science* 62:265, 2012.
- [61] A. Thomas, S. Théberge, G. Miller. *Physical Review D* 24:216, 1981.
- [62] I. Zahed, G. Brown. *Physical Reports* 142:1, 1986.
- [63] U. Vogl, W. Weise. *Progress in Particle and Nuclear Physics* 27:195, 1991.
- [64] Z. Fodor, C. Hoelbling. *Reviews of Modern Physics* 84:449, 2012.
- [65] C. Burgess, G. Moore. *The Standard Model: A Primer*. Cambridge University Press, 2006.
- [66] J. Peláez. arXiv:1510.00653, 2015.
- [67] J. Donoghue. *Physics Letters B* 643:165, 2006.
- [68] S. Scherer. *Advances in Nuclear Physics* 27:277, 2003.
- [69] S. Weinberg. *The Quantum Theory of Fields, Volume 2*. Cambridge University Press, 1996.
- [70] J. Walecka. *Theoretical Nuclear and Subnuclear Physics* Imperial College Press, 2004.
- [71] A. Afanazjev, H. Abusara. *Physical Review C* 81:014309, 2010.
- [72] M. Mayer, J. Jensen. *Elementary Theory of Nuclear Shell Structure*. John Wiley and Sons, 1955.
- [73] R. Furnstahl, B. Serot. *Comments on Nuclear and Particle Physics* 2:A23, 2000.
- [74] J. Jackson, *Classical Electrodynamics* John Wiley and Sons, 1999.
- [75] R. Furnstahl, B. Serot, H. Tang. *Nuclear Physics A* 615:441, 1997.
- [76] J. Walecka. *Annals of Physics* 83:491, 1974.
- [77] J. Sakurai. *Annals of Physics* 11:1, 1960.

- [78] P. Guichon. *Physics Letters B* 200:234, 1988.
- [79] J. Sakurai. *Currents and Mesons*. University of Chicago Press, 1969.
- [80] R. Bhaduri. *Models of the Nucleon: From Quarks to Solitons*. Addison-Wesley Publishing Company 1988.
- [81] C. DeTar, J. Donoghue. *Annual Review of Nuclear and Particle Science* 33:235, 1983.
- [82] J. Donoghue, K. Johnson. *Physical Review D* 21:1975, 1980.
- [83] G. Höhler, E. Pietarinen. *Nuclear Physics B* 95:210, 1975.
- [84] W. Grein. *Nuclear Physics B* 131:255, 1977.
- [85] P. Mergell, U. Meißner, D. Drechsel. *Nuclear Physics A* 596:367, 1996.
- [86] S. Furuichi, K. Watanabe. *Progress in Theoretical Physics* 82:581, 1989.
- [87] D. Jido, E. Oset, J. Palomar. *Nuclear Physics A* 709:345, 2002.
- [88] G. Höhler *et al.* *Nuclear Physics B* 114:505, 1976.
- [89] E. Epelbaum, U. Meißner. *Annual Review of Nuclear and Particle Physics* 62:159, 2012.
- [90] M. Kortelainen *et al.* *Physical Review C* 82:024313, 2010.
- [91] M. Kortelainen *et al.* *Physical Review C* 85:024304, 2012.
- [92] M. Kortelainen *et al.* *Physical Review C* 89:054314, 2014.
- [93] E. Chabanat *et al.* *Nuclear Physics A* 635:231, 1998.
- [94] J. Bartel *et al.* *Nuclear Physics A* 386:79, 1982.
- [95] P.G. Reinhard and H. Flocard. *Nuclear Physics A* 584:467, 1995.
- [96] M. Samyn *et al.* *Nuclear Physics A* 700:142, 2002.
- [97] J. Stone, P. G. Reinhard. *Progress in Particle and Nuclear Physics* 58:587, 2007.
- [98] S. Goriely *et al.* *Physical Review C* 68:054325, 2003.
- [99] B. Brown. *Physical Review C* 58:220, 1998.
- [100] E. Chabanat *et al.* *Nuclear Physics A* 627:710, 1997.
- [101] G. Lalazissis, J. König, P. Ring. *Physical Review C* 55:540, 1997.
- [102] M. Bender *et al.* *Physical Review C* 60:034304, 1999.
- [103] P. Stevenson *et al.* *Physical Review C* 93:054617, 2016.
- [104] M. Bender *et al.* *Physical Review C* 80:064302, 2009.
- [105] V. Hellemans, P. Heenen, M. Bender. *Physical Review C* 85:014326, 2012.
- [106] T. Otsuka *et al.* *Physical Review Letters* 86:082502, 2001.

- 
- [107] N. Schunck *et al.* *Journal of Physics G* 42:034024, 2015.
- [108] M. Kortelainen *et al.* *Physical Review C* 77:064307, 2008.
- [109] R. Machleidt, I. Slaus. *Journal of Physics G* 27:69, 2001.
- [110] R. Machleidt, D. Entem. *Physics Reports* 503:1, 2011.
- [111] S. Weinberg. *Physics Letters B* 251:288, 1990.
- [112] S. Weinberg. *Physics Letters B* 295:144, 1991.
- [113] S. Weinberg. *Physics Letters B* 363:3, 1992.
- [114] D. Vretenar. *The European Physical Journal: Special Topics* 156:37, 2008.
- [115] S. Aoki. *European Physics Journal A* 49:81, 2013.
- [116] J. Boyd. *Acta Applicandae Mathematicae* 56:1, 1999.
- [117] G. Källén. *Helvetica Physica Acta* 25:417, 1952.
- [118] H. Lehmann. *Nuovo Cimento* 11:342, 1954.
- [119] T. Padmanabhan. *Quantum Field Theory: The Why, What and How*. Springer, 2016.
- [120] Y. Engel *et al.* *Nuclear Physics A* 249:215, 1975.